NEDO-24615
80NED023
Class I
June 1980

MARK I CONTAINMENT PROGRAM

1/4 SCALE PRESSURE

SUPPRESSION POOL SWELL TEST PROGRAM: SUPPLEMENTAL PLANT UNIQUE TESTS

TASK NUMBERS 5.5.4/10.1

Volume 2, Appendices A and B

This work was performed with the support of
Quadrex Corporation, Nuclear Services Division,
and Aerotherm Division of Acurex Corporation
under contract to General Electric.

Reviewed by: John M. Humphrey
John M. Humphrey
Mark I Containment Design

Approved by:
G. E. Wade, Manager
Mark I Containment Design

Approved by:
P. W. Ianni, Manager
Containment Design

NUCLEAR ENGINEERING DIVISION • GENERAL ELECTRIC COMPANY
SAN JOSE, CALIFORNIA 95125

GENERAL ELECTRIC

TABLE OF CONTENTS - APPENDICES

*The Monticello tests are discussed in Section 3 of the main report.

INTRODUCTION - APPENDICES

The large quantity of data and descriptive material produced by each test series has necessitated the inclusion of a set of appendices with this report. The main report highlights data from a typical plant's tests and summarizes information of general interest. Ten appendices have been included to present data for the remaining plants, to discuss in detail certain phenomena of particular interest, and to document areas that have received additional investigative effort. The contents of these appendices are summarized below.

Appendix A (a continuation of Section 3) presents the test data for the other six plant configurations not discussed in the main report. The data in Section 3 and Appendix A are not necessarily design basis data. The Task 5.5.3-2 Plant Unique Tests were performed at conditions being evaluated for plant operation. Supplementary tests in this report were performed to evaluate alternate conditions (including variations in water level, submergence, drywell/wetwell pressure differential and vent header deflector design) for seven Mark I utilities. After a review of these data, a set of test conditions will be selected for each plant to serve as a design basis for pool swell loads.

Appendix B defines the method used for vent header pressure integration. The values used for the six-point fits to the impact pressure transducer transients and the resulting pressure integrals are also provided.

Appendix C presents plant unique data comparisons and the results of a linear regression correlation of the test data from the Plant Unique Tests, Supplemental Plant Unique Tests, and Generic Sensitivity Tests.

Appendix D presents the results of a measurement uncertainty analysis.

Appendix E presents a series of pool swell pictures for each plant configuration.

Appendix F presents smoothed window-related download oscillations.

Appendix G presents the specification for vent system resistance and the method used to meet the specification.

Appendix H describes the method used to calculate the internal drag forces in the vent system.

Appendix I presents measured deflector forces and an analysis of dye injection tests to investigate the fluid velocity and acceleration history at the deflector.

APPENDIX A
TEST RESULTS

The data for one typical test configuration was presented and discussed in Section 3. The data for the other six configurations tested during the Task 5.5.4 Supplemental Plant Unique Tests are presented and discussed in this appendix in the same format as Section 3.

A.1 Duane Arnold Tests

A.1.1 Typical Data

Time-history plots of the driving conditions and pool response are presented in this section for Duane Arnold Test 7. Test 7 was conducted with a zero initial drywell/wetwell differential pressure (0" H_2O ΔP), a downcomer submergence of 12.08 inches, and a 9.06-inch width wedge deflector (30 inches full scale).

A.1.1.1 Driving Conditions

Driving conditions for Duane Arnold Test 7 are presented in Figures A-1 through A-5. Driving conditions for the Duane Arnold tests had the same characteristics as the "typical" plant discussed in Section 3.0 of this report.

A.1.1.2 Pool Response

Downcomer internal pressure and wetwell pressures for Duane Arnold Test 7 are presented in Figures A-6 and A-7, respectively. Net torus force from the pressure integral (Figure A-8) shows some oscillations in downforce as well as in upforce. Net torus force that is determined from the torus load cell (Figure A-9) by applying inertial correction with the torus accelerometer (Figure A-10) is shown in Figure A-11 and compared with net torus force determined from the pressure integral. Figure A-12 presents the net torus force based on the torus pressure integral, corrected for water inertia.

The "average" pool pressure for Duane Arnold Test 7 is shown in Figure A-13. Figure A-14 is similar to Figure A-12, with force replaced by average pressure (force/torus projected area).

The vent header impact pressures for Duane Arnold Test 7 are presented in Figures A-15 and A-16. These figures indicate that the deflector eliminated any measurable load on the vent header.

A.1.2 Pool Dynamics

The pool contours at various times during pool swell are shown in Figures A-17 through A-19 for Duane Arnold Tests 6, 7, and 8. Pool surface displacement curves for Tests 6 through 9 (combined data) are shown in Figure A-20. The pool surface velocity profiles for Tests 6 through 9 (combined data) are shown in Figure A-21.

The pool surface displacement and velocity profile viewed from the side window during Test 9 are shown in Figure A-22. The downcomer water slug displacement, velocity, and acceleration versus time for Test 8 are presented in Figure A-23.

A.1.3 Data Summaries

A.1.3.1 Wetwell Vertical Forces

Table A-1 presents the Duane Arnold test data for wetwell vertical forces. Graphical comparison of the data is shown in Figures A-24 through A-26. All parameters in the figures are sensitive to ΔP, and trends in the data are comparable to those for the "typical plant" in Section 3.0.

A.1.3.2 Vent Header Impact Forces

Table A-2 presents the Duane Arnold test data for vent header impact forces. These tests were conducted with a wedge deflector installed

below the vent header. The 9.06 inch deflector (30 inches full scale) was effective in mitigating the vent header impact. Tests 6 and 7 were conducted with the deflector supported from the torus by cables (deflector load transmitted to the torus), while Tests 8 and 9 were conducted with the deflector welded directly onto the vent header (deflector load transmitted to the vent header). These two different attachment methods made it possible to measure the force on the deflector. Results of the deflector load analysis are given in Appendix I.

A.1.4 Discussion and Analysis

The Duane Arnold plant unique tests (Task 5.5.3-2) and supplemental tests (Task 5.5.4) were conducted with drywell/wetwell differential pressures of 0" and 9.19" H_2O. The torus vertical forces (downforce and upforce) were sensitive to drywell/wetwell ΔP and decreased with increase in ΔP. The wedge deflector (30-inch width full scale) effectively mitigated the vent header impact. A comparison of torus load cell and pressure integral data shows that these redundant measurements are in good agreement. The vent header impact force was negligibly small. The photographic results in Appendix E show that there was no direct impact of water on the bottom of the vent header.

During the Duane Arnold tests, a torus downforce spike with subsequent oscillations and a torus pressure spike with oscillations appeared at approximately 600 milliseconds after test initiation. Section C.5 presents an analysis of that phenomenon. It was concluded that the torus downforce at 600 milliseconds is real and the localized impulsive loading should be considered in load evaluation.

FIGURE A-1

DRYWELL ORIFICE UPSTREAM PRESSURE

TASK 5.5.4 DUANE ARNOLD TEST 7

*

*General Electric Company proprietary information has been deleted.

FIGURE A-2

DRYWELL PRESSURE

TASK 5.5.4 DUANE ARNOLD TEST 7

*

*General Electric Company proprietary information has been deleted.

FIGURE A-3

DOWNCOMER ORIFICE DIFFERENTIAL PRESSURE

TASK 5.5.4 DUANE ARNOLD TEST 7

*

*General Electric Company proprietary information has been deleted.

FIGURE A-4

DOWNCOMER ORIFICE UPSTREAM TEMPERATURE

TASK 5.5.4 DUANE ARNOLD TEST 7

*

*General Electric Company proprietary information has been deleted.

FIGURE A-5

ENTHALPY FLOW INTO POOL

Task 5.5.4 Duane Arnold Test 7

*

*General Electric Company proprietary information has been deleted.

FIGURE A-6

DOWNCOMER INTERNAL PRESSURE

TASK 5.5.4 DUANE ARNOLD TEST 7

*

*General Electric Company proprietary information has been deleted.

FIGURE A-7

WETWELL PRESSURES

TASK 5.5.4 DUANE ARNOLD TEST 7

*

*General Electric Company proprietary information has been deleted.

FIGURE A-8

NET TORUS FORCE FROM PRESSURE INTEGRAL *

TASK 5.5.4 DUANE ARNOLD TEST 7

*General Electric Company proprietary information has been deleted.

FIGURE A-9

TORUS LOAD CELL

TASK 5.5.4 DUANE ARNOLD TEST 7

*

*General Electric Company proprietary information has been deleted.

FIGURE A-10

TORUS VERTICAL ACCELERATION

TASK 5.5.4 DUANE ARNOLD TEST 7

*

*General Electric Company proprietary information has been deleted.

FIGURE A-11

COMPARISON OF NET TORUS FORCE FROM PRESSURE INTEGRAL

WITH NET TORUS FORCE FROM LOAD CELL CORRECTED FOR TORUS INERTIA

TASK 5.5.4 DUANE ARNOLD TEST 7

*

*General Electric Company proprietary information has been deleted.

FIGURE A-12

NET TORUS FORCE FROM PRESSURE INTEGRAL, CORRECTED FOR WATER INERTIA *

TASK 5.5.4 DUANE ARNOLD TEST 7

*General Electric Company proprietary information has been deleted.

FIGURE A-13

AVERAGE POOL PRESSURE, CORRECTED FOR WATER INERTIA

TASK 5.5.4 DUANE ARNOLD TEST 7

*

*General Electric Company proprietary information has been deleted.

FIGURE A-14

NET AVERAGE POOL PRESSURE, CORRECTED FOR WATER INERTIA

TASK 5.5.4 DUANE ARNOLD TEST 7

*

*General Electric Company proprietary information has been deleted.

FIGURE A-15

VENT HEADER IMPACT PRESSURES

TASK 5.5.4 DUANE ARNOLD TEST 7

*

*General Electric Company proprietary information has been deleted.

FIGURE A-16

VENT HEADER IMPACT PRESSURES

TASK 5.5.4 DUANE ARNOLD TEST 7

*

*General Electric Company proprietary information has been deleted.

FIGURE A-17

TIME HISTORY OF

POOL DISPLACEMENT

DUANE ARNOLD, TEST 6

*

*General Electric Company proprietary information has been deleted.

FIGURE A-18
TIME HISTORY OF
POOL DISPLACEMENT
DUANE ARNOLD, TEST 7

*

*General Electric Company proprietary information has been deleted.

FIGURE A-19
A TIME HISTORY OF
POOL DISPLACEMENT

DUANE ARNOLD, TEST 8

*

*General Electric Company proprietary information has been deleted.

FIGURE A-20

POOL SURFACE DISPLACEMENT

DUANE ARNOLD, TESTS 6, 7, 8, 9

(Combined Data)

*

*General Electric Company proprietary information has been deleted.

FIGURE A-21

POOL SURFACE VELOCITY PROFILES

DUANE ARNOLD, TESTS 6, 7, 8, 9

(Combined Data)

*

*General Electric Company proprietary information has been deleted.

FIGURE A-22

POOL BOUNDARY DISPLACEMENT AND VELOCITY PROFILES ALONG SIDE WINDOW

DUANE ARNOLD, TEST 9

*

*General Electric Company proprietary information has been deleted.

FIGURE A-23

DOWNCOMER WATER SLUG EJECTION

DUANE ARNOLD, TEST 3

*

*General Electric Company proprietary information has been deleted.

FIGURE A-24

SENSITIVITY OF DOWNFORCE AND UPFORCE TO DRYWELL/WETWELL ΔP

TASKS 5.5.3-2 & 5.5.4 DUANE ARNOLD TESTS

*

*General Electric Company proprietary information has been deleted.

FIGURE A-25

SENSITIVITY OF TORUS DOWNFORCE IMPULSE TO DRYWELL/WETWELL ΔP

TASKS 5.5.3-2 & 5.5.4 DUANE ARNOLD TESTS

*

*General Electric Company proprietary information has been deleted.

FIGURE A-26

SENSITIVITY OF TIMES TO PEAK DOWNFORCE AND UPFORCE

TO DRYWELL/WETWELL ΔP

TASKS 5.5.3-2 & 5.5.4 DUANE ARNOLD TESTS *

*General Electric Company proprietary information has been deleted.

TABLE A-1

DATA FOR WETWELL VERTICAL LOADS

Task 5.5.4 Duane Arnold Tests

*

*General Electric Company proprietary information has been deleted.

TABLE A-1

DATA FOR WETWELL VERTICAL LOADS (continued)

Task 5.5.4 Duane Arnold Tests

*

*General Electric Company proprietary information has been deleted.

TABLE A-2

*

DATA FOR VENT HEADER IMPACT LOADS

Task 5.5.4 Duane Arnold Tests

*General Electric Company proprietary information has been deleted.

A.2 Pilgrim Tests

A.2.1 Typical Data

Time-history plots of the driving conditions and pool response are presented in this section for Pilgrim Tests 7 and 11. Test 7 was conducted with a drywell/wetwell differential pressure of 8.52" H_2O ΔP and with a 6.727-inch winged deflector (25.61 inches full scale).* Test 11 was conducted with a zero initial drywell/wetwell differential pressure (0" H_2O ΔP) and with the same 6.727-inch winged deflector. All Pilgrim tests were performed with an initial downcomer submergence of 10.25 inches.

A.2.1.1 Driving Conditions

Driving conditions for Pilgrim Tests 7 and 11 are presented in Figures A-27 through A-31. Driving conditions for the Pilgrim tests had the same characteristics as the "typical" plant discussed in Section 3.0 of this report.

2.1.2 Pool Response

Downcomer internal pressure and wetwell pressures for Pilgrim Tests 7 and 11 are presented in Figures A-32 and A-33, respectively. These pressure plots have the same characteristics as the "typical" plant in Section 3.0. At 0" H_2O ΔP, however, the characteristic one-cycle oscillation of the downcomer internal pressure is negligibly small (Test 11).

Figure A-34 presents net torus force based on the torus pressure integral for Pilgrim Tests 7 and 11. The net torus force exhibits no significant oscillations in downforce and upforce.

The net torus force which was determined by applying the inertial correction from the torus accelerometer (Figure A-36) to the torus load cell (Figure A-35) is compared with the net torus force obtained from the torus pressure integral in Figure A-37. Residual oscillations are

---

* A "winged" deflector is a standard pipe with structural angles welded to the sides.

present in the corrected load cell for the 0"H_2O ΔP run (Test 11). Figure A-38 presents the net torus force based on the torus pressure integral corrected for inertia.

The "average" pool pressures for Pilgrim Tests 7 and 11 are shown in Figure A-39. Figure A-40 is similar to Figure A-38, with force replaced by average pressure (force/torus projected area).

The vent header impact pressures for Pilgrim Tests 7 and 11 are presented in Figures A-41 through A-44. These figures indicate that the deflector was effective in mitigating vent header impact.

Figure A-45 presents a comparison of the vent header impact force derived from pressure integral with that derived from the corrected load cell.

A.2.2 Pool Dynamics

The pool contours at various times during pool swell are shown in Figures A-46 through A-51 for Pilgrim Tests 6, 7, 8, 10, 11, and 12.

Pool surface displacement curves for Tests 6 through 9 (combined data) are shown in Figure A-52. The pool surface velocities for Tests 6 through 9 (combined data) are shown in Figure A-53. The pool surface displacement curves and pool surface velocity profiles for Tests 10 through 13 (combined data) are shown in Figures A-54 and A-55, respectively.

The pool surface displacement and velocity profile viewed from the side window during Tests 9 and 13 are shown in Figures A-56 and A-57, respectively. The downcomer water slug displacement, velocity, and acceleration versus time for Tests 8 and 12 are presented in Figures A-58 and A-59. Pilgrim pool dynamics are similar to those of the "typical" plant discussed in Section 3.0.

A.2.3 Data Summaries

A.2.3.1 Wetwell Vertical Forces

Tables A-3 and A-5 present the Pilgrim test data for wetwell vertical forces. Graphical comparison of the data is shown in Figures A-60 through A-62. All parameters in the figures are sensitive to the initial downcomer submergence and ΔP; trends in the data are comparable to those for the "typical plant" in Section 3.0.

A.2.3.2 Vent Header Impact Forces

Tables A-4 and A-6 present the Pilgrim test data for vent header impact forces. These tests were conducted with a winged deflector installed below the vent header. The 6.727-inch deflector (25.61 inches full scale) was effective in mitigating the vent header impact. Two of the four tests at the same test condition were conducted with the deflector supported from the torus by cables (deflector load transmitted to the torus), while the other two tests were conducted with the deflector bolted onto the vent header (deflector load transmitted to the vent header). These two different attachment methods made it possible to measure the force on the deflector. Results of the deflector load analysis are reported in Appendix I.

A.2.4 Discussion and Analysis

The Pilgrim plant unique tests (Task 5.5.3-2) and supplemental tests (Task 5.5.4) were conducted with drywell/wetwell differential presssures of 0", 8.52", and 10.9" H_2O and with initial downcomer submergences of 10.25 and 15.13 inches. The torus vertical forces (downforce and upforce) were sensitive to both drywell/wetwell ΔP and downcomer submergence. The torus vertical forces decreased with increase in ΔP or decrease in downcomer submergence or both. ΔP was more effective in reducing the torus vertical forces than the downcomer submergence over the ranges of ΔP and downcomer submergence varied during the test series.

The winged deflector (25.61 inches full scale) effectively mitigated vent header impact. The four tests which were run at a same test condition show excellent reproducibility and consistency. A comparison of load cell data and pressure integral data for torus shows that these redundant measurements are in good agreement. The peak vent header impact force from corrected load cell also agrees reasonably well with the peak force from pressure integral.

FIGURE A-27

DRYWELL ORIFICE UPSTREAM PRESSURE

TASK 5.5.4 PILGRIM TESTS

TEST 7

TEST 11

*

*General Electric Company proprietary information has been deleted.

FIGURE A-28

DRYWELL PRESSURE

TASK 5.5.4 PILGRIM TESTS

TEST 7

TEST 11

*General Electric Company proprietary information has been deleted.

FIGURE A-29

DOWNCOMER ORIFICE DIFFERENTIAL PRESSURE

TASK 5.5.4 PILGRIM TESTS

TEST 7

TEST 11

*General Electric Company proprietary information has been deleted.

FIGURE A-30

DOWNCOMER ORIFICE UPSTREAM TEMPERATURE

TASK 5.5.4 PILGRIM TESTS

TEST 7

TEST 11

*

*General Electric Company proprietary information has been deleted.

FIGURE A-31

ENTHALPY FLOW INTO POOL

TASK 5.5.4 PILGRIM TESTS

TEST 7

TEST 11

*

*General Electric Company proprietary information has been deleted.

FIGURE A-32

DOWNCOMER INTERNAL PRESSURE

TASK 5.5.4 PILGRIM TESTS

TEST 7

Tf - 11

*

*General Electric Company proprietary information has beer deleted.

FIGURE A-33

WETWELL PRESSURES

TASK 5.5.4 PILGRIM TESTS

TEST 7

TEST 11

*

*General Electric Company proprietary information has been deleted.

FIGURE A-34

NET TORUS FORCE FROM PRESSURE INTEGRAL

TASK 5.5.4 PILGRIM TESTS

TEST 7

Test 11

*General Electric Company proprietary information has been deleted.

FIGURE A-35

TORUS LOAD CELL

TASK 5.5.4 PILGRIM TESTS

TEST 7

TEST 11

*

*General Electric Company proprietary information has been deleted.

FIGURE A-36

TORUS VERTICAL ACCELERATION

TASK 5.5.4 PILGRIM TESTS

TEST 7

TEST 11

*General Electric Company proprietary information has been deleted.

FIGURE A-37

COMPARISON OF NET TORUS FORCE FROM PRESSURE INTEGRAL
WITH NET TORUS FORCE FROM LOAD CELL CORRECTED FOR TORUS INERTIA

TEST 7

TEST 11

*General Electric Company proprietary information has been deleted.

FIGURE A-38

NET TORUS FORCE FROM PRESSURE INTEGRAL, CORRECTED FOR WATER INERTIA

TASK 5.5.4 PILGRIM TESTS

TEST 7

TEST 11

*

*General Electric Company proprietary information has been deleted.

FIGURE A-39

AVERAGE POOL PRESSURE, CORRECTED FOR WATER INERTIA

TASK 5.5.4 PILGRIM TESTS

TEST 7

TEST 11

*General Electric Company proprietary information has been deleted.

FIGURE A-40

NET AVERAGE POOL PRESSURE, CORRECTED FOR WATER INERTIA

TASK 5.5.4 PILGRIM TESTS

TEST 7

TEST 11

*General Electric Company proprietary information has been deleted.

FIGURE A-41

VENT HEADER IMPACT PRESSURES

TASK 5.5.4 PILGRIM TESTS

TEST 7

TEST 11

*General Electric Company proprietary information has been deleted.

FIGURE A-42

VENT HEADER IMPACT PRESSURES

TASK 5.5.4 PILGRIM TESTS

TEST 7

TEST 11

*

*General Electric Company proprietary information has been deleted.

FIGURE A-43

VENT HEADER IMPACT PRESSURES

TASK 5.5.4 PILGRIM TESTS

TEST 7

TEST 11

*

*General Electric Company proprietary information has been deleted.

FIGURE A-45

COMPARISON OF VENT HEADER IMPACT RESULTS

Task 5.5.4 Pilgrim Tests 7 and 11

*

Test 7

Test 11

*General Electric Company proprietary information has been deleted.

FIGURE A-46
TIME HISTORY OF
POOL DISPLACEMENT
PILGRIM, TEST 6

*

*General Electric Company proprietary information has been deleted.

FIGURE A-47
TIME HISTORY OF
POOL DISPLACEMENT

PILGRIM, TEST 7

*

*General Electric Company proprietary information has been deleted.

FIGURE A-48

TIME HISTORY OF
POOL DISPLACEMENT
PILGRIM, TEST 8

*

*General Electric Company proprietary information has been deleted.

FIGURE A-49

TIME HISTORY OF
POOL DISPLACEMENT

PILGRIM, TEST 10

*

*General Electric Company proprietary information has been deleted.

FIGURE A-50

TIME HISTORY OF

POOL DISPLACEMENT

PILGRIM, TEST 11

*General Electric Company proprietary information has been deleted.

FIGURE A-51

TIME HISTORY OF

POOL DISPLACEMENT

PILGRIM, TEST 12

*

*General Electric Company proprietary information has been deleted.

FIGURE A-52

POOL SURFACE DISPLACEMENT

PILGRIM, TESTS 6, 7, 8, 9

(Combined Data)

*

FIGURE A-33

POOL SURFACE VELOCITY PROFILES

PILGRIM, TESTS 6, 7, 8, 9

(Combined Data)

*

*General Electric Company proprietary information has been deleted.

FIGURE A-54

POOL SURFACE DISPLACEMENT

PILGRIM, TESTS 10, 11, 12, 13

(Combined Data)

*

FIGURE A-55

POOL SURFACE VELOCITY PROFILES

PILGRIM, TESTS 10, 11, 12, 13

(Combined Data)

*

*General Electric Company proprietary information has been deleted.

FIGURE A-56

PILGRIM, TEST 9

POOL BOUNDARY DISPLACEMENT AND VELOCITY PROFILES ALONG SIDE WINDOW

*

*General Electric Company proprietary information has been deleted.

FIGURE A-57

PILGRIM, TEST 13

POOL BOUNDARY DI PLACEMENT AND VELOCITY PROFILES ALONG SIDE WINDOW *

*General Electric Company proprietary information has been deleted.

FIGURE A-58

DOWNCOMER WATER SLUG EJECTION

PILGRIM, TEST 8

*

*General Electric Company proprietary information has been deleted.

FIGURE A-59

DOWNCOMER WATER SLUG EJECTION

PILGRIM, TEST 12

*

*General Electric Company proprietary information has been deleted.

FIGURE A-60

SENSITIVITY OF PEAK DOWNFORCE AND UPFORCE TO DRYWELL/WETWELL ΔP

Task 5.5.3-2 & 5.5.4 Pilgrim Tests

*

*General Electric Company proprietary information has been deleted.

FIGURE A-61

SENSITIVITY OF TORUS DOWNFORCE IMPULSE TO DRYWELL/WETWELL ΔP *

Tasks 5.5.3-2 & 5.5.4 Pilgrim Tests

*General Electric Company proprietary information has been deleted.

FIGURE A-62

SENSITIVITY OF TIMES TO PEAK DOWNFORCE AND UPFORCE TO DRYWELL/WETWELL ΔP *

Tasks 5.5.3-2 & 5.5.4 Pilgrim Tests

*General Electric Company proprietary information has been deleted.

TABLE A-3

DATA FOR WETWELL VERTICAL LOADS

Task 5.5.4 Pilgrim Tests

*

*General Electric Company proprietary information has been deleted.

TABLE A-3

DATA FOR WETWELL VERTICAL LOADS (continued)

Task 5.5.4 Pilgrim Tests *

*General Electric Company proprietary information has been deleted.

TABLE A-4

DATA FOR VENT HEADER IMPACT LOADS

Task 5.5.4 Pilgrim Tests

*

*General Electric Company proprietary information has been deleted.

TABLE A-5

DATA FOR WETWELL VERTICAL LOADS

Task 5.5.4 Pilgrim Tests

*

*General Electric company proprietary information has been deleted.

TABLE A-5

DATA FOR WETWELL VERTICAL LOADS (continued)

Task 5.5.4 Pilgrim Tests

*

*General Electric Company proprietary information has been deleted.

TABLE A-6

DATA FOR VENT HEADER IMPACT LOADS

Task 5.5.4 Pilgrim Tests

*

*General Electric Company proprietary information has been deleted.

A.3 Oyster Creek Tests

A.3.1 Typical Data

Time-history plots of the driving conditions and pool response are presented in this section for Oyster Creek Tests 6, 10, 11, and 15. Test 6 was conducted with a drywell/wetwell differential pressure of 7.15" H_2O ΔP, an initial downcomer submergence of 12.59 inches, and a 7.75 inch "T" deflector (30 inches full scale).* Test 10 was conducted with a zero initial drywell/wetwell differential pressure (0" H_2O ΔP), a submergence of 12.59 inches, and the same 7.75 inch "T" deflector. Test 11 was conducted with a drywell/wetwell differential pressure of 7.00" H_2O; Test 15 was conducted with a zero drywell/wetwell differential pressure. Both Tests 11 and 15 were performed with an initial submergence of 9.30 inches and the 7.75 inch "T" deflector.

A.3.1.1 Driving Conditions

Driving conditions for Oyster Creek Tests 6, 10, 11, and 15 are presented in Figures A-63 through A-72. Driving conditions for the Oyster Creek tests had the same characteristics as the "typical" plant discussed in Section 3.0 of this report.

A.3.1.2 Pool Response

Downcomer internal pressure and wetwell pressures for Oyster Creek Tests 6, 10, 11, and 15 are presented in Figures A-73 and A-76. These pressure plots have the same characteristics as the "typical" plant in Section 3.0.

Figures A-77 and A-78 present net torus force based on the torus pressure integral for Oyster Creek Tests 6, 10, 11, and 15. Some downforce oscillations are present, but they dampen out rapidly after the first oscillation.

---

*A "T" deflector is a pipe with a structural "T" welded on each side.

The net torus force which was determined by applying the inertial correction from the torus accelerometer (Figures A-81 and A-82) to the torus load cell (Figures A-79 and A-80) is compared with the torus force obtained from the torus integral in Figures A-83 and A-84. Residual oscillations are present in the corrected load cell. Figures A-85 and A-86 present the net torus force based on the torus pressure integral corrected for water inertia. Window related download oscillations were noted in Test 11. Filtering (see Appendix F) significantly smoothed these oscillations.

The "average" pool pressures for Oyster Creek Tests 6, 10, 11, and 15 are shown in Figures A-87 and A-88. Figures A-89 and 90 are similar to Figures A-85 and A-86, with force replaced by average pressure (force/torus projected area).

The vent header impact pressures for Oyster Creek Tests 6, 10, 11, and 15 are presented in Figures A-91 through A-97. These figures indicate that the "T" deflector was effective in reducing the peak local vent header impact pressure.

Figures A-98 and A-99 present a comparison of the vent header impact force derived from the pressure integral with that derived from the corrected load cell.

A.3.2 Pool Dynamics

The pool contours at various times during pool swell are shown in Figures A-100 through A-106 for Oyster Creek Tests 6, 7, 8, 10, 11, 13, and 15.*

The pool surface displacement curves for Oyster Creek Tests 6, 7, 8, and 9 (combined data) are shown in Figure A-107. The pool surface velocities for Tests 6, 7, 8, and 9 (combined data) are shown in Figure A-108. The pool surface displacement graph and pool surface

*The high-speed camera was not operable during Test 12.

velocity profiles for Test 10 are shown in Figures A-109 and A-110, respectively. The pool surface displacement curves for Tests 11, 13, and 14 (combined data) are shown in Figure A-111. The pool surface velocities for Tests 11, 13, and 14 (combined data) are shown in Figure A-112. The pool surface displacement graph and pool surface velocity profiles for Test 15 are shown in Figures A-113 and A-114, respectively.

The pool surface displacements and velocity profile viewed from the side window during Tests 9 and 14 are shown in Figures A-115 and A-116, respectively. The downcomer water slug displacement, velocity, and acceleration versus time for Tests 8, 10, 13, and 15 are presented in Figures A-117 through A-120.

A.3.3 Data Summaries

A.3.3.1 Wetwell Vertical Forces

Tables A-7 and A-8 present the Oyster Creek test data for wetwell vertical forces. Graphical comparisons of the data is shown in Figures A-121 through A-123. All parameters in the figures are sensitive to the initial downcomer submergence and ΔP (with the exception of time to the peak downforce, which shows little or no sensitivity to downcomer submergence). Trends in the data are comparable to those for the "typical plant" in Section 3.0.

A.3.3.2 Vent Header Impact Forces

Tables A-9 and A-10 present the Oyster Creek test data for vent header impact forces. These tests were conducted with a "T" deflector installed below the vent header. The 7.15-inch deflector (30 inches full scale) was effective in mitigating the vent header impact. Two of the four tests at the same test condition were conducted with the deflector supported from the torus by cables (deflector load transmitted to the

torus), while the other two tests were conducted with the deflector bolted onto the vent header (deflector load transmitted to the vent header). These two different attachment methods made it possible to measure the force on the deflector. Results of the deflector load analysis are reported in Appendix I.

A.3.4 Discussion and Analysis

The Oyster Creek plant unique tests (Task 5.5.3-2) and supplemental tests (Task 5.5.4) were conducted with drywell/wetwell differential pressures of 0" and 7.15" H_2O and with initial downcomer submergences of 9.30 and 12.59 inches. The torus vertical forces (downforce and upforce) were sensitive to both drywell/wetwell ΔP and downcomer submergence. The torus vertical forces decreased with increase in ΔP or decrease in downcomer submergence or both. ΔP was more effective in reducing the torus vertical forces than the downcomer submergence over the ranges of ΔP and downcomer submergence varied during the test series. The "T" deflector (30 inches full scale) effectively mitigated vent header impact. The four tests which were run at a same test condition show excellent reproducibility and consistency. A comparison of torus load cell and pressure integral data shows that these redundant measurements are in good agreement. The measured peak vent header impact forces were small and the peak force from pressure integral was somewhat lower than the peak force from corrected load cell.

FIGURE A-63

DRYWELL ORIFICE UPSTREAM PRESSURE

TASK 5.5.4 OYSTER CREEK TESTS

TEST 6

TEST 10

*

NEDO-24615

*General Electric Company proprietary information has been deleted.

FIGURE A-64
DRYWELL ORIFICE UPSTREAM PRESSURE

TASK 5.5.4 OYSTER CREEK TESTS

TEST 11

TEST 15

*

*General Electric Company proprietary information has been deleted.

FIGURE A-65

DRYWELL PRESSURE

TASK 5.5.4 OYSTER CREEK TESTS

TEST 6

TEST 10

*

*General Electric Company proprietary information has been deleted.

FIGURE A-66

DRYWELL PRESSURE

TASK 5.5.4 OYSTER CREEK TESTS

TEST 11

TEST 15

*

*General Electric Company proprietary information has been deleted.

FIGURE A-67

DOWNCOMER ORIFICE DIFFERENTIAL PRESSURE

TASK 5.5.4 OYSTER CREEK TESTS

TEST 6

TEST 19

FIGURE A-68

DOWNCOMER ORIFICE DIFFERENTIAL PRESSURE

TASK 5.5.4 OYSTER CREEK TESTS

TEST 11

TEST 15

*

*General Electric Company proprietary information has been deleted.

FIGURE A-69

DOWNCOMER ORIFICE UPSTREAM TEMPERATURE

TASK 5.5.4 OYSTER CREEK TESTS

TEST 6

TEST 10

*

*General Electric Company proprietary information has been deleted.

FIGURE A-70
DOWNCOMER ORIFICE UPSTREAM TEMPERATURE

TASK 5.5.4 OYSTER CREEK TESTS

TEST 11

TEST 15

*

NEDO-24615

*General Electric Company proprietary information has been deleted.

FIGURE A-71

ENTHALPY FLOW INTO POOL

TASK 5.5.4 OYSTER CREEK TESTS

TEST 6

TEST 10

*General Electric Company proprietary information has been deleted.

FIGURE A-72

ENTHALPY FLOW INTO POOL

TASK 5.5.4 OYSTER CREEK TESTS

TEST 11

TEST 15

*

*General Electric Company proprietary information has been deleted.

FIGURE A-73

DOWNCOMER INTERNAL PRESSURE

TASK 5.5.4 OYSTER CREEK TESTS

TEST 6

TEST 10

*

*General Electric Company proprietary information has been deleted.

FIGURE A-74

DOWNCOMER INTERNAL PRESSURE

TASK 5.5.4 OYSTER CREEK TESTS

TEST 11

TEST 15

*

*General Electric Company proprietary information has been deleted.

FIGURE A-75

WETWELL PRESSURES

TASK 5.5.4 OYSTER CREEK TESTS

TEST 6

TEST 10

*General Electric Company proprietary information has been deleted.

FIGURE A-76

WETWELL PRESSURES

TASK 5.5.4 OYSTER CREEK TESTS

TEST 1[illegible]

TEST 15

*General Electric Company proprietary information has been deleted.

TEST 6

TEST 10

*

*General Electric Company proprietary information has been deleted.

FIGURE A-78 NET TORUS FORCE FROM PRESSURE INTEGRAL

TASK 5.5.4 OYSTER CREEK TESTS

TEST 11

TEST 15

*

*General Electric Company proprietary information has been deleted.

FIGURE A-79 TORUS LOAD CELL

TASK 5.5.4 OYSTER CREEK TESTS

TEST 6

TEST 10

NEDO-24615

*General Electric Company proprietary information has been deleted.

FIGURE A-80

TORUS LOAD CELL

TASK 5.5.4 Oyster Creek Tests

TEST 11

TEST 15

*General Electric Company proprietary information has been deleted.

FIGURE A-81

TORUS VERTICAL ACCELERATION

TASK 5.5.4 OYSTER CREEK TESTS

TEST 6

TEST 10

*General Electric Company proprietary information has been deleted.

NEDO-24615

FIGURE A-82

TORUS VERTICAL ACCELERATION
TASK 5.5.4 OYSTER CREEK TESTS

TEST 11

TEST 15

*General Electric Company proprietary information has been deleted.

FIGURE A-83 COMPARISON OF NET TORUS FORCE FROM PRESSURE INTEGRAL WITH NET TORUS FORCE FROM LOAD CELL CORRECTED FOR TORUS INERTIA

TASK 5.5.4 OYSTER CREEK TESTS

TEST 6 TEST 10

*General Electric Company proprietary information has been deleted.

FIGURE A-84

COMPARISON OF NET TORUS FORCE FROM PRESSURE INTEGRAL
WITH NET TORUS FORCE FROM LOAD CELL CORRECTED FOR TORUS INERTIA
TASK 5.5.4 OYSTER CREEK TESTS

TEST 11

TEST 15

*

*General Electric Company proprietary information has been deleted.

FIGURE A-85 NET TORUS FORCE FROM PRESSURE INTEGRAL CORRECTED FOR WATER INERTIA

TASK 5.5.4 OYSTER CREEK TESTS

TEST 6

TEST 10

*General Electric Company proprietary information has been deleted.

NET TORUS FORCE FROM PRESSURE INTEGRAL CORRECTED FOR WATER INERTI

FIGURE A-86

TASK 5.5.4 OYSTER CREEK TESTS

TEST 11

TEST 15

*

*General Electric Company proprietary information has been deleted.

FIGURE A-87 AVERAGE POOL PRESSURE CORRECTED FOR WATER INERTIA

TASK 5.5.4 OYSTER CREEK TESTS

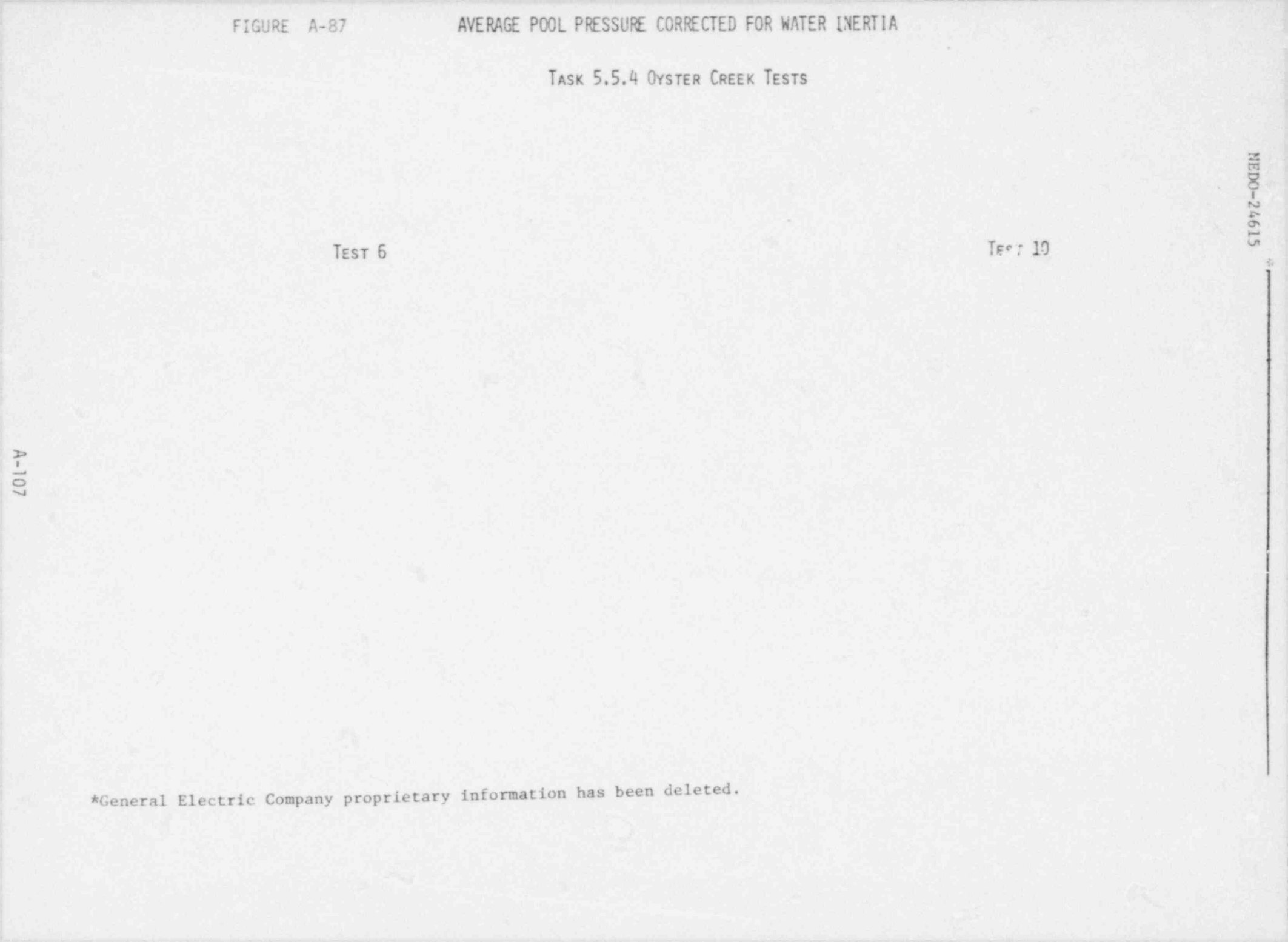

*General Electric Company proprietary information has been deleted.

FIGURE A-88

AVERAGE POOL PRESSURE CORRECTED FOR WATER INERTIA
TASK 5.5.4 OYSTER CREEK TESTS

TEST 11

TEST 15

*General Electric Company proprietary information has been deleted.

FIGURE A-89 NET AVERAGE FUEL PRESSURE CORRECTED FOR WATER HEIGHT

TASK 5.5.4 OYSTER CREEK TESTS

TEST 6

TEST 10

*General Electric Company proprietary information has been deleted.

FIGURE A-90

NET AVERAGE POOL PRESSURE CORRECTED FOR WATER INERTIA

TASK 5.5.4 OYSTER CREEK TESTS

TEST 11

TEST 15

*

*General Electric Company proprietary information has been deleted.

FIGURE A-91

VENT HEADER IMPACT PRESSURES

TASK 5.5.4 OYSTER CREEK TESTS

TEST 6

TEST 10

*General Electric Company proprietary information has been deleted.

FIGURE A-92

VENT HEADER IMPACT PRESSURES

TASK 5.5.4 OYSTER CREEK TESTS

TEST 6

TEST 10

*

*General Electric Company proprietary information has been deleted.

FIGURE A-93

VENT HEADER IMPACT PRESSURES

TASK 5.5.4 OYSTER CREEK TESTS

TEST 6

TEST 10

*

*General Electric Company proprietary information has been deleted.

FIGURE A-94
VENT HEADER IMPACT PRESSURES

TASK 5.5.4 OYSTER CREEK TESTS

TEST 11

TEST 15

*General Electric Company proprietary information has been deleted.

FIGURE A-95
VENT HEADER IMPACT PRESSURES

TASK 5.5.4 OYSTER CREEK TESTS

TEST 11

TEST 15

*General Electric Company proprietary information has been deleted.

FIGURE A-96

VENT HEADER IMPACT PRESSURES

TASK 5.5.4 OYSTER CREEK TESTS

TEST 11

TEST 15

*General Electric Company proprietary information has been deleted.

FIGURE A-97
VENT HEADER IMPACT PRESSURES

TASK 5.5.4 OYSTER CREEK TESTS

TEST 11

TEST 15

*

*General Electric Company proprietary information has been deleted.

FIGURE A-98

COMPARISON OF VENT HEADER IMPACT RESULTS

Task 5.5.4 Oyster Creek Tests

Test 6

Test 10

*

*General Electric Company proprietary information has been deleted.

FIGURE A-99

COMPARISON OF VENT HEADER IMPACT RESULTS

Task 5.5.4 Oyster Creek Tests

Test 11

Test 15

*General Electric Company proprietary information has been deleted.

Figure A-100

TIME HISTORY OF

POOL DISPLACEMENT

Oyster Creek Test 6

*

*General Electric Company proprietary information has been deleted.

Figure A-101

TIME HISTORY OF

POOL DISPLACEMENT

Oyster Creek Test 7

*

*General Electric Company proprietary information has been deleted.

Figure A-102

TIME HISTORY OF
POOL DISPLACEMENT

Oyster Creek Test 8

*

*General Electric Company proprietary information has been deleted.

Figure A-103

TIME HISTORY OF
POOL DISPLACEMENT

Oyster Creek Test 10

*

*General Electric Company proprietary information has been deleted.

Figure A-104

TIME HISTORY OF
POOL DISPLACEMENT

Oyster Creek Test 11

*

*General Electric Company proprietary information has been deleted.

Figure A-105

TIME HISTORY OF

POOL DISPLACEMENT

Oyster Creek Test 13

*

*General Electric Company proprietary information has been deleted.

Figure A-106

TIME HISTORY OF

POOL DISPLACEMENT

Oyster Creek Test 15

*

*General Electric Company proprietary information has been deleted.

POOL SURFACE DISPLACEMENT

Oyster Creek Tests 6, 7, 8, 9
(Combined Data)

*

*General Electric Company proprietary information has been deleted.

Figure A-108

POOL SURFACE VELOCITY PROFILES

Oyster Creek 6, 7, 8, 9
(Combined Data)

POOL SURFACE DISPLACEMENT

Oyster Creek Test 10

*

*General Electric Company proprietary information has been deleted.

Figure A-110

POOL SURFACE VELOCITY PROFILES

Oyster Creek, 10

*

*General Electric Company proprietary information has been deleted.

Figure A-111

POOL SURFACE DISPLACEMENT

Oyster Creek, Tests 11, 13, 14
(Combined Data)

*

*General Electric Company proprietary information has been deleted.

Figure A-112

POOL SURFACE VELOCITY PROFILES

Oyster Creek, 11, 13, 14

(Combined Data)

POOL SURFACE DISPLACEMENT

Oyster Creek, 15

*

*General Electric Company proprietary information has been deleted.

Figure A-114

POOL SURFACE VELOCITY PROFILES

OYSTER CREEK, TEST 15

FIGURE A-115

OYSTER CREEK TEST 9

POOL BOUNDARY DISPLACEMENT AND VELOCITY PROFILES ALONG SIDE WINDOW

*

*General Electric Company proprietary information has been deleted.

Figure A-115

Oyster Creek Test 14

POOL BOUNDARY DISPLACEMENT AND VELOCITY PROFILES ALONG SIDE WINDOW *

*General Electric Company proprietary information has been deleted.

Figure 4-117
Oyster Creek, Test 8

DOWNCOMER WATER SLUG EJECTION

*

*General Electric Company proprietary information has been deleted.

Figure A-118

Oyster Creek, Test 10

DOWNCOMER WATER SLUG EJECTION

*

*General Electric Company proprietary information has been deleted.

Figure A-119

Oyster Creek, Test 13

DOWNCOMER WATER SLUG EJECTION

*

*General Electric Company proprietary information has been deleted.

Figure A-120

Oyster Creek, Test 15

DOWNCOMER WATER SLUG EJECTION

*

*General Electric Company proprietary information has been deleted.

FIGURE A-121

SENSITIVITY OF PEAK DOWNFORCE AND UPFORCE TO DRYWELL/WETWELL ΔP

Tasks 5.5.3-2 and 5.5.4 Oyster Creek Tests

*

*General Electric Company proprietary information has been deleted.

FIGURE A-122

SENSITIVITY OF TORUS DOWNFORCE IMPULSE TO DRYWELL/WETWELL ΔP

Tasks 5.5.3-2 and 5.5.4 Oyster Creek Tests

*

*General Electric Company proprietary information has been deleted.

FIGURE A-123

SENSIVITITY OF TIMES TO PEAK DOWNFORCE AND UPFORCE

TO DRYWELL/WETWELL ΔP

Tasks 5.5.3-2 and 5.5.4 Oyster Creek Tests

*

*General Electric Company proprietary information has been deleted.

DATA FOR WETWELL VERTICAL LOADS

Task 5.5.4 Oyster Creek Tests

*

*General Electric Company proprietary information has been deleted.

TABLE A-7

DATA FOR WETWELL VERTICAL LOADS (Continued)

Task 5.5.4 Oyster Creek Tests

*

*General Electric Company proprietary information has been deleted.

DATA FOR WETWELL VERTICAL LOADS

Task 5.5.4 Oyster Creek Tests

*General Electric Company proprietary information has been deleted.

TABLE A-8

DATA FOR WETWELL VERTICAL LOADS (Continued)

Task 5.5.4 Oyster Creek Tests

*

*General Electric Company proprietary information has been deleted.

TABLE A-9

DATA FOR VENT HEADER IMPACT LOADS

Task 5.5.4 Oyster Creek Tests

*

*General Electric Company proprietary information has been deleted.

TABLE A-10

DATA FOR VENT HEADER IMPACT LOADS

Task 5.5.4 Oyster Creek Tests

*

*General Electric Company proprietary information has been deleted.

A.4 Nine Mile Point Tests

A.4.1 Typical Data

Time-history plots of the driving conditions and pool response are presented in this section for Nine Mile Point Tests 6, 10A, 12, and 15. Test 6 was conducted at a drywell/wetwell differential pressure of 7.94" H_2O ΔP and a downcomer submergence of 14.64 inches. Test 10 was conducted with a zero drywell/wetwell differential pressure and a submergence of 14.64 inches. Test 12 was conducted at a drywell/wetwell differential pressure of 7.94" H_2O ΔP and a submergence of 11.19 inches. Test 15 was conducted with a zero initial drywell/wetwell differential pressure (0" H_2O ΔP) and a submergence of 11.19 inches. All tests were conducted with a 7.35 inch winged deflector (25.61 inches full scale).*

A.4.1.1 Driving Conditions

Driving conditions for Nine Mile Point Tests 6, 10A, 12, and 15 are presented in Figures A-124 through A-133. Driving conditions for the Nine Mile Point tests had the same characteristics as the "typical" plant discussed in Section 3.0.

A.4.1.2 Pool Response

Downcomer internal pressure and wetwell pressures for Nine Mile Point Tests 6, 10A, 12, and 15 are presented in Figures A-134 through A-137. These pressure plots have the same characteristics as the "typical" plant in Section 3.0.

Figures A-138 and A-139 present net torus force based on the torus pressure integral for Nine Mile Point Tests 6, 10A, 12, and 15. The non-zero ΔP runs (Tests 6 and 12) show relatively smooth net torus force, but the zero ΔP runs (Test 10A and 15) have a one-cycle oscillation in downforce.

*A "winged" deflector is a standard pipe with structural angles welded to the sides.

The net torus force which was determined by applying the inertial correction from the torus accelerometer (Figures A-142 and A-143) to the torus load cell (Figures A-140 and A-141) is compared with the net torus force obtained from the torus pressure integral in Figures A-144 and 145. Figures A-145 and A-147 present the net torus force based on the pressure integral corrected for water inertia.

The "average" pool pressures for Nine Mile Point Tests 6, 10A, 12, and 15 are shown in Figures A-148 and A-149. Figures A-150 and A-151 are similar to Figures A-145 and A-146, with force replaced by average pressure (force/torus projected area).

The vent header impact pressures for Nine Mile Point Tests 6, 10A, 12, and 15 are presented in Figures A-152 through A-158. These figures indicate that the deflector was effective in mitigating vent header impact.

Figures A-159 and A-160 present a comparison of the vent header impact force derived from pressure integral with that derived from the corrected load cell.

A.4.2 Pool Dynamics

The pool contours at various times during pool swell are shown in Figures A-161 through A-170 for Nine Mile Point Tests 6, 7, 8, 10A, 11, 12, 13, 15, 16, and 17.

Pool surface displacement curves for Tests 6 through 9 (combined data) are shown in Figure A-171. The pool surface velocities for Tests 6 through 9 (combined data) are shown in Figure A-172. The pool surface displacement curves and pool surface velocity profiles for Test 10A are shown in Figures A-173 and A-174, respectively. Pool surface displacement curves for Tests 11 through 14 (combined data) are shown in Figure A-175.

The pool surface velocities for Tests 11 through 14 (combined data) are shown in Figure A-176. The pool surface displacement curves and pool surface velocity profiles for Tests 15 through 18 (combined data) are shown in Figures A-177 and A-178, respectively.

The pool surface displacement and velocity profile viewed from the side window during Tests 9, 14, and 18 are shown in Figures A-179 through A-181. The downcomer water slug displacement, velocity, and acceleration versus time for Tests 8, 10A, 13, and 17 are presented in Figures A-182 through A-185.

A.4.3 Data Summaries

A.4.3.1 Wetwell Vertical Forces

The Nine Mile Point test data for wetwell vertical forces are presented in Tables A-11 through A-13. Graphical comparison of the data is shown in Figures A-186 through A-188. All parameters in the figures are sensitive to the initial downcomer submergence and ΔP; trends in the data are comparable to those for the "typical plant" in Section 3.0.

A.4.3.2 Vent Header Impact Forces

The Nine Mile Point test data for vent header impact forces are presented in Tables A-14 through A-16. These tests were conducted with a winged deflector installed below the vent header. The 7.35-inch deflector (25.61 inches full scale) was effective in mitigating the vent header impact. Two of the four tests at the same test condition were conducted with the deflector supported from the torus by cables (deflector load transmitted to the torus), while the other two tests were conducted with the deflector bolted onto the vent header (deflector load transmitted to the vent header). These two different attachment methods made it possible to measure the force on the deflector. Results of the deflector load analysis are reported in Appendix I.

A.4.4 Discussion and Analysis

The Nine Mile Point plant unique tests (Task 5.5.3-2) and supplemental tests (Task 5.5.4) were conducted with drywell/wetwell differential pressures of 0" and 7.94" H_2O and with initial downcomer submergences of 11.9 and 14.64 inches. The torus vertical forces (downforce and upforce) were sensitive to both drywell/wetwell ΔP and downcomer submergence. The torus vertical forces decreased with increase in ΔP or decrease in downcomer submergence or both. The winged deflector (25.61 inches full scale) effectively mitigated vent header impact. The four tests which were run at a same test condition generally show excellent reproducibility and consistency. A comparison of load cell data and pressure integral data for torus shows that these redundant measurements are in good agreement. The peak vent header impact force from corrected load cell also agrees reasonably well with the peak force from pressure integral.

FIGURE A-124

DRYWELL ORIFICE UPSTREAM PRESSURE

TASK 5.5.4 NINE MILE POINT TESTS

TEST 6

TEST 10A

*

*General Electric Company proprietary information has been deleted.

FIGURE A-125

DRYWELL ORIFICE UPSTREAM PRESSURE

TASK 5.5.4 NINE MILE POINT TESTS

TEST 12

TEST 15

*

NEDO-24615

*General Electric Company proprietary information has been deleted.

FIGURE A-126
DRYWELL PRESSURE

TASK 5.5.4 NINE MILE POINT TESTS

TEST 6

TEST 10A

*

*General Electric Company proprietary information has been deleted.

FIGURE A-127

DRYWELL PRESSURE

TASK 5.5.4 NINE MILE POINT TESTS

TEST 12

TEST 15

*

*General Electric Company proprietary information has been deleted.

FIGURE A-128

DOWNCOMER ORIFICE DIFFERENTIAL PRESSURE

TASK 5.5.4 NINE MILE POINT TESTS

TEST 6

TEST 10A

*

*General Electric Company proprietary information has been deleted.

FIGURE A-129

DOWNCOMER ORIFICE DIFFERENTIAL PRESSURE

TASK 5.5.4 NINE MILE POINT TESTS

TEST 12

TEST 15

*General Electric Company proprietary information has been deleted.

FIGURE A-130

DOWNCOMER ORIFICE UPSTREAM TEMPERATURE

TASK 5.5.4 NINE MILE POINT TESTS

TEST 6

TEST 10A

*General Electric Company proprietary information has been deleted.

FIGURE A-131

DOWNCOMER ORIFICE UPSTREAM TEMPERATURE

TASK 5.5.4 NINE MILE POINT TESTS

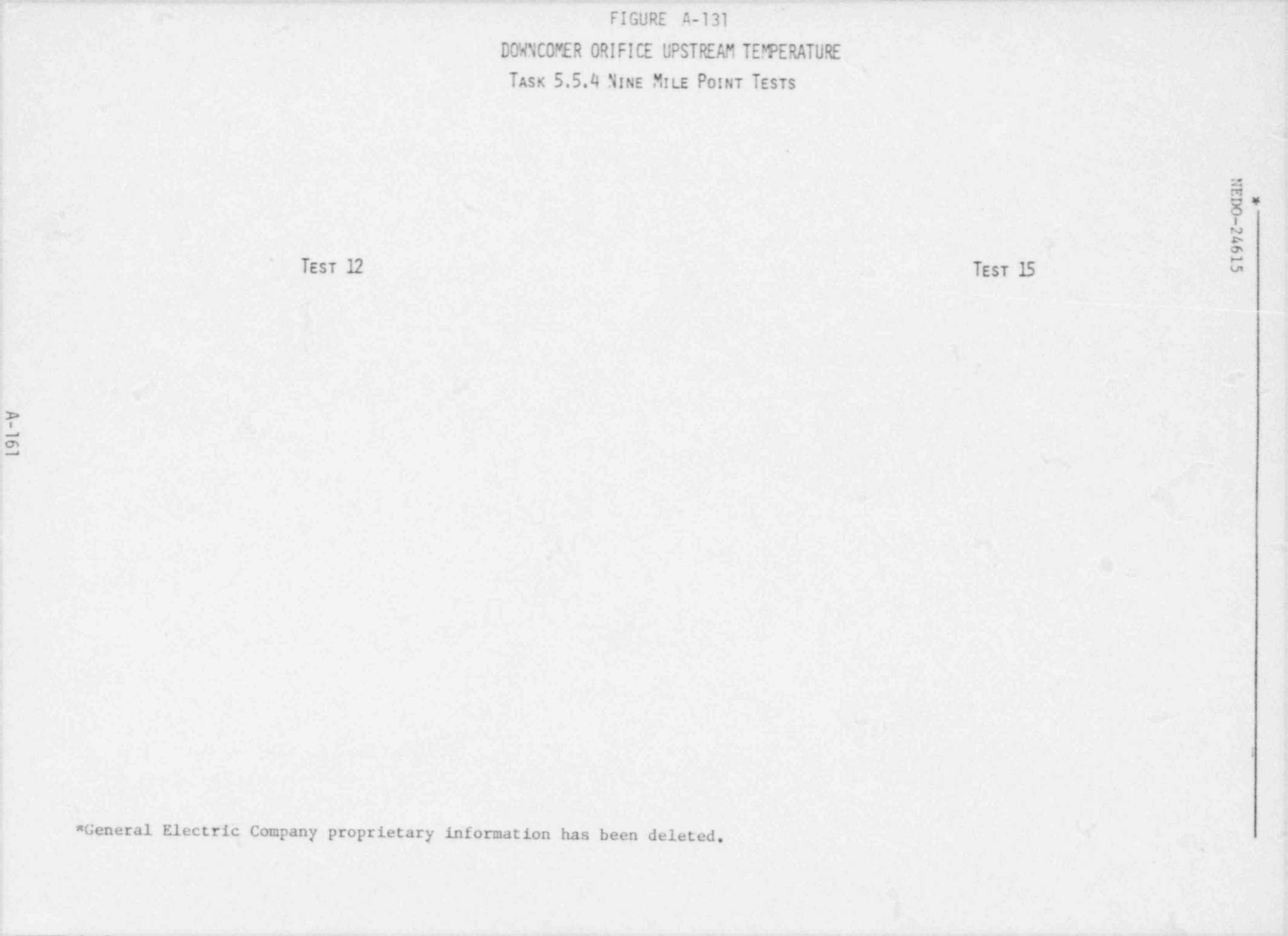

*General Electric Company proprietary information has been deleted.

FIGURE A-132
ENTHALPY FLOW INTO POOL

TASK 5.5.4 NINE MILE POINT TESTS

TEST 6

TEST 10A

*

*General Electric Company proprietary information has been deleted.

FIGURE A-133

ENTHALPY FLOW INTO POOL

TEST 5.5.4 NINE MILE POINT TESTS

TEST 12

TEST 15

*

*General Electric Company proprietary information has been deleted.

FIGURE A-134

DOWNCOMER INTERNAL PRESSURE

TASK 5.5.4 NINE MILE POINT TESTS

TEST 6

TEST 10A

*General Electric Company proprietary information has been deleted.

FIGURE A-135

DOWNCOMER INTERVAL PRESSURE

TASK 5.5.4 NINE MILE POINT TESTS

TEST 12

TEST 15

*General Electric Company proprietary information has been deleted.

FIGURE A-136
WETWELL PRESSURES
TASK 5.5.4 NINE MILE POINT TESTS

TEST 6

TEST 10A

*General Electric Company proprietary information has been deleted.

*

FIGURE A-137

WETWELL PRESSURES

TASK 5.5.4 NINE MILE POINT TESTS

TEST 12

TEST 15

*General Electric Company proprietary information has been deleted.

FIGURE A-138

NET TORUS FORCE FROM PRESSURE INTEGRAL

TASK 5.5.4 NINE MILE POINT TESTS

TEST 6 TEST 19A *

*General Electric Company proprietary information has been deleted.

TASK 5.5.4 NINE MILE POINT TESTS

TEST 12

TEST 15

*General Electric Company proprietary information has been deleted.

FIGURE A-140

TORUS LOAD CELL

TASK 5.5.4 NINE MILE POINT TESTS

TEST 6

TEST 10A

*

*General Electric Company proprietary information has been deleted.

FIGURE 4-141
TORUS LOAD CELL

TASK 5.5.4 NINE MILE POINT TESTS

TEST 12

TEST 15

*General Electric Company proprietary information has been deleted.

FIGURE A-142

TORUS VERTIAL ACCELERATION

TASK 5.5.4 NINE MILE POINT TESTS

TEST 6

TEST 10 A

*

*General Electric Company proprietary information has been deleted.

FIGURE A-143

TORUS VERTICAL ACCELERATION

TASK 5.5.4 NINE MILE POINT TESTS

TEST 12

TEST 15

*

*General Electric Company proprietary information has been deleted.

FIGURE A-144

COMPARISON OF NET TORUS FORCE FROM PRESSURE INTEGRAL
WITH NET TORUS FORCE FROM LOAD CELL CORRECTED FOR TORUS INERTIA
TASK 5.5.4 NINE MILE POINT TESTS

TEST 6

TEST 10A

*

*General Electric Company proprietary information has been deleted.

FIGURE A-145 COMPARISON OF NET TORUS FORCE FROM PRESSURE INTEGRAL WITH NET TORUS FORCE FROM LOAD CELL CORRECTED FOR TORUS INERTIA

TASK 5.5.4 NINE MILE POINT TESTS

TEST 12 TEST 15

*

*General Electric Company proprietary information has been deleted.

FIGURE A-146 NET TORUS FORCE FROM PRESSURE INTEGRAL CORRECTED FOR WATER INERTIA

TASK 5.5.4 NINE MILE POINT TESTS

TEST 6

TEST 10A

*

*General Electric Company proprietary information has been deleted.

FIGURE A-147 NET TORUS FORCE FROM PRESSURE INTEGRAL CORRECTED FOR WATER INERTIA

TASK 5.5.4 NINE MILE POINT TESTS

TEST 12

TEST 15

*

*General Electric Company proprietary information has been deleted.

FIGURE A-148

AVERAGE POOL PRESSURE CORRECTED FOR WATER INERTIA

TASK 5.5.4 NINE MILE POINT TESTS

TEST 6

TEST 10A

*General Electric Company proprietary information has been deleted.

FIGURE A-149

AVERAGE POOL PRESSURE CORRECTED FOR WATER INERTIA

TASK 5.5.4 NINE MILE POINT TESTS

TEST 12

TEST 15

*

NEDO-24615

A-179

*General Electric Company proprietary information has been deleted.

FIGURE A-150

NET AVERAGE POOL PRESSURE CORRECTED FOR WATER INERTIA

TASK 5.5.4 NINE MILE POINT TESTS

TEST 6

TEST 114

*

*General Electric Company proprietary information has been deleted.

FIGURE A-151

NET AVERAGE POOL PRESSURE CORRECTED FOR WATER INERTIA

TASK 5.5.4 NINE MILE POINT TESTS

TEST 12

TEST 15

*General Electric Company proprietary information has been deleted.

FIGURE A-152
VENT HEADER IMPACT PRESSURES

TASK 5.5.4 NINE MILE POINT TESTS

TEST 6 TEST 10A

*General Electric Company proprietary information has been deleted.

FIGURE A-153

VENT HEADER IMPACT PRESSURES

TASK 5.5.4 NINE MILE POINT TESTS

TEST 6

TEST 10A

*

*General Electric Company proprietary information nas been deleted.

FIGURE A-154

VENT HEADER IMPACT PRESSURES

TASK 5.5.4 NINE MILE POINT TESTS

TEST 6

TEST 10A

*General Electric Company proprietary information has been deleted.

FIGURE A-155
VENT HEADER IMPACT PRESSURES

TASK 3.3.4 NINE MILE POINT TESTS

TEST 6 - "Bad Transducer"

TEST 10A

*

*General Electric Company proprietary information has been deleted.

FIGURE A-156

VENT HEADER IMPACT PRESSURES

TASK 5.5.4 NINE MILE POINT TESTS

TEST 12

TEST 15

*General Electric Company proprietary information has been deleted.

FIGURE A-157

VENT HEADER IMPACT PRESSURES

TASK 5.5.4 NINE MILE POINT TESTS

TEST 12

TEST 15

*

FIGURE A-158

VENT HEADER IMPACT PRESSURES

TASK 5.5.4 NINE MILE POINT TESTS

TEST 12

TEST 15

*

*General Electric Company proprietary information has been deleted.

FIGURE A-159

COMPARISON OF VENT HEADER IMPACT RESULTS

Task 5.5.4 Nine Mile Point Tests

Test 6

*

Test 10A

*General Electric Company proprietary information has been deleted.

FIGURE A-160

COMPARISON OF VENT HEADER IMPACT RESULTS

Task 5.5.4 Nine Mile Point Tests

Test 15

*

Test 12

*General Electric Company proprietary information has been deleted.

Figure A-161

TIME HISTORY OF

POOL DISPLACEMENT

NINE MILE POINT TEST 6

*

*General Electric Company proprietary information has been deleted.

Figure A-162

TIME HISTORY OF

POOL DISPLACEMENT

NINE MILE POINT TEST 7

*General Electric Company proprietary information has been deteted.

Figure A-163

TIME HISTORY OF -

POOL DISPLACEMENT

NINE MILE POINT TEST 8

*

*General Electric Company proprietary information has been deleted.

Figure A-164

TIME HISTORY OF

POOL DISPLACEMENT

NINE MILE POINT TEST 10

*

*General Electric Company proprietary information has been deleted.

Figure A-165

TIME HISTORY OF -

POOL DISPLACEMENT

NINE MILE POINT TEST 11

*

*General Electric Company proprietary information has been deleted.

Figure A-166

TIME HISTORY OF

POOL DISPLACEMENT

NINE MILE POINT TEST 12

*General Electric Company proprietary information has been deleted.

Figure A-167

TIME HISTORY OF
POOL DISPLACEMENT

NINE MILE POINT TEST 13

*

*General Electric Company proprietary information has been deleted.

Figure A-168

TIME HISTORY OF
POOL DISPLACEMENT

NINE MILE POINT TEST 15

*General Electric Company proprietary information has been deleted.

Figure A-169

TIME HISTORY OF

POOL DISPLACEMENT

NINE MILE POINT TEST 16

*

*General Electric Company proprietary information has been deleted.

Figure A-170

TIME HISTORY OF

POOL DISPLACEMENT

NINE MILE POINT TEST 17

*General Electric Company proprietary information has been deleted.

POOL SURFACE DISPLACEMENT

(Combined Data)

NINE MILE POINT TESTS 6, 7, 8, 9

*

*General Electric Company proprietary information has been deleted.

FIGURE A-172 POOL SURFACE VELOCITY PROFILES

NINE MILE POINT TESTS 6, 7, 8, 9

(Combined Data)

*

*General Electric Company proprietary information has been deleted.

NINE MILE POINT TEST 10

*

*General Electric Company proprietary information has been deleted.

Figure A-174

POOL SURFACE VELOCITY PROFILES

NINE MILE POINT TEST 10

POOL SURFACE DISPLACEMENT

NINE MILE POINT TESTS 11, 12, 13, 14

(Combined Data)

*

*General Electric Company proprietary information has been deleted.

Figure A-176

POOL SURFACE VELOCITY PROFILES

NINE MILE POINT TESTS 11, 12, 13, 14

(Combined Data)

FIGURE A-177 POOL SURFACE DISPLACEMENT

NINE MILE POINT TESTS 15, 16, 17, 18

(Combined Data)

*

*General Electric Company proprietary information has been deleted.

FIGURE A-178

POOL SURFACE VELOCITY PROFILES

NINE MILE POINT TESTS 15, 16, 17, 18

(Combined Data)

Figure A-179

NINE MILE POINT, TEST 9

POOL BOUNDARY DISPLACEMENT AND VELOCITY PROFILES ALONG SIDE WINDOW

*

*General Electric Company proprietary information has been deleted.

Figure A-180

NINE MILE POINT, TEST 14

POOL BOUNDARY DISPLACEMENT AND VELOCITY PROFILES ALONG SIDE WINDOW *

*General Electric Company proprietary information has been deleted.

Figure A-181

NINE MILE POINT, TEST 18

POOL BOUNDARY DISPLACEMENT AND VELOCITY PROFILES ALONG SIDE WINDOW

*

*General Electric Company proprietary information has been deleted.

Figure A-182

NINE MILE POINT, TEST 8

DOWNCOMER WATER SLUG EJECTION

*

*General Electric Company proprietary information has been deleted.

Figure A-183

DOWNCOMER WATER SLUG EJECTION

NINE MILE POINT, TEST 10

*General Electric Company proprietary information has been deleted.

Figure A-184

NINE MILE POINT, TEST 13

DOWNCOMER WATER SLUG EJECTION

*

*General Electric Company proprietary information has been deleted.

Figure A-185

NINE MILE POINT, TEST 17

DOWNCOMER WATER SLUG EJECTION

*

*General Electric Company proprietary information has been deleted.

FIGURE A-186
SENSITIVITY OF PEAK DOWNFORCE AND UPFORCE TO DRYWELL/WETWELL ΔP

Tasks 5.5.3-2 and 5.5.4 Nine Mile Point Tests

*General Electric Company proprietary information has been deleted.

FIGURE A-187

SENSITIVITY OF TORUS DOWNFORCE IMPULSE TO DRYWELL/WETWELL ΔP

Tasks 5.5.3-2 and 5.5.4 Nine Mile Point Tests

*

*General Electric Company proprietary information has been deleted.

FIGURE A-188

SENSITIVITY OF TIMES TO PEAK DOWNFORCE AND UPFORCE

TO DRYWELL/WETWELL ΔP

Tasks 5.5.3-2 and 5.5.4 Nine Mile Point Tests

*General Electric Company proprietary information has been deleted.

Table A-11

DATA FOR WETWELL VERTICAL LOADS

Task 5.5.4 Nine Mile Point Tests

*

*General Electric Company proprietary information has been deleted.

TABLE A-11

DATA FOR WETWELL VERTICAL LOADS (continued)

Task 5.5.4 Nine Mile Point Tests

*General Electric Company proprietary information has been deleted.

DATA FOR WETWELL VERTICAL LOADS

Task 5.5.4 Nine Mile Point Tests

*

*General Electric Company proprietary information has been deleted.

TABLE A-12

DATA FOR WETWELL VERTICAL LOADS (continued)

Task 5.5.4 Nine Mile Point Tests

*

*General Electric Company proprietary information has been deleted.

DATA FOR WETWELL VERTICAL LOADS

Task 5.5.4 Nine Mile Point Tests

*

*General Electric Company proprietary information has been deleted.

TABLE A-13

DATA FOR WETWELL VERTICAL LOADS (continued)

Task 5.5.4 Nine Mile Point Tests

*

*General Electric Company proprietary information has been deleted.

TABLE A-14

DATA FOR VENT HEADER IMPACT LOADS

Task 5.5.4 Nine Mile Point Tests

*

*General Electric Company proprietary information has been deleted.

TABLE A-15

DATA FOR VENT HEADER IMPACT LOADS

Task 5.5.4 Nine Mile Point Tests

*

*General Electric Company proprietary information has been deleted.

TABLE A-16

DATA FOR VENT HEADER IMPACT LOADS

Task 5.5.4 Nine Mile Point Tests

*

*General Electric Company proprietary information has been deleted.

A.5 Millstone Tests

A.5.1 Typical Data

Time-history plots of the driving conditions and pool response are presented in this section for Millstone Tests 8 and 10. Test 8 was conducted with a drywell/wetwell differential pressure of 7.27" H_2O ΔP and a 6.73-inch winged deflector (25.6 inches full scale).* Test 10 was conducted with a zero initial drywell/wetwell differential pressure (0" H_2O ΔP) and the same 6.73-inch winged deflector. Both tests were performed with a downcomer submergence of 10.50 inches.

A.5.1.1 Driving Conditions

Driving conditions for Millstone Tests 8 and 10 are presented in Figures A-189 through A-193. Driving conditions for the Millstone tests had the same characteristics as the "typical" plant discussed in Section 3.0 of this report.

A.5.1.2 Pool Response

Downcomer internal pressure and wetwell pressures for Millstone Tests 8 and 10 are presented in Figures A-194 and A-195, respectively. These pressure plots have the same characteristics as the "typical" plant in Section 3.0.

Figure A-196 presents net torus force based on the torus pressure integral for Millstone Tests 8 and 10. The downforce in Test 8 indicates some oscillations which dampen out rapidly after the peak downforce. For the zero ΔP test (Test 10), the torus pressure integral shows a pronounced downforce oscillation which is thought to be caused by bubble pressure variations during vent clearing.

The net torus force which was determined by applying the inertial correction from the torus accelerometer (Figure A-198) to the torus load

*A "winged" deflector is a standard pipe with structural angles welded to the sides.

cell (Figure A-197) is compared with the net torus force obtained from torus pressure integral in Figure A-199. Figure A-200 presents the net torus force based on the torus pressure integral corrected for water inertia. Filtering to remove window related oscillations (see Appendix F) significantly smoothed the download for Test 8, but had little effect on the download for Test 10.

The "average" pool pressures for Millstone Tests 8 and 10 are shown in Figure A-201. Figure A-202 is similar to Figure A-200, with force replaced by average pressure (force/torus projected area).

The vent header impact pressures for Millstone Tests 8 and 10 are presented in Figures A-203 through A-206. These figures indicate that the deflector was effective in mitigating vent header impact. Vent header forces for the integration of impact pressures are presented in Appendix B.

A.5.2 Pool Dynamics

The pool contours at various times during pool swell are shown in Figures A-207 through A-210 for Millstone Tests 6, 7, 8, and 10.

Pool surface displacement curves for Tests 6 through 9 (combined data) are shown in Figure A-211. The pool surface velocities for Tests 6 through 9 (combined data) are shown in Figure A-212. The pool surface displacement curves and pool surface velocity profiles for Test 10 are shown in Figures A-213 and A-214, respectively.

The pool surface displacement and velocity profile viewed from the side window during Test 9 are shown in Figure A-215. The downcomer water slug displacement, velocity, and acceleration versus time for Tests 8 and 10 are presented in Figures A-216 and A-217, respectively.

A.5.3 Data Summaries

A.5.3.1 Wetwell Vertical Forces

Table A-17 presents the Millstone test data for wetwell vertical forces. Graphical comparison of the data is shown in Figures A-218 through A-220.

All parameters in these figures are sensitive to drywell/wetwell ΔP; trends in the data are comparable to those for the "typical" plant in Section 3.0.

A.5.3.2 Vent Header Impact Forces

Table A-18 presents the Millstone test data for vent header impact forces. These tests were conducted with a winged deflector installed below the vent header. The 6.73-inch deflector (25.6 inches full scale) was effective in mitigating the vent header impact. Two of the four tests at the same test condition were conducted with the deflector supported from the torus by cables (deflector load transmitted to the torus), while the other two tests were conducted with the deflector bolted onto the vent header (deflector load transmitted to the vent header). These two different attachment methods made it possible to measure force on the deflector. Results of the deflector load analysis are reported in Appendix I.

A.5.4 Discussion and Analysis

The Millstone plant unique tests (Task 5.5.3-2) and supplemental tests (Tasks 5.5.4) were conducted with drywell/wetwell differential pressures of 0", 7.27", and 8.73" H_2O and with an initial downcomer submergence of 10.50 inches. The torus vertical forces (downforce and upforce) were sensitive to drywell/wetwell ΔP and decreased with increase in ΔP. The winged deflector (25.3 inches full scale) effectively mitigated vent header impact. The four tests which were run at the same test condition show reasonably good reproducibility and consistency. A comparison of torus load cell and pressure integral data shows that these redundant measurements are in good agreement.

FIGURE A-189

DRYWELL ORIFICE UPSTREAM PRESSURE

TASK 5.5.4 MILLSTONE TESTS

TEST 8

TEST 10

*General Electric Company proprietary information has been deleted.

FIGURE A-190

DRYWELL PRESSURE

TASK 5.5.4 MILLSTONE TESTS

TEST 8

TEST 10

*

NEDO-24615

A-232

*General Electric Company proprietary information has been deleted.

FIGURE A-191

DOWNCOMER ORIFICE DIFFERENTIAL PRESSURE

TASK 5.5.4 MILLSTONE TESTS

TEST 8

TEST 10

*

*General Electric Company proprietary information has been deleted.

FIGURE 4-192

DOWNCOMER ORIFICE UPSTREAM TEMPERATURE

TASK 5.5.4 MILLSTONE TESTS

TEST 8

TEST 10

*

NEDO-24615

A-234

*General Electric Company proprietary information has been deleted.

FIGURE A-193

ENTHALPY FLOW INTO POOL

TASK 5.5.4 MILLSTONE TESTS

TEST 8

TEST 10

*

*General Electric Company proprietary information has been deleted.

FIGURE A-194

DOWNCOMER INTERNAL PRESSURE

TASK 5.5.4 MILLSTONE TESTS

TEST 8

TEST 10

*

*General Electric Company proprietary information has been deleted.

WETWELL PRESSURES

TASK 5.5.4 MILLSTONE TESTS

TEST 8

TEST 10

*

*General Electric Company proprietary information has been deleted.

FIGURE A-196 NET TORUS FORCE FROM PRESSURE INTEGRAL

TASK 5.5.4 MILLSTONE TESTS

TEST 8

TEST 10

*

*General Electric Company proprietary information has been deleted.

FIGURE A-197

TORUS LOAD CELL

TASK 5.5.4 MILLSTONE TESTS

TEST 8

TEST 10

*General Electric Company proprietary information has been deleted.

FIGURE A-198

TORUS VERTICAL ACCELERATION

TASK 5.5.4 MILLSTONE TESTS

TEST 8

TEST 10

*General Electric Company proprietary information has been deleted.

COMPARISON OF NET TORUS FORCE WITH PRESSURE INTERNAL

WITH NET TORUS FORCE FROM LOAD CELL CORRECTED FOR TOURS INERTIA

TASK 5.5.4 MILLSTONE TESTS

TEST 8

TEST 10

*General Electric Company proprietary information has been deleted.

FIGURE A-200

NET TORUS FORCE FROM PRESSURE INTEGRAL

CORRECTED FOR WATER INERTIA

TASK 3.3.4 MILLSTONE TESTS

TEST 8

TEST 10

AVERAGE POOL PRESSURE CORRECTED FOR WATER INERTIA

TASK 5.5.4 MILLSTONE TESTS

TEST 8

TEST 10

*

*General Electric Company proprietary information has been deleted.

FIGURE A-202

NET AVERAGE POOL PRESSURE CORRECTED FOR WATER INERTIA

TASK 5.5.4 MILLSTONE TESTS

TEST 8

TEST 10

*General Electric Company proprietary information has been deleted.

FIGURE A-203

VENT HEADER IMPACT PRESSURES

TASK 5.5.4 MILLSTONE TESTS

TEST 8

TEST 10 *

*General Electric Company proprietary information has been deleted.

FIGURE A-204

VENT HEADER IMPACT PRESSURES

TASK 5.5.4 MILLSTONE TESTS

TEST 9

TEST 10

*General Electric Company proprietary information has been deleted.

FIGURE A-205

VENT HEADER IMPACT PRESSURES

TASK 5.5.4 MILLSTONE TESTS

TEST 8

TEST 10

*

*General Electric Company proprietary information has been deleted.

FIGURE A-206

VENT HEADER IMPACT PRESSURES

TASK 5.5.4 Millstone Tests

TEST 8

TEST 19

*General Electric Company proprietary information has been deleted.

TIME HISTORY OF
POOL DISPLACEMENT

MILLSTONE, TEST 6

*

*General Electric Company proprietary information has been deleted.

FIGURE A-208

TIME HISTORY OF

POOL DISPLACEMENT

Millstone, Test 7

*General Electric Company proprietary information has been deleted.

FIGURE A-209

TIME HISTORY OF

POOL DISPLACEMENT

MILLSTONE, TEST 8

*

*General Electric Company proprietary information has been deleted.

FIGURE A-210
TIME HISTORY OF

POOL DISPLACEMENT

MILLSTONE, TEST 10

*General Electric Company proprietary information has been deleted.

POOL SURFACE DISPLACEMENT

MILLSTONE TESTS 6, 7, 8, 9

(Combined Data)

*

*General Electric Company proprietary information has been deleted.

FIGURE A-212

POOL SURFACE VELOCITY PROFILES

MILLSTONE, TEST 6, 7, 8, 9

(Combined Data)

*General Electric Company proprietary information has been deleted.

FIGURE A-213 POOL SURFACE DISPLACEMENT

MILLSTONE, TEST 10

*

*General Electric Company proprietary information has been deleted.

FIGURE A-214 POOL SURFACE VELOCITY PROFILES

MILLSTONE, TEST 10

*

*General Electric Company proprietary information has been deleted.

FIGURE A-215

Millstone, Test 9

POOL BOUNDARY DISPLACEMENT AND VELOCITY PROFILES ALONG SIDE WINDOW *

*General Electric Company proprietary information has been deleted.

FIGURE A-216

DOWNCOMER WATER SLUG EJECTION
MILLSTONE, TEST 8

*

*General Electric Company proprietary information has been deleted.

FIGURE A-217

DOWNCOMER WATER SLUG EJECTION
MILLSTONE, TEST 10

*

*General Electric Company proprietary information has been deleted.

FIGURE A-218

SENSITIVITY OF DOWNFORCE AND UPFORCE TO DRYWELL/WETWELL ΔP

Tasks 5.5.3-2 and 5.5.4 Millstone Tests

*General Electric Company proprietary information has been deleted.

FIGURE A-219

SENSITIVITY OF TORUS DOWNFORCE IMPULSE TO DRYWELL/WETWELL

Tasks 5.5.3-2 and 5.5.4 Millstone Tests

*

*General Electric Company proprietary information has been deleted.

FIGURE A-220

SENSITIVITY OF TIMES TO PEAK DOWNFORCE AND UPFORCE

TO DRYWELL/WETWELL ΔP

Tasks 5.5.3-2 and 5.5.4 Millstone Tests

*General Electric Company proprietary information has been deleted.

TABLE A-17

DATA FOR WETWELL VERTICAL LOADS

Task 5.5.4 Millstone Tests

*

*General Electric Company proprietary information has been deleted.

TABLE A-17
DATA FOR WETWELL VERTICAL LOADS (continued)

Task 5.5.4 Millstone Tests

*General Electric Company proprietary information has been deleted.

TABLE A-18

DATA FOR VENT HEADER IMPACT LOADS

Task 5.5.4 Millstone Tests

*

*General Electric Company proprietary information has been deleted.

A.6 Cooper Station Tests

A.6.1 Typical Data

Time-history plots of the driving conditions and pool response are presented in this section for Cooper Station Tests 7 and 11. Test 7 was conducted with a drywell/wetwell differential pressure of 7.46" H_2O ΔP and a 6.82-inch winged deflector (25.3 inches full scale).* Test 11 was conducted with a zero initial drywell/wetwell differential pressure (0" H_2O ΔP) and with the same 6.82-inch winged deflector. Both tests were performed with a downcomer submergence of 10.78 inches.

A.6.1.1 Driving Conditions

Driving conditions for Cooper Station Tests 7 and 11 are presented in Figures A-221 through A-225. Driving conditions for the Cooper Station tests had the same characteristics as the "typical" plant discussed in Section 3.0 of this report.

A.6.1.2 Pool Response

Downcomer internal pressure and wetwell pressures are presented in Figures A-226 and A-227, respectively. These plots have the same characteristics as the "typical" plant in Section 3.0.

Figure A-228 presents net torus force based on the torus pressure integral for Cooper Station Tests 7 and 11. Some downforce oscillations are present, but they dampen out rapidly. There are no upforce oscillations.

The net torus force which was determined by applying the inertial correction from the torus accelerometer (Figure A-230) to the torus load cell (Figure A-229) is compared with the net torus force obtained from the torus pressure integral in Figure A-231. Figure A-232 presents the net torus force based on the torus pressure integral corrected for water inertia. Filtering to remove window related oscillations (see Appendix F) significantly smoothed the download for Test 7.

*A "winged" deflector is a standard pipe with structural angles welded to the sides.

The "average" pool pressures for Cooper Station Tests 7 and 11 are shown in Figure A-233. Figure A-234 is similar to Figure A-232, with force replaced by average pressure (force/torus projected area).

The vent header impact pressures for Cooper Station Tests 7 and 11 are presented in Figures A-235 through A-237. These figures indicate that the deflector was effective in mitigating vent header impact. Vent header forces from the integration of impact pressures are presented in Appendix B.

A.6.2 Pool Dynamics

The pool contours at various times of pool swell are shown in Figures A-238 through A-243 for Cooper Station Tests 6, 7, 8, 10, 11, and 12.

Pool surface displacement curves for Tests 6 through 9 (combined data) are shown in Figure A-244. The pool surface velocities for Tests 6 through 9 (combined data) are shown in Figure A-2.45 The pool surface displacement curves and pool surface velocity profiles for Tests 10 through 13 (combined data) are shown in Figures A-246 and A-247, respectively.

The pool surface displacement and velocity profile viewed from the side window during Tests 9 and 13 are shown in Figures A-248 and A-249, respectively. The downcomer water slug displacement, velocity, and acceleration versus time for Tests 8 and 12 are presented in Figures A-250 and A-251.

A.6.3 Data Summaries

A.6.3.1 Wetwell Vertical Forces

Tables A-19 and A-20 present the Cooper Station test data for wetwell vertical forces. Graphical comparison of the data is shown in Figures A-252 through A-254. All parameters (with the exception of time to peak downforce) in the figures are sensitive to the initial downcomer submer-

gence and ΔP; trends in the data are comparable to those for the "typical" plant in Section 3.0.

A.6.3.2 Vent Header Impact Forces

Tables A-21 and A-22 present the Cooper Station test data for vent header impact forces. These tests were conducted with a winged deflector installed below the vent header. The 6.82-inch deflector (25.3 inches full scale) was effective in mitigating the vent header impact. Two of the four tests at the same test condition were conducted with the deflector supported from the torus by cables (deflector load transmitted to the torus), while the other two tests were conducted with the deflector bolted onto the vent header (deflector load transmitted to the vent header). These two different attachment methods made it possible to measure the force on the deflector. Results of the deflector load analysis are reported in Appendix I.

A.6.4 Discussion and Analysis

The Cooper Station plant unique tests (Task 5.5.3-2) and supplemental tests (Task 5.5.4) were conducted at drywell/wetwell differential pressures of 0" and 7.46" H_2O and with initial downcomer submergences of 10.78 and 14.15 inches. The torus vertical forces (downforce and upforce) were sensitive to both drywell/wetwell ΔP and downcomer submergence. The torus vertical forces decreased with increase in ΔP or decrease in downcomer submergence or both. The winged deflector (25.3 inches full scale) effectively mitigated vent header impact. The four tests which were run at a same test condition show reasonably good reproducibility and consistency. A comparison of load cell data and pressure integral data for torus shows that these redundant measurements are in good agreement.

FIGURE A-221

DRYWELL ORIFICE UPSTREAM PRESSURE

TASK 5.5.4 COOPER STATION TESTS

TEST 7

TEST 11

*

*General Electric Company proprietary information has been deleted.

FIGURE A-222

DRYWELL PRESSURE

TASK 5.5.4 COOPER STATION TESTS

TEST 7

TEST 11

*

*General Electric Company proprietary information has been deleted.

FIGURE A-223

DOWNCOMER ORIFICE DIFFERENTIAL PRESSURE

TASK 5.5.4 COOPER STATION TESTS

TEST 7

TEST 11

*

*General Electric Company proprietary information has been deleted.

FIGURE A-224

DOWNCOMER ORIFICE UPSTREAM TEMPERATURE

TASK 5.5.4 COOPER STATION TESTS

TEST 7

TEST 11

*

*General Electric Company proprietary information has been deleted.

FIGURE A-225

ENTHALPY FLOW INTO POOL

TASK 5.5.4 COOPER STATION TESTS

TEST 7

TEST 11

*

*General Electric Company proprietary information has been deleted.

FIGURE A-226

DOWNCOMER INTERNAL PRESSURE

TASK 5.5.4 COOPER STATION TESTS

TEST 8A*

TEST 12A*

*

*General Electric Company proprietary information has been deleted.

FIGURE A-227

WETWELL PRESSURES

TASK 5.5.4 COOPER STATION TESTS

TEST 7

TEST 11

*

*General Electric Company proprietary information has been deleted.

FIGURE A-223

NET TORUS FORCE FROM PRESSURE INTEGRAL

TASK 5.5.4 COOPER STATION TESTS

TEST 7

TEST 11

FIGURE A-229

TORUS LOAD CELLS

TASK 5.5.4 COOPER STATION TESTS

TEST 7

TEST 11

*

*General Electric Company proprietary information has been deleted.

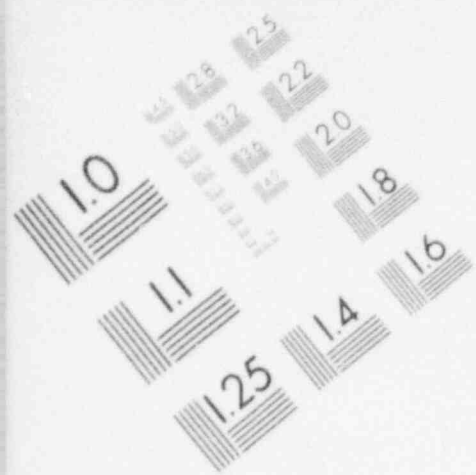

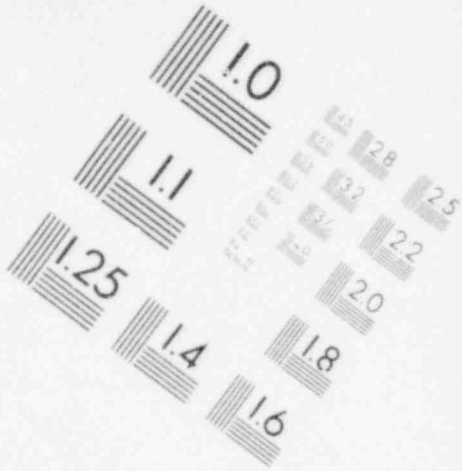

IMAGE EVALUATION
TEST TARGET (MT-3)

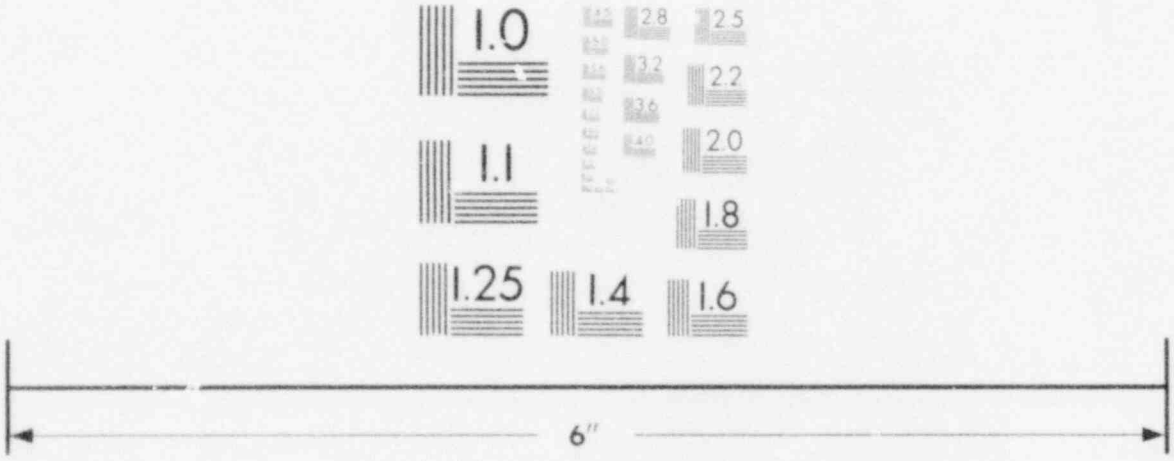

MICROCOPY RESOLUTION TEST CHART

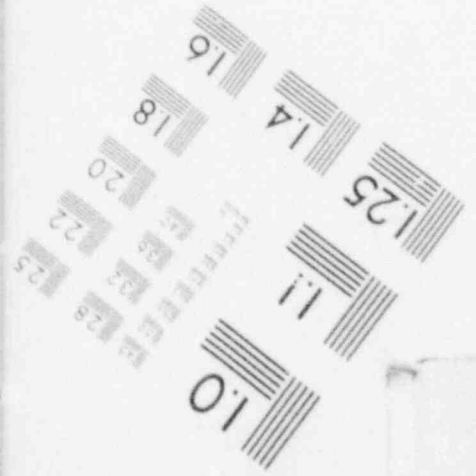

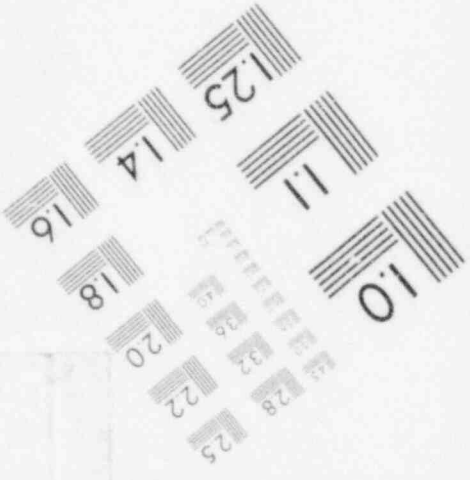

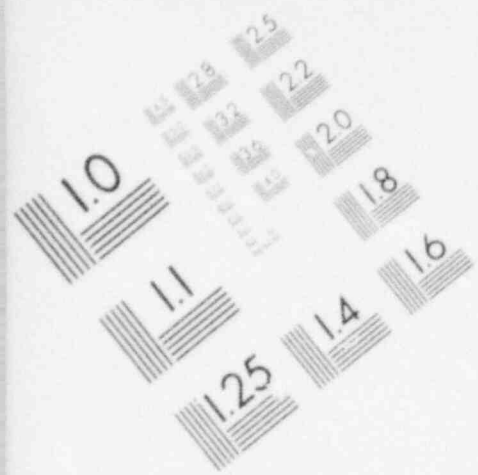

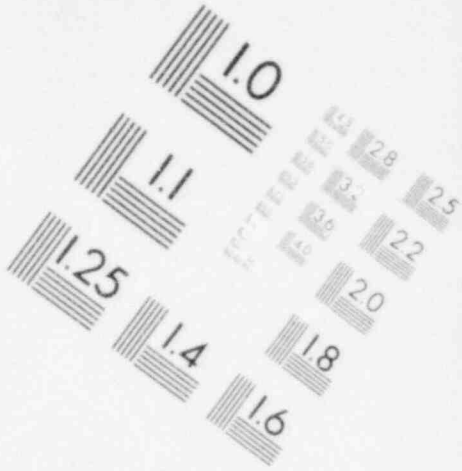

IMAGE EVALUATION
TEST TARGET (MT-3)

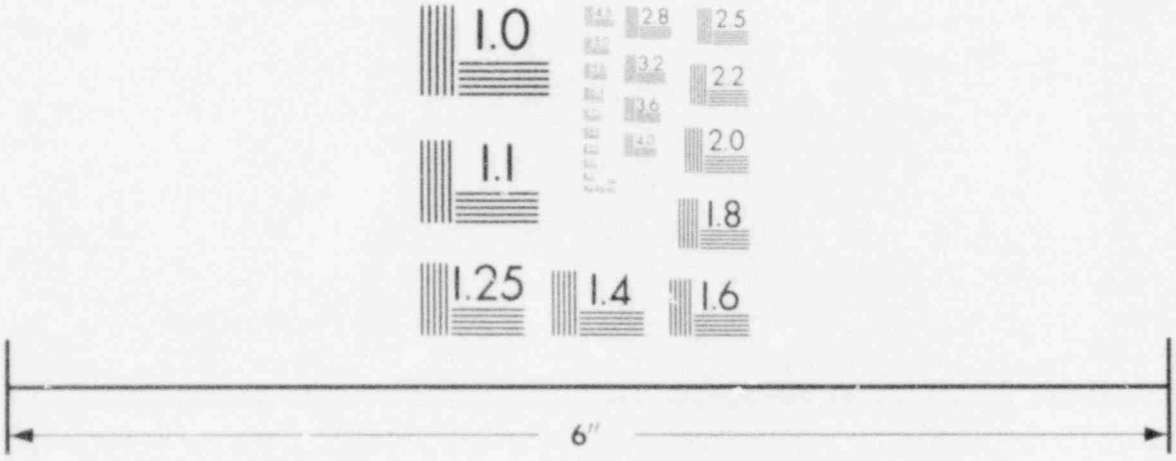

MICROCOPY RESOLUTION TEST CHART

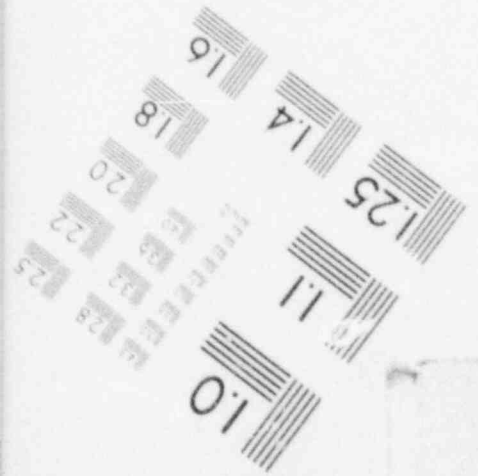

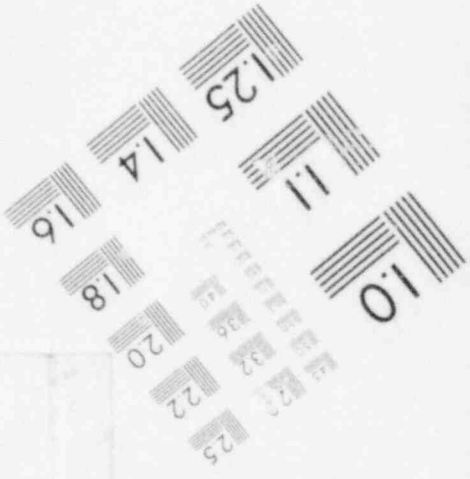

FIGURE A-230

TORUS VERTICAL ACCELERATION

TASK 5.5.4 COOPER STATION TESTS

TEST 7

TEST 11

*General Electric Company proprietary information has been deleted.

COMPARISON OF NET TORUS FORCE FROM PRESSURE INTEGRAL

WITH NET TORUS FORCE FROM LOAD CELL CORRECTED FOR TORUS INERTIA

TEST 7 TASK 5.5.4 COOPER STATION TESTS TEST 11

*General Electric Company proprietary information has been deleted.

FIGURE A-232

NET TORUS FORCE FROM PRESSURE INTEGRAL CORRECTED FOR WATER INERTIA

TASK 5.5.4 COOPER STATION TESTS

TEST 7

TEST 11

*

*General Electric Company proprietary information has been deleted.

FIGURE A-233

AVERAGE POOL PRESSURE CORRECTED FOR WATER INERTIA

TASK 5.5.4 COOPER STATION TESTS

*General Electric Company proprietary information has been deleted.

FIGURE A-234

NET AVERAGE POOL PRESSURE CORRECTED FOR WATER INERTIA

TEST 7 TASK 5.5.4 COOPER STATION TESTS TEST 11

*

NEDO-24615

A-282

*General Electric Company proprietary information has been deleted.

FIGURE A-235

VENT HEADER IMPACT PRESSURES

TASK 5.5.4 COOPER STATION TESTS

TEST 7

TEST 11

*

*General Electric Company proprietary information has been deleted.

FIGURE A-236

VENT HEADER IMPACT PRESSURES

TASK 5.5.4 COOPER STATION TESTS

TEST 7 TEST 11

*General Electric Company proprietary information has been deleted.

FIGURE A-237

VENT HEADER IMPACT PRESSURES

TASK 5.5.4 COOPER STATION TESTS

TEST 7

TEST 11

*

neral Electric Company proprietary information has been deleted.

TIME HISTORY OF

POOL DISPLACEMENT

Cooper Station, Test 6

*General Electric Company proprietary information has been deleted.

TIME HISTORY OF

POOL DISPLACEMENT

Cooper Station Test 7

*

*General Electric Company proprietary information has been deleted.

TIME HISTORY OF

POOL DISPLACEMENT

Cooper Station Test 8

*General Electric Company proprietary information has been deleted.

FIGURE A-241

TIME HISTORY OF

POOL DISPLACEMENT

Cooper Station Test 10

*

eneral Electric Company proprietary information has been deleted.

TIME HISTORY OF

POOL DISPLACEMENT

Cooper Station Test 11

*General Electric Company proprietary information has been deleted.

FIGURE A-243

TIME HISTORY OF

POOL DISPLACEMENT

Cooper Station Test 12

*

*General Electric Company proprietary information has been deleted.

FIGURE A-244 POOL SURFACE DISPLACEMENT

Cooper Station Tests 6, 7, 8, 9

(Combined Data)

*

NEDE-24615

*General Electric Company proprietary information has been deleted.

FIGURE A-245 POOL SURFACE VELOCITY PROFILES

Cooper Station Tests 6, 7, 8, 9

(Combined Data)

*General Electric Company proprietary information has been deleted.

FIGURE A-246

POOL SURFACE DISPLACEMENT

Cooper Station Tests 10, 11, 12, 13

(Combined Data)

*

*General Electric Company proprietary information has been deleted.

FIGURE A-247 POOL SURFACE VELOCITY PROFILES

Cooper Station Tests 10, 11, 12, 13

(Combined Data)

*General Electric Company proprietary information has been deleted.

FIGURE A-248

COOPER STATION, TEST 9

POOL BOUNDARY DISPLACEMENT AND VELOCITY PROFILES ALONG SIDE WINDOW

*

*General Electric Company proprietary information has been deleted.

COOPER STATION, TEST 13

FIGURE A-249

POOL BOUNDARY DISPLACEMENT AND VELOCITY PROFILES ALONG SIDE WINDOW *

*General Electric Company proprietary information has been deleted.

FIGURE A-250

DOWNCOMER WATER SLUG EJECTION Cooper Station, Test 8

*

*General Electric Company proprietary information has been deleted.

FIGURE A-251

DOWNCOMER WATER SLUG EJECTION Cooper Station, Test 12

*

*General Electric Company proprietary information has been deleted.

FIGURE A-252

SENSITIVITY OF PEAK DOWNFORCE AND UPFORCE TO DRYWELL/WETWELL ΔP

Task 5.5.3-2 & 5.5.4 Cooper Station Tests

*General Electric Company proprietary information has been deleted.

FIGURE A-253

SENSITIVITY OF TORUS DOWNFORCE IMPULSE TO DRYWELL/WETWELL ΔP

Task 5.5.3-2 & 5.5.4 Cooper Station Tests

*

*General Electric Company proprietary information has been deleted.

FIGURE A-254

SENSITIVITY OF TIMES TO PEAK DOWNFORCE AND UPFORCE TO DRYWELL/WETWELL ΔP

Task 5.5.3-2 & 5.5.4 Cooper Station Tests

*

*General Electric Company proprietary information has been deleted.

TABLE A-19

DATA FOR WETWELL VERTICAL LOADS

Task 5.5.4 Cooper Station Tests

*

*General Electric Company proprietary information has been deleted.

TABLE A-19

DATA FOR WETWELL VERTICAL LOADS (continued)

Task 5.5.4 Cooper Station Tests

*

*General Electric Company proprietary information has been deleted.

TABLE A-20

DATA FOR WETWELL VERTICAL LOADS

Task 5.5.4 Cooper Station Tests

*

*General Electric Company proprietary information has been deleted.

TABLE A-20

DATA FOR WETWELL VERTICAL LOADS (continued)

Task 5.5.4 Cooper Station Tests

*General Electric Company proprietary information has been deleted.

TABLE A-21

DATA FOR VENT HEADER IMPACT LOADS

Task 5.5.4 Cooper Station Tests

*

*General Electric Company proprietary information has been deleted.

TABLE A-22

DATA FOR VENT HEADER IMPACT LOADS

Task 5.5.4 Cooper Station Tests

*

*General Electric Company proprietary information has been deleted.

APPENDIX B

VENT HEADER PRESSURE INTEGRATION

B.1 Impact Symmetry

The vent header impact force was determined from an area integration of local pressures measured by pressure transducers on the bottom of the vent header. During the Generic Sensitivity Tests (conducted during February and March 1978), several different vent header transducer patterns were utilized in order to investigate the symmetry of vent header impact pressures. The test results indicated that pool water impacted the vent header symmetrically (Reference 1). Because of this vent header symmetry, pressure transducers were placed in only one quadrant for the remaining tests.

B.2 Typical Data

Time-history plots of the vent header impact pressures for Monticello Tests 18 and 22 are presented in Section 3.1. Similarly, typical time-history plots of the vent header impact pressures for Duane Arnold, Pilgrim, Oyster Creek, Nine Mile Point, Millstone, and Cooper Station tests are presented in Appendix A.

B.3 Pressure Integral Calculation

The vent header impact force was obtained from two different sources during this test series: a load cell with acceleration and thrust corrections* and an area integration of pressures measured by transducers on the bottom of the vent header. This section describes the procedure and results of the pressure integration method.

---

*See Appendix H.

B.3.1 Test Hardware Description

The vent headers used for plant unique testing were specially constructed to closely match individual utility design input. Each vent header had provision made for approximately 18 pressure transducer locations on a bottom quadrant. The layout of a typical transducer pattern is shown in Figure B-1. Not all locations were used in a single test, due to transducer and recording channel limitations. The basic pressure map was created in one quadrant from 12 or 13 measurements extending out to 60° from bottom dead center. (For some tests the thirteenth transducer was placed on one downcomer bend.)

The test matrix included 56 tests. Thirteen transducers (T1 through T13) were used in all runs. The measurement locations were varied slightly for each of the plants tested (based on the deflector geometry) to obtain a good impact pressure distribution pattern.

Two types of pressure transducers were used, Kulite Model CQ-140-100A and Bell & Howell Model 4-312-0001, both 0-100 psia. Mounting configurations for each are shown in Figure B-2.

B.3.2 Data Reduction

Twelve or thirteen pressure locations are insufficient to produce a smooth area integral in time. Therefore, an interpolation scheme was used to create pressure histories at intermediate locations. Figure B-3 and Table B-1 illustrate the nodal scheme used. Measurements are made at numbered stations and interpolated histories are created for areas A through MM. The impact load at a given time is formed by summing the product of the pressure for that time at a given node (either a measured or interpolated function) and its corresponding area. The area used is the projection of the nodal area on the horizontal plane in order to calculate the vertical

force component. A more detailed description of the interpolation technique can be found in Reference B-1.

Each measured pressure history is approximated by 5 line segments defined by 6 points. An example of this approximation is shown in Figure B-4. The 6 defining points for each measurement are the input data for the integration computer program. A complete tabulation of the 6-point input data from this program is included.

B.3.3 Results and Discussion

Table B-2 presents typical input data and Table B-3 lists the 6-point approximations used for the integration program for all runs. Figures B-5 through B-56 show the pressure integral results for the Supplemental Plant Unique Tests (time shown is the test run time and not corrected for T_o). Duane Arnold results are not presented because the vent header impact loads were negligibly small.

B.4 Comparison of Pressure Integral and Load Cell

The vent header impact force was obtained from two sources during this test series: a load cell and an area integration of pressure measured by transducers on the vent header. The time-history plots of vent header force determined from the inertia- and thrust-corrected vent header load cell and the pressure integration are compared in Section 3.1.2 for typical Monticello test runs and in Appendix A for other plants. In general, these figures indicate reasonably good agreement between the two methods at peak vent header impact force.

B.5 References

B-1, W. Kennedy et al, "Rigid and Flexible Vent Header Testing in the Quarter-Scale Test Facility Mark I Containment Program, Task 5.3.3," Acurex Corporation, NEDE-24520-P, Class III, March 1978.

TYPICAL VENT HEADER INSTRUMENTATION LOCATIONS

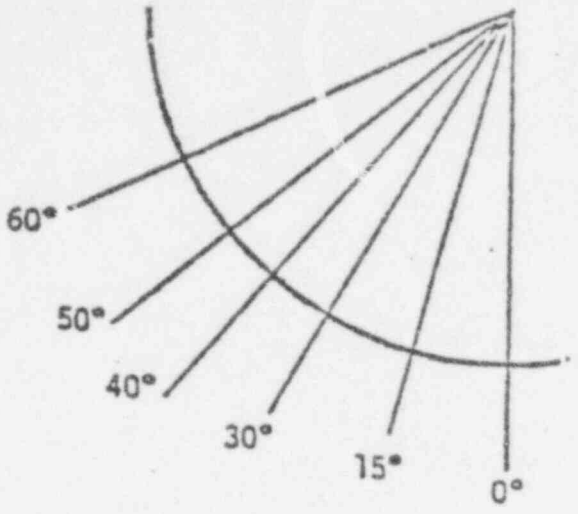

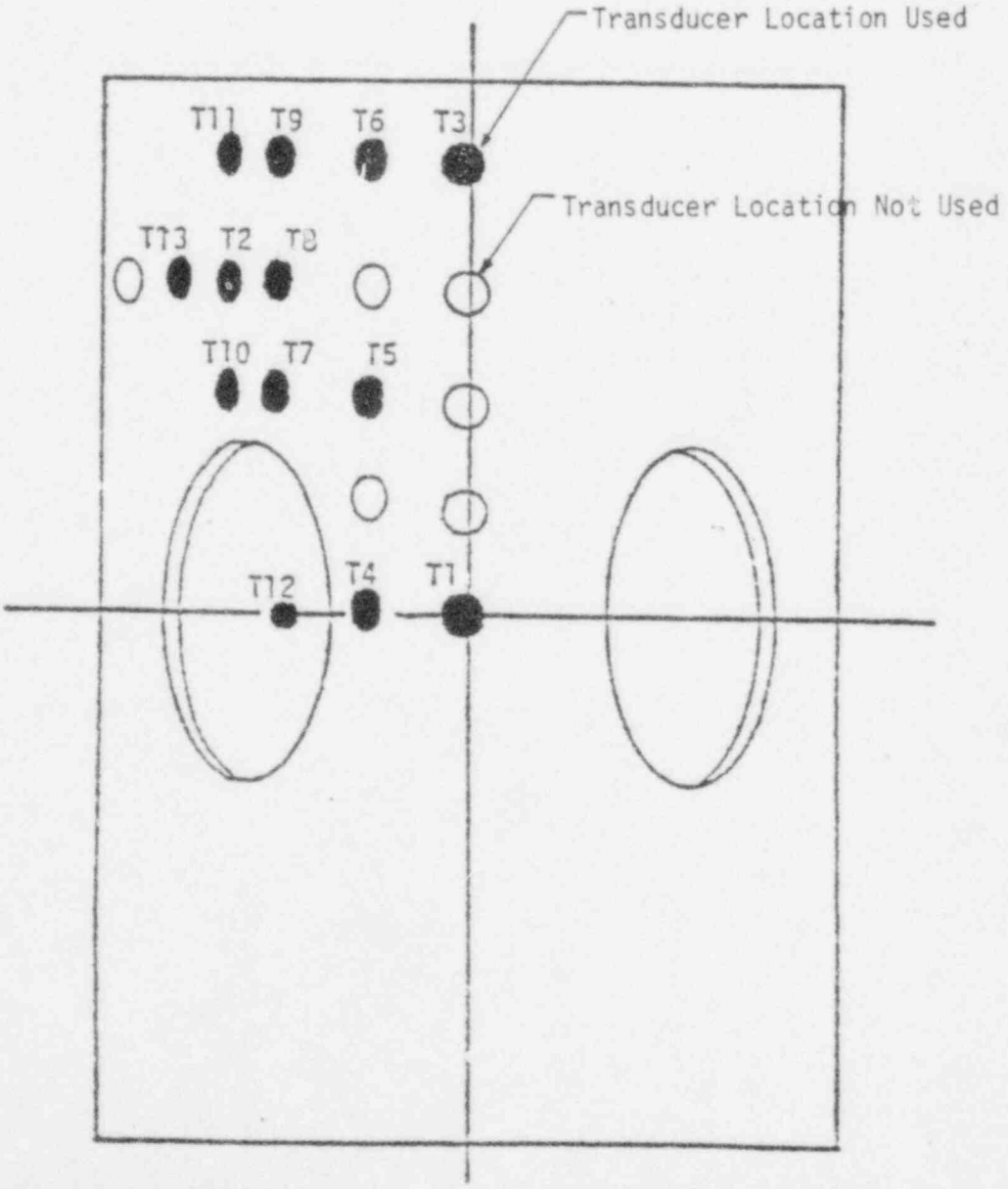

FIGURE B-2

VENT HEADER TRANSDUCER MOUNT DETAILS

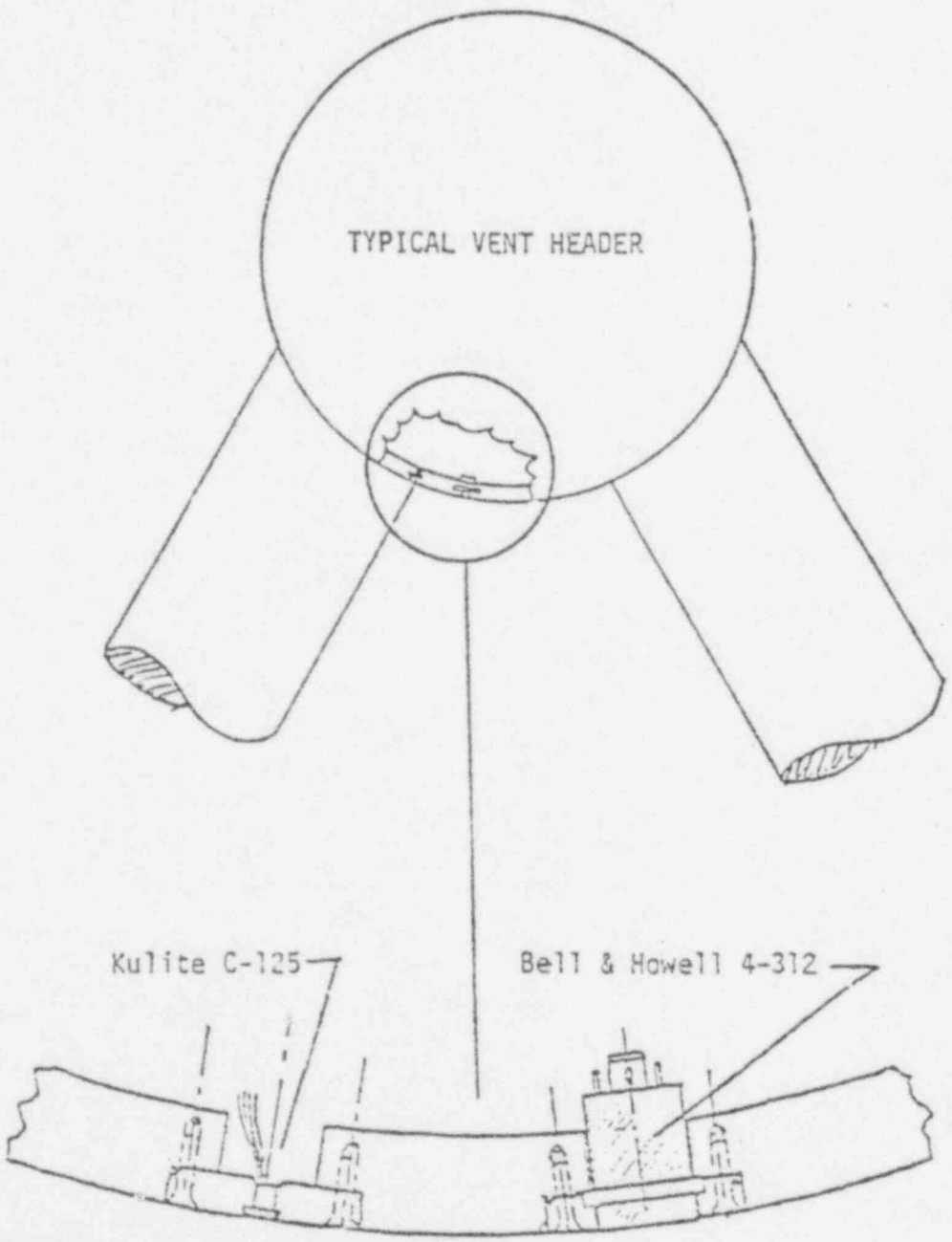

FIGURE B-3

TYPICAL PRESSURE INTEGRAL NODAL SCHEME

VENT HEADER RADIUS = 7.5"

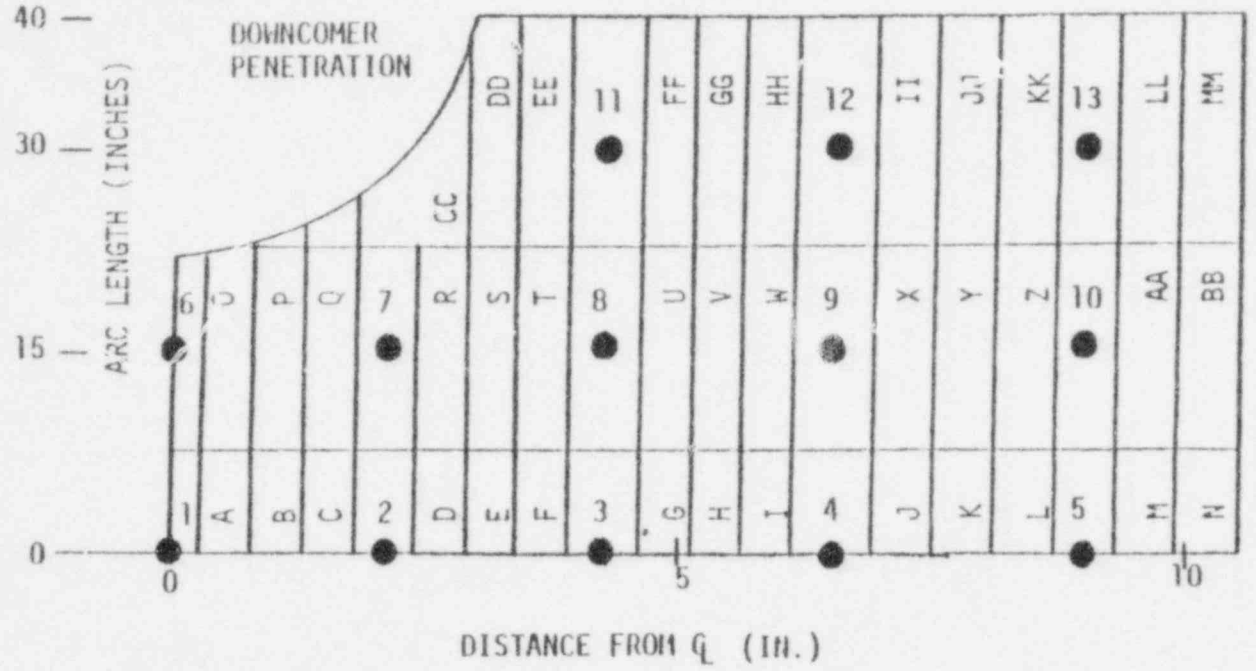

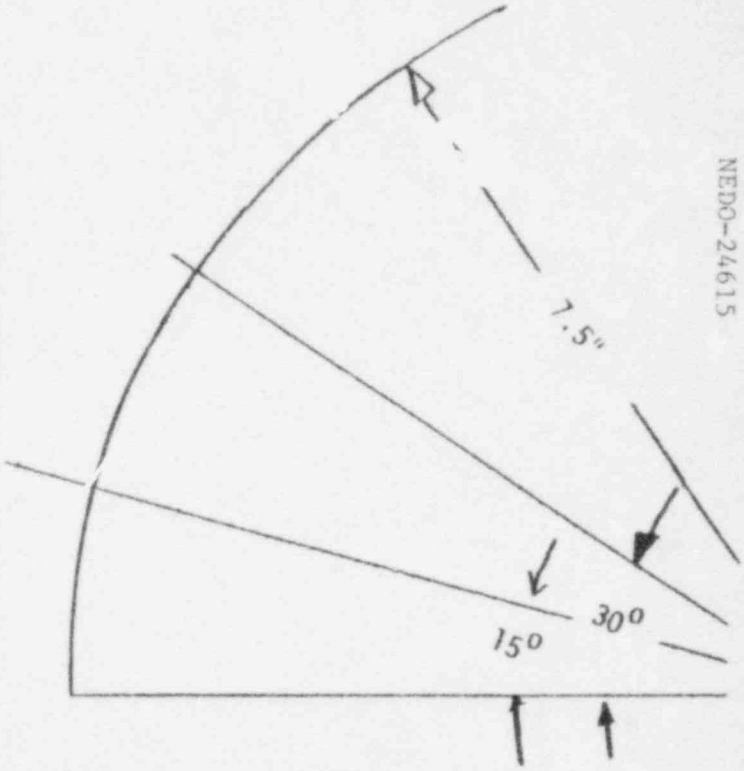

FIGURE B-4

TYPICAL SIX POINT APPROXIMATION
TO VENT HEADER IMPACT PRESSURE TRACE

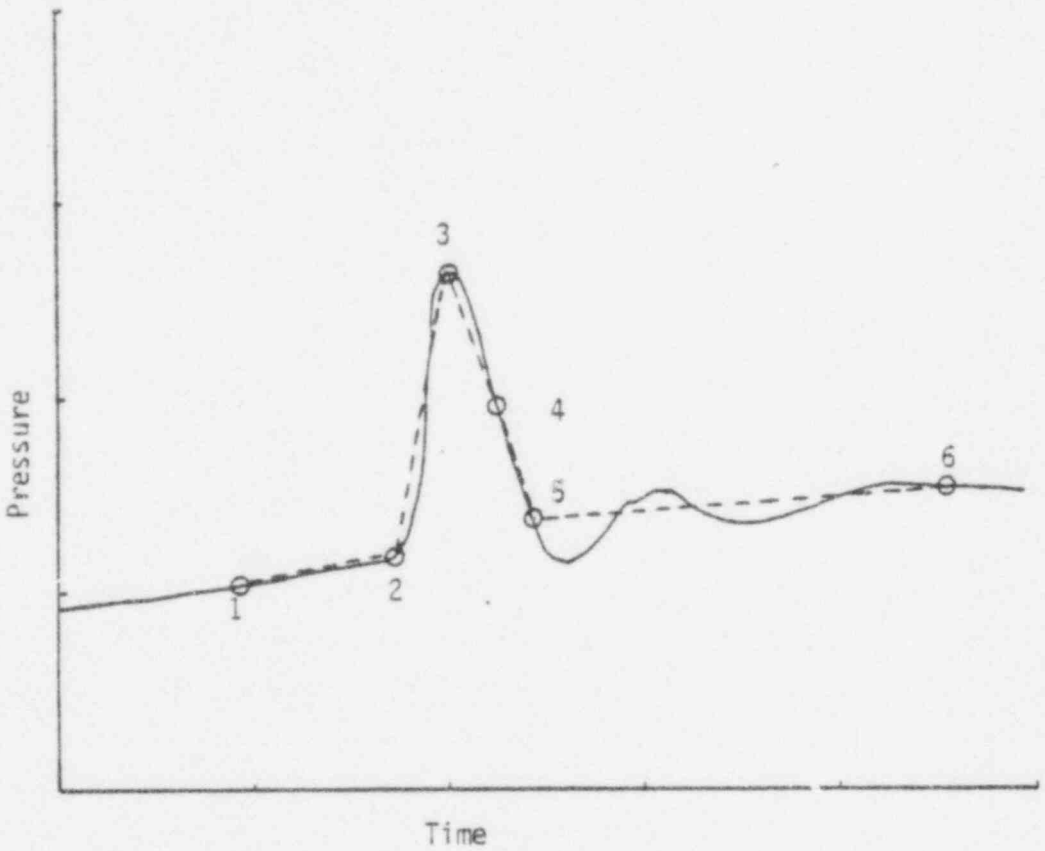

Note: Point 1 is at the earliest time of impact on any pressure transducer. All vent impact pressures are adjusted to the torus freespace pressure at that time.

FIGURE B-5

*General Electric Company proprietary information has been deleted.

FIGURE B-6

*

*General Electric Company proprietary information has been deleted.

FIGURE B-7

*General Electric Company proprietary information has been deleted.

FIGURE B-8

*

*General Electric Company proprietary information has been deleted.

FIGURE B-9

*General Electric Company proprietary information has been deleted.

FIGURE B-10

*General Electric Company proprietary information has been deleted.

FIGURE B-11

*

*General Electric Company proprietary information has been deleted.

FIGURE B-12

*

*General Electric Company proprietary information has been deleted.

FIGURE B-13

*

*General Electric Company proprietary information has been deleted.

FIGURE B-14

*General Electric Company proprietary information has been deleted.

FIGURE B-15

*

*General Electric Company proprietary information has been deleted.

FIGURE B-16

*

*General Electric Company proprietary information has been deleted.

FIGURE B-17

*General Electric Company proprietary information has been deleted.

FIGURE B-18

*

*General Electric Company proprietary information has been deleted.

FIGURE B-19

*

*General Electric Company proprietary information has been deleted.

FIGURE B-20

*

*General Electric Company proprietary information has been deleted.

FIGURE B-21

*

*General Electric Company proprietary information has been deleted.

FIGURE B-22

*

*General Electric Company proprietary information has been deleted.

FIGURE B-23

*

*General Electric Company proprietary information has been deleted.

FIGURE B-24

*

*General Electric Company proprietary information has been deleted.

FIGURE B-25

*General Electric Company proprietary information has been deleted.

FIGURE B-26

*

*General Electric Company proprietary information has been deleted.

FIGURE B-27 *

*General Electric Company proprietary information has been deleted.

FIGURE B-28 *

*General Electric Company proprietary information has been deleted.

FIGURE B-29

*

*General Electric Company proprietary information has been deleted.

FIGURE B-30

*

*General Electric Company proprietary information has been deleted.

FIGURE B-31

*

*General Electric Company proprietary information has been deleted.

FIGURE B-32

*

*General Electric Company proprietary information has been deleted.

FIGURE B-33

*

*General Electric Company proprietary information has been deleted.

FIGURE B-34

*

*General Electric Company proprietary information has been deleted.

FIGURE B-35

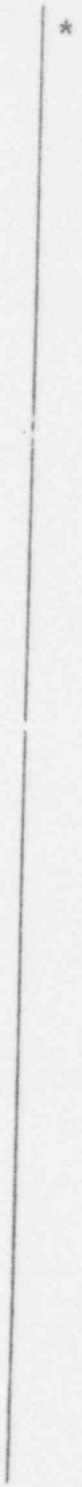

*General Electric Company proprietary information has been deleted.

FIGURE B-36

*

*General Electric Company proprietary information has been deleted.

FIGURE B-37

*General Electric Company proprietary information has been deleted.

FIGURE B-38

*

*General Electric Company proprietary information has been deleted.

FIGURE B-39

*

*General Electric Company proprietary information has been deleted.

FIGURE B-40 *

*Ge .eral Electric Company proprietary information has been deleted.

FIGURE B-41

*General Electric Company proprietary information has been deleted.

FIGURE B-42

*

*General Electric Company proprietary information has been deleted.

FIGURE B-43

*

*General Electric Company proprietary information has been deleted.

FIGURE B-44

*

*General Electric Company proprietary information has been deleted.

FIGURE B-45 *

*General Electric Company proprietary information has been deleted.

FIGURE B-46

*

*General Electric Company proprietary information has been deleted.

FIGURE B-47

*

*General Electric Company proprietary information has been deleted.

FIGURE B-48

*

*General Electric Company proprietary information has been deleted.

FIGURE B-49

*

*General Electric Company proprietary information has been deleted.

FIGURE B-50

*

*General Electric Company proprietary information has been deleted.

FIGURE B-51

*

*General Electric Company proprietary information has been deleted.

FIGURE B-52

*

*General Electric Company proprietary information has been deleted.

FIGURE B-53

*

*General Electric Company proprietary information has been deleted.

FIGURE B-54

*

*General Electric Company proprietary information has been deleted.

FIGURE B-55

*

*General Electric Company proprietary information has been deleted.

FIGURE B-56

*

*General Electric Company proprietary information has been deleted.

TABLE B-1

TYPICAL NODAL LAYOUT DATA

NAME	ANGULAR POSITION	DISTANCE FROM ℄ [in]	AREA [in^2]
PT3001	0.0	0.0	1.20
PT3002	0.0	2.125	2.40
PT3003	0.0	4.25	2.80
PT3004	0.0	6.50	3.20
PT3005	0.0	9.0	2.4
PT3006	15.0	0.0	2.28
PT3007	15.0	2.125	4.80
PT3008	15.0	4.25	5.60
PT3009	15.0	6.50	6.40
PT3010	15.0	9.0	4.80
PT3011	30.0	4.25	6.16
PT3013	30.0	9.0	5.28
A	0.0	0.55	2.00
B	0.0	1.05	2.00
C	0.00	1.55	2.00
D	0.0	2.65	2.00
E	0.00	3.15	2.00
F	0.00	3.65	2.00
G	0.00	4.85	2.00
H	0.00	5.35	2.00
I	0.00	5.85	2.00
J	0.00	7.20	2.40
K	0.00	7.80	2.40
L	0.00	8.40	2.40
M	0.00	9.60	2.40
N	0.00	10.20	2.40
O	15.0	0.55	3.84
P	15.0	1.05	4.20
Q	15.0	1.55	4.68
R	15.0	2.65	4.00
S	15.0	3.15	4.00
T	15.0	3.65	4.00
U	15.0	4.85	4.00
V	15.0	5.35	4.00
W	15.0	5.85	4.00
X	15.0	7.20	4.80
Y	15.0	7.80	4.80
Z	15.0	8.40	4.80
AA	15.0	9.60	4.80
BB	15.0	10.20	4.80
CC	30.00	2.65	5.44
DD	30.00	3.15	4.40
EE	30.00	3.65	4.40
FF	30.00	4.85	4.40
GG	30.00	5.35	4.40
HH	30.00	5.85	4.40
PT3012	30.0	6.50	7.04
II	30.00	7.20	5.28
JJ	30.00	7.80	5.28
KK	30.00	8.40	5.28
LL	30.00	9.60	5.28
MM	30.00	10.2	5.28

TABLE B-2

TYPICAL VENT HEADER INPUT DATA

Note: This table is for illustrative purposes only - All Vent Header Digital Data is included in microfiche form as Table B-3

DIGITAL INPUT VALUES FOR VENT HEADER IMPACT PRESSURE INTEGRATION

DATA REDUCED BY ..... N. W. .....

TABLE B-2

(Continued)

*

DATA CHECKED BY .....

MONT 17A REV 0 12/17/78

ROW NO. TRANSDUCERS INTERPOLATED POINTS

*General Electric Company proprietary information has been deleted.

TABLE B-2

(Continued)

PRESSURE BASE (PSIA)
CALIBRATION FACTOR
TONI

*General Electric Company proprietary information has been deleted.

TABLE B-3

VENT HEADER INPUT DATA

This table will be provided on microfilm.
All the microfilm pages are proprietary.

NEDO-24615
80NED023
Class I
June 1980

MARK I CONTAINMENT PROGRAM

1/4 SCALE PRESSURE

SUPPRESSION POOL SWELL TEST PROGRAM: SUPPLEMENTAL PLANT UNIQUE TESTS

TASK NUMBERS 5.5.4/10.1

Volume 3, Appendices C through I

This work was performed with the support of Quadrex Corporation, Nuclear Services Division, and Aerotherm Division of Acurex Corporation under contract to General Electric.

Reviewed by: John M. Humphrey
John M. Humphrey
Mark I Containment Design

Approved by:
G. E. Wade, Manager
Mark I Containment Design

Approved by:
P. W. Ianni, Manager
Containment Design

NUCLEAR ENGINEERING DIVISION • GENERAL ELECTRIC COMPANY
SAN JOSE, CALIFORNIA 95125

GENERAL ELECTRIC

DISCLAIMER OF RESPONSIBILITY

Neither the General Electric Company nor any of the contributors to this document makes any warranty or representation (express or implied) with respect to the accuracy, completeness, or usefulness of the information contained in this document or that the use of such information may not infringe privately owned rights; nor do they assume any responsibility for liability or damage of any kind which may result from the use of any of the information contained in this document.

TABLE OF CONTENTS - APPENDICES

*The Monticello tests are discussed in Section 3 of the main report.

INTRODUCTION - APPENDICES

The large quantity of data and descriptive material produced by each test series has necessitated the inclusion of a set of appendices with this report. The main report highlights data from a typical plant's tests and summarizes information of general interest. Ten appendices have been included to present data for the remaining plants, to discuss in detail certain phenomena of particular interest, and to document areas that have received additional investigative effort. The contents of these appendices are summarized below.

Appendix A (a continuation of Section 3) presents the test data for the other six plant configurations not discussed in the main report. The data in Section 3 and Appendix A are not necessarily design basis data. The Task 5.5.3-2 Plant Unique Tests were performed at conditions being evaluated for plant operation. Supplementary tests in this report were performed to evaluate alternate conditions (including variations in water level, submergence, drywell/wetwell pressure differential and vent header deflector design) for seven Mark I utilities. After a review of these data, a set of test conditions will be selected for each plant to serve as a design basis for pool swell loads.

Appendix B defines the method used for vent header pressure integration. The values used for the six-point fits to the impact pressure transducer transients and the resulting pressure integrals are also provided.

Appendix C presents plant unique data comparisons and the results of a linear regression correlation of the test data from the Plant Unique Tests, Supplemental Plant Unique Tests, and Generic Sensitivity Tests.

Appendix D presents the results of a measurement uncertainty analysis.

Appendix E presents a series of pool swell pictures for each plant configuration.

Appendix F presents smoothed window-related download oscillations.

Appendix G presents the specification for vent system resistance and the method used to meet the specification.

Appendix H describes the method used to calculate the internal drag forces in the vent system.

Appendix I presents measured deflector forces and an analysis of dye injection tests to investigate the fluid velocity and acceleration history at the deflector.

APPENDIX C
PLANT UNIQUE DATA COMPARISONS

C.1 Comparison of Equivalent Quarter-Scale Loads

Direct comparison of plant unique test results requires adjustment of the test data to account for the different scale factors and projected areas. Table C-1 describes the basic scaling equations used to compare the results of different plant unique tests. These formulas are based on Dr. F. J. Moody's scaling laws described in Section 2.1 and Reference 2. The Scale Factor (SF) referenced is the ratio of the plant full-scale torus diameter to the actual diameter of the test facility torus. The (.250/SF) multiplier is used to ratio every value back to a nominal quarter scale. Using the scaling equations shown in Table C-1, quarter-scale values of average pressure loads and pressure impulses have been calculated for the Mark I plants tested. These values, which are based on QSTF scaled mean data, do not represent a load definition. They do, however, allow a quantitative comparison of test results to be made for the plants tested.

Previously-run QSTF test data from Tasks 5.5.1 and 5.5.3-1 (References 3 and 1) are given in Table C-2 for comparison with the plant unique test data. Task 5.5.4 (this report) test data (normalized to quarter scale) are given in Tables C-3a through C-3e. In these tables, the test conditions and deflector pipe sizes are given in full scale/values.

C.1.1 Comparison of Torus Forces

As discussed in Section C.3, increasing drywell/wetwell differential pressure significantly mitigates torus forces. For the non-zero ΔP tests, all of the plants except Pilgrim were run at 2.31 ft H_2O (1.0 psi) ΔP, full scale. The Pilgrim non-zero ΔP tests were run at 3.46 ft. H_2O (1.5 psi) ΔP full scale. For these non-zero ΔP tests, the torus forces (peak average downforce pressure) varied between 1.33 and 1.96 psi. Variation of the torus forces was primarily caused by submergence varying between 3.00 and 4.25 ft. (full scale). Although both non-zero and zero

ΔP forces are presented in Tables C-3a through C-3e, the most direct plant comparisons are at the zero ΔP condition. At zero ΔP the equivalent quarter-scale torus forces showed considerable variation. The Duane Arnold tests exhibited a downforce pressure of 1.42 psi, the lowest pressure among the plants tested. The Duane Arnold test conditions had relatively shallow submergence, low drywell pressurization rate, and the largest pool area to vent area ratio of any of the plants. Those plants tested with deep submergence (Oyster Creek and Nine Mile Point) or high drywell pressurization rate (Monticello) had higher torus downforces (2.78 to 3.16 psi).

Both Oyster Creek and Nine Mile Point were tested at two different submergences. The effect of submergence on torus downforce is clearly shown in Tables C-3c and C-3d.

C.1.2 Comparison of Vent Header Forces

With the use of large vent header deflectors, the vent header loads are reduced to a very low level relative to unprotected values. The residual vent header load variations due to other test parameters (e.g., ΔP, submergence, etc.) are then relatively insignificant. All the deflector geometries tested in this series were large enough to substantially reduce the vent header load values (listed in Tables 3a through 3e) compared to values observed without deflectors (see Section C.2).

---

*Full scale deflector width

C.2 Effects of Vent Header Deflectors

Non-dimensionalized vent header impact parameters were developed to evaluate the effectiveness of deflectors on vent header impact mitigation. Non-dimensionalized values for peak local pressure (P^*_{LOCAL}), vent impact force (F^*) and hydrodynamic mass (M^*_H) are developed in Tables C-4a and C-4b. P^*_{LOCAL} is the ratio of the peak local impact pressure to the dynamic pressure at the estimated header impact velocity. The non-dimensional force (F^*) is the peak force divided by the bulk pool dynamic pressure times the vent header projected area and is analogous to a drag coefficient. The non-dimensional hydrodynamic mass (M^*_H) is the ratio of the apparent hydrodynamic mass (M_H = Impulse/ Bulk Velocity) and the deeply submerged hydrodynamic mass based on the cylindrical volume of the header. Values around 0.2 are typical of thick slug cylinder impact. Task 5.5.4 non-dimensional data are summarized in Tables C-4a and C-4b. The non-dimensional impact parameters are plotted against the ratio of deflector width/vent header diameter in Figures C-1 through C-3. Some scatter in the data would be expected since these first-order correlations neglect the effects of deflector geometry, deflector height above the pool, and submergence.

As discussed in the previous paragraph and shown in Figure C-1, even relatively small deflectors are very effective mitigators of peak local impact pressure. Values of P^*_{LOCAL} on the order of 1.0 indicate primarily drag load. Non-zero differential pressure mitigates impact pressure for unprotected headers by reducing the slug thickness at impact. Deflectors break up the slug and seem to wash out the mitigating effects of ΔP on vent header impact. Non-dimensionalized values for vent impact force (Figure C-2) and impulse (Figure C-3) show that, although these parameters are harder to mitigate than local peak pressure, they can be essentially eliminated with a large enough deflector. The non-dimensional correlations indicate that deflectors roughly half the width of the header reduce vent impact loads to negligible values. All three correlations show that the mitigating effects of ΔP for unprotected headers tend to disappear for large deflectors.

The following observations were made on the effects of vent header deflectors:

a) In general, pipe deflectors (especially those with structural angles or "Ts") whose width is half the width of the vent header effectively mitigate the vent header impact.

b) Smaller pipes significantly reduce peak local pressures, but are not as effective at reducing peak force or impact impulse.

c) Plain pipes located too close to the water (before the pool swell can approach terminal velocity) are less effective in mitigating vent header impact than pipes located at least one foot (full scale) above the initial water surface.

d) Adding structural angles or "Ts" to a plain pipe seems to provide greater mitigation of header impact than would be expected for a plain pipe of the same total width as the "T" deflector.

e) Adding structural angles or "Ts" to a plain pipe seems to remove the penalty of locating the deflector too close to the water. The deflector acts more as a flow diverter and is less sensitive to the impact velocity.

f) The wedge deflector for the Duane Arnold single downcomer configuration effectively mitigates vent header impact.

g) High-speed movies show that vent header deflectors divert water flow past the vent header and promote higher local penetration of the freespace.

C.3 Effects of Drywell/Wetwell Differential Pressurization (ΔP)

The effects of ΔP on measured torus forces for Tasks 5.5.3-2 and 5.5.4 have been examined by plotting the ratio of the force at non-zero ΔP to the force with zero ΔP on the Y-axis against the ratio of ΔP/submergence (normalized measure of ΔP) on the X-axis. Implicit in these correlations are data points at (0, 1.0). Both the peak downforce ratio (Figure C-4) and downforce impulse ratio (Figure C-5) seem to have a well-defined linear relationship, with the exception of the Monticello, Peach Bottom, and Millstone data. Because the water level in the Monticello, Peach Bottom, and Millstone zero ΔP tests was above the downcomer bends, the stream line length is shorter on the outside of the downcomers and the downcomers clear first on that side. This phenomenon (staged clearing) resulted in a reduction of downforce for the zero ΔP tests.

The peak upforce ratio (Figure C-6) follows but lies below the general trend developed earlier from GE 1/12-scale tests* at 4 ft. submergence, with the exception of the Browns Ferry test data. Some of the type II (30° bend) downcomer plants exhibited upforce oscillation, especially at zero ΔP conditions. The fact that less upforce oscillation was observed at non-zero ΔP conditions may account for the increased effect of ΔP on maximum upforce observed during those tests.

Although the downforce and impulse ratios for the Browns Ferry runs (Figures C-4 and C-5) fit the data trends, the upforce ratio stayed above the trend (Figure C-6). It should be noted that Browns Ferry has 45° downcomers with the bend well above the waterline. As the pool rises past the bend the flow is observed to separate, leaving a column of air from the bend into the torus air space. During the Generic Sensitivity Tests with the standard 45° downcomers, the plot of peak upforce versus drywell pressurization rate ($\dot{p}$) indicated that as pressurization rate increases, the peak upforce reaches a maximum and then declines (Reference 1). This maximum may occur because driving the pool harder (higher $\dot{p}$) causes the bubble to reach the air column above the

*"Mark I Containment Evaluation Short Term Program - Final Report, Addendum 2," NEDC 20989-P, Class III, June 1976, Company Proprietary.

downcomer bend earlier during the upforce transient, thus causing early breakthrough. Although the impulse increases as the pressurization rate is increased, the upforce flattens out and does not oscillate. Early bubble breakthrough in the Browns Ferry tests with the 45° downcomers may have reduced the ΔP sensitivity of peak upforce.

The vent header impact pressure ratios are presented in Figure C-7. The failure of the peak pressure ratio to show a correlation with ΔP indicates that deflector size controls the vent impact characteristics. Monticello data appear to confirm this conclusion.

C.4 Statistical Study of Quarter Scale Data

Linear regression correlations of the data from plant unique testing successfully explain most of the observed variations in Task 5.5.4 data. These results indicate a high degree of consistency of the plant unique pool swell data over the wide range of Mark I conditions tested.

C.4.1 Introduction

The purpose of this statistical study is to analyze the relationships between twelve important pool swell variables and a set of vent header, torus, and pool parameters. A previous study using the 5.5.3-2 tests as the data base (Reference 2) produced equations which have proved useful in predicting pool swell variables for the Task 5.5.4 Supplemental Plant Unique Tests documented in this report, as well as for the Task 5.3.3-1 Generic Sensitivity Tests (Reference 1). The accuracy of the previous study was good, but several improvements are made in this study. First, the data base is expanded from 96 to 173 tests by the inclusion of sixteen typical 5.5.3-1 Generic Sensitivity Tests (1-8, 29-36), the five 5.5.3-2 Duane Arnold tests which were purposely excluded from the data base of the previous study, and the fifty-six Task 5.5.4 tests. Since the Duane Arnold tests were not well explained by the equations from the previous study, a variable was included which successfully incorporates the Duane Arnold tests into the analysis. Since torus uploads were not

as well explained as other torus variables in the previous study, the effect of distance from the deflector bottom to the water surface upon uploads was examined and found to be helpful in explaining variations in upload data. One of the purposes of this study was to improve the explanation of vent header variables. With the expanded range of the data and the very small header forces, however, both the non-linearity of load sensitivity and the larger scatter in the data prevented further improvement in the accuracy of vent header load correlations.

The simplicity and flexibility of the predictive equations are improved in this study by allowing no second order variables into the set of explaining variables. With first order variables the effects of varying the important parameters can be more conveniently studied. The significance of, and percentage of variation explained by, the regression equations are maintained at levels comparable to those of the previous study even though the data base is broadened, the ranges of the variables increased, and the choice of explaining variables limited to first order variables. Even though one to three extra variables are included per equation in this study, the maintenance of high levels of significance (measured by the F-statistic, which drops sharply as insignificant variables are added) and explanatory power (measured by R^2) indicate a consistent data base and a better set of models for the torus variables.

The consistency of the large and varied data base with these simple linear models shows the regularity of the variations observed in the torus variables. The vent header variables are significantly less consistent with the linear models than the torus variables, because of the larger relative data scatter in the vent header data and because of apparent non-linearities in the load response to changes in deflector parameters.

Before discussing the new data base and regression equations, the predictions produced by the previous study (based on 5.5.3-2 tests) will be

compared to the actual quantities of the pool swell variables observed for the tests which we wish to add to the data base (i.e., the 5.5.3-1 and 5.5.4 tests). The estimates for these added tests (based on the previous regression equations), the corresponding observed values, and the deviations of the estimate from the observed in units of standard deviation are presented in Tables C-5 through C-11. Approximately ninety percent of all estimates are expected to fall within $\pm$ two standard deviations of the observed, provided that the quantities being estimated come from the same distribution as the data base which underlies the estimating equation and the estimating equation is properly specified. If the Duane Arnold tests are neglected, 88.5 percent of the torus estimates are within two standard deviations of the observed. Almost none of the estimates for the Duane Arnold torus variables are within two standard deviations, the estimate tending to be much higher than the observed. Thus, although the Supplemental Plant Unique Test data seem to belong with previous Plant Unique Test data base, the equations seem to be insufficient to account for the Duane Arnold tests. If the Duane Arnold tests are neglected, 30 percent of the vent header estimates are outside of two standard deviations from the observed. This would be an abnormally high rate of deviance if the parameters of new tests were within the range of the old, but the tests which produced parameters outside the two standard deviation band were run with a larger deflector farther above the water surface than most tests in the 5.5.3-2 data base. There seems to be significant non-linear aspects in the response of vent header variables at the extremes of deflector height and deflector to vent header width ratio.

Estimates for peak downforce impulse and time to peak torus downforce were not generated for the Generic Sensitivity Tests because volume between orifices is an argument in the estimating equations for those two torus variables and the Generic Sensitivity Tests were run with only one orifice.

Estimates for the vent header forces could not be made for the Generic Sensitivity Tests because many of the arguments in the estimating equation are undefined, since the Generic Sensitivity Tests were run with a bare header.

C.4.2 Multiple Regression--Some Definitions

Multiple regression produces the linear combination of independent variables, i.e., test parameters such as pressurization rate, fL/D, etc., which best estimates a given dependent variable, such as peak torus downforce.

The linear model is as follows:

$$Y_j = a + b_1X_{1j} + b_2X_{2j} + \ldots + b_nX_{nj} + e_j$$

where Y_j is the value of the dependent variable for test j. The Y_j is considered dependent in the sense that its magnitude is influenced by the values of the independent variables, X_{ij}, (the value of plant parameter i for test j) in a linear fashion, which is described by the constant terms a_1, $b_1 \ldots$, b_n. The e_j are error terms composed of measurement errors and the influence of variables which are excluded.

If assumptions can be made about the distribution of the error terms, then estimates made with the regression can be accompanied by confidence intervals (which estimate the probability that the observed will be within a given interval).

The total sum of squared differences between the mean of the dependent variable, $\bar{Y}$, and its observed values, Y_i, can be partitioned into the sum of squares which is predicted by the regression equation (SS_1), and the sum of squared error terms (SS_2):

$$\sum_i (Y_i - \bar{Y})^2 = \sum_i (Y_i' - \bar{Y})^2 + \sum_i (Y_i - Y_i')^2$$

$$SS_{TOTAL} = SS_1 + SS_2$$

where $Y_i' = a + b_1 X_{1i} + \ldots + b_n X_{ni}$ and $Y_i - Y_i' = e_i$.

The ratio of SS_1/SS_{TOT} is called R^2 and increases from zero toward one as the equation accounts for more of the observed variation in the dependent variable.

The ratio of SS_2 to the number of independent squares in SS_2 (the degrees of freedom of SS_2) is the variance of the estimate (the square of the standard error of the estimate (SEE) = variance of residuals).

Since the load definition tests are groups of tests run under identical conditions, information can be gained by further partitioning SS_2:

$$SS_2 = \sum_i \sum_j (Y_{ij} - Y_{ij}')^2 = \sum_i \sum_j (Y_{ij} - \bar{Y}_{i\cdot})^2 + SS_0$$

where Y_{ij}, and Y_{ij}' are the observed and estimated Ys for the jth test in load definition tests group i, and $\bar{Y}_{i\cdot}$ is the mean of observed Y in group i. The ratio:

$$\frac{\sum_i \sum_j (Y_{ij} - \bar{Y}_{i\cdot})^2}{\sum_i \sum_j (Y_{ij} - \bar{Y})^2} = r\%$$

is a measure of a proportion of the total variation which is completely random, i.e., the proportion which comes from differences in pool swell parameters from identical tests. The r% rises as Y gets smaller in relation to its measurement error.

If two sums of squares come from the identical distributions, then the ratio of the ratio of one sum of squares to its degrees of freedom to the other sum of squares to its degrees of freedom is distributed F. An F test of the following form can be used to test if SS_1 is significantly greater than SS_2 which is the same as testing if the regression equation which produced SS_1 and SS_2 is significant:

$$\frac{SS_{1/k}}{SS_2/n-k-1} = F$$

where k = the number of variables in the equation, and n = the number of tests examined.

An F test of the following form can be used to test if an individual variable is significant:

$$\frac{SS_{i/1}}{SS_2/n-k-1} = F$$

where SS_i is the difference between SS_1 before variable i is introduced into the regression and SS_1 after i is introduced. The F-statistics are calculated, compared to an F distribution and the probability that the two sums of squares come from identical distributions is known.*

C.4.3 Test Matrix

The data base is composed of 173 tests in 48 different configurations (all 101 tests from Task 5.5.3-2 Plant Unique Tests, all 56 from Task 5.5.4 Supplemental Plant Unique Tests and 16 tests selected from the 36 Task 5.5.3-1

*For further reading, see Mood, Graybill, Boes., Introduction to The Theory of Statistics. McGraw Hill, 1974, Chapter X.

Generic Sensitivity Tests)**. Twelve plant parameters and twelve pool swell variables are included in the analysis.

C.4.3.1 Plant Parameters -- Definition, [Ranges] adjusted to 1/4 scale, and (Abbreviation)

1. Total fL/D is a measure of system flow resistance; its calculation is described in Appendix G. Range [11.0, 20.3], (fL/D).

2. Pressurization rate, dP/dt, measured in psi/second is the linear rate of drywell pressurization measured with capped downcomers (constant volume charging) during calibration tests run for each drywell/orifice configuration [23.3, 41.4], (PDOT).

3. Submergence, measured in inches, is the distance from the downcomer exit to the water surface. [9.0, 14.4], (SUB).

4. The pressure difference between the drywell and wetwell is measured in inches of water and is equal to the displacement of the water inside the downcomer. [0.0, 13.0], (ΔP).

5. The width of the torus test segment (representing an average cell) is measured in inches. [15.9, 27.0], (CW).

6. The distance from the vent header to the water surface is measured in inches. [6.5, 12.2], (VH-W).

7. The distance from the deflector bottom to the water surface is measured in inches. [0, 5.8], (DF-W).

**The 16 tests selected (4 each at 4 conditions) were 1) at the reference condition of 3' 4" submergence with maximum ΔP, 2) with vent orifices, 3) with partial ΔP and 4) with deeper submergence (4' 4"). The 20 tests which were not included were at vent system fL/D or had dyrwell $\dot{p}$ values well outside the range evaluated for plant unique testing.

8. The ratio of the width of the deflector to the width of the vent header is dimensionless. [0, 0.706], (DF/VH).

9. A dummy variable is included to account for differences in vent header loads due to differences between an angle deflector and a pipe deflector of equal width. [0 or 1], (TYPE).

10. The vent header diameter is measured in inches. [10.6, 15.0], (VHD).

11. Vent System Capacitance for this correlation is defined as the area above the test characteristic line(s) on a vent system volume versus normalized static pressure plot. This quantity provides a linearized measure of the ability of the vent system to transiently store and discharge air into the suppression pool. [38, 231], (CAP).

12. The ratio of cell width to the number of downcomers is measured in inches/downcomer. [7.95, 19.50], (CW/DC).

C.4.3.2 Pool Swell Parameters

1. Peak torus downforce and peak torus down pressure. The first is the peak downforce value of the torus pressure integral, corrected for water inertia, and the second value is the first divided by torus area.

2. Peak torus upforce and peak torus up pressure. The first is the peak upforce value of the torus pressure integral, uncorrected for water inertia, and the second is the first divided by torus area.

3. Peak torus downforce impulse and peak torus downpressure impulse. The first is the integral of the torus pressure integral, uncorrected for water inertia, from To, the start of pressurization of the drywell, to the time that the torus pressure integral reaches zero again, and the second is the first divided by torus area.

4. Peak vent header force and peak vent header average pressure. The first is the maximum value of the vent header force from the integral of vent header pressure transducers, and the second is the first divided by vent header area.

5. Peak vent header force impulse and peak vent header pressure impulse. The first is the integral of the vent header force from the first vent header impact until peak impulse. The second is the first divided by the vent header area.

6. Time to peak torus downforce is the difference between the time at which peak torus downforce occurred and To.

7. Time to peak torus upforce is the difference between the time at which peak torus upforce occurred and To.

All variables were scaled from the actual scale factor at which the tests were conducted to 1/4-scale. This scaling was performed according to laws developed by Dr. Moody of G.E. (discussed in Section 2.1 of Reference 2) in order to provide a common basis for comparison.

Regressions on the twelve pool swell variables were performed using the computer program, Statistical Package for the Social Sciences (SPSS). The twelve plant parameters listed above were found to be significant in the determination of one or more of the twelve pool swell parameters. Other plant parameters were tested and discarded because of lack of significance or because the sign of the coefficient of the variable was not explainable or consistent.

High degrees of correlation between explaining variables cause the variability of the coefficients of the highly correlated pair to rise and will increase the variability of the estimates produced by the equation. The correlation matrix of all variables entered in any equation is reproduced in Table C-12 and contains no number greater than 0.814. The data base can be considered sufficiently diverse to permit the effects of all of the explaining variables chosen here to be statistically separated from each other.

The regression equations produced by analysis of this data base can produce accurate estimates for plant configurations within and possibly slightly beyond the ranges of the plant parameters of the data base. Assuming that the relationships described in the next section are linear over the ranges tested was a useful simplification. Deviations from linear behavior might be expected beyond the ranges tested.

C.4.4 Regression Results

The regression equations presented in this chapter were chosen by admitting any variable of the set of plant parameters listed in Section C.4.3 if the variable could be considered significant with 90% confidence. This approach was taken in favor of maximizing the significance or F-statistic of the entire equation to quantify the effect of as many of the important plant parameters as possible. In general, variables were not included in the list in Section C.4.3 if their effect tended to change as the data base changed or tended to change from equation to equation. Some variables were eliminated due to low levels of significance. For that reason the distance from the downcomer exit to torus bottom was eliminated, despite having a consistent and explainable sign.

The emphasis is shifted in this study from best explanation with fewest variables, to the development of a complete and consistent picture of the effects of a set of plant parameters on the pool swell variables.

The 90% confidence intervals (CI) are based on the assumption that the errors of the estimates are normally distributed. A chi-squared test of this assumption was made, and each residual distribution was found to be within a normal range (i.e., in no case could the null hypothesis that the residuals were normally distributed be rejected with even 75% confidence).

The coefficient of variability (CV), the ratio of the standard error of the estimate (SEE) to the mean of the dependent variable, is a more comparable measure of the variability of the estimates and is reported along with R^2, r%, F, and SEE, all of which have been defined in Section C.4.2.

The overall Fs reported indicate that each equation is significant with 99% confidence.

The order of the variables, from left to right corresponds to their relative significance to the equation presented.

The following equations summarize the results of this study:

1. Peak Torus Downforce from pressure integral corrected for water inertia (DN).

$$DN = -3067.2 - 233.5\ (\Delta P) + 326.6\ (SUB) + 166.3\ (CW) - 130.0\ (CW/DC) + 61.0\ (PDOT) + 1.1\ (CAP)$$

a) $R^2 = 0.92308$

b) SEE = 346.0

1) 90% CI = 569.2

2) CV = 10.0%

c) Overall $F_{6,166} = 332.0$

d) r% = 1.2%

2. Peak Torus Downpressure from pressure integral corrected for water inertia (PDN).

$$PDN = 0.0988 - 0.1303\ (\Delta P) + 0.1892\ (SUB) + 0.0421\ (PDOT) - 0.0653\ (CW/DC) - 0.0088\ (CW)$$

a) $R^2 = 0.91920$
b) SEE = 0.19500
   1) 90% CI = 0.3209
   2) CV = 10.3%
c) Overall $F_{5,167} = 380.0$
d) r% not calculated

3. Peak Torus Impulse from uncorrected pressure integral (IM).

$$IM = -197.8 - 12.9\ (\Delta P) + 29.5\ (SUB) + 6.6\ (CW) - 7.7\ (CW/DC) + 3.8\ (PDOT)$$

a) $R^2 = 0.95847$
b) SEE = 15.1
   1) 90% CI = 24.8
   2) CV = 6.4%
c) Overall $F_{5,167} = 770.9$
d) r% = 0.9%

4. Peak Torus Pressure Impulse from uncorrected pressure integral (PIM).

$$PIM = 0.0654 - 0.0070\ (\Delta P) + 0.0164\ (SUB) - 0.0053\ (CW/DC) + 0.0019\ (PDOT) - 0.0026\ (fL/D) - 0.0019\ (CW)$$

a) $R^2 = 0.96187$

b) SEE = 0.00862

1) 90% CI = 0.0142

2) CV 6.6%

c) Overall $F_{6,166} = 697.8$

d) r% not calculated

5. Time to Peak Torus Downforce (B1).

$$B1 = 92.2 - 5.3\ (\Delta P) + 6.4\ (SUB) - 1.2\ (PDOT) + 1.3\ (CW/DC) - 0.7\ (fL/D)$$

a) $R^2 = 0.84972$

b) SEE = 10.2

1) 90% CI = 16.8

2) CV = 9.7%

c) Overall $F_{5,167} = 188.9$

d) r% = 2.8%

6. Peak Torus Upforce, from pressure integral uncorrected for water inertia (UP).

$$UP = -3982.5 - 98.9\ (\Delta P) + 264.7\ (SUB) + 71.3\ (CW) + 37.4\ (PDOT) + 10.3\ (CAP) - 32.3\ (DF\text{-}W) - 32.4\ (CW/DC) - 14.0\ (fL/D)$$

a) $R^2 = 0.87335$

b) SEE = 218.0

1) 90% CI = 358.5

2) CV = 10.8%

c) Overall $F_{7,121} = 119.2$

d) r% = 1.0%

7. Peak Torus Uppressure, from pressure integral uncorrected for water inertia (PUP).

$$PUP = -0.5933 - 0.0567\,(\Delta P) + 0.1521\,(SUB) + 0.0192\,(PDOT) + 0.0367\,(CW/DC) - 0.0336\,(fL/D) + 0.0043\,(CAP) - 0.0189\,(DF\text{-}W)$$

a) $R^2 = 0.90157$

b) SEE = 0.11082

1) 90% CI = 0.1823

2) CV = 9.6%

c) Overall $F_{7,121} = 158.3$

d) r% not calculated

8. Time to Peak Torus Upforce (B3).

$$B3 = 154.0 - 9.1\,(\Delta P) + 16.6\,(SUB) - 1.8\,(PDOT) - 0.1\,(CAP) + 0.4\,(CW/DC)$$

a) $R^2 = 0.94676$

b) SEE = 10.1

1) 90% CI = 16.6

2) CV = 4.3%

c) Overall $F_{5,167} = 593.9$

d) r% = 0.4%

9. Peak Vent Header Force, from pressure integral (VP).

$$VP = 760\ 8 - 75.7\,(DF/VH) - 110.1\,(TYPE) - 4.2\,(\Delta P) - 10.4\,(DF\text{-}$$

a) $R^2 = 0.71637$

b) SEE = 92.7

1) 90% CI = 152.5

2) CV = 54.4%

c) Overall $F_{4,97} = 61.2$

d) r% = 5.4%

10. Peak Vent Header Average Pressure, from pressure integral (PVP).

PVP = 10.0840 - 4.9179 (DF/VH) - 0.4079 (VHD) - 0.1192 (CW/DC)
-0.3803 (TYPE) - 0.0450 (DF-W) - 0.0090 (ΔP)

a) R^2 = 0.76174
b) SEE = 0.33065
   1) 90% CI = 0.5439
   2) CV = 52.3%
c) Overall $F_{6,95}$ = 50.6
d) r% not calculated

11. Peak Vent Header Impulse, from load cell (VM).

VM = 20.7 - 5.5 (TYPE) - 17.0 (DF/VH) - 0.2 (ΔP) - 0.3 (DF-W)
-0.3 (CW/DC)

a) R^2 = 0.69885
b) SEE = 2.67894
   1) 90% CI = 4.408
   2) CV = 49.1%
c) Overall $F_{5,96}$ = 44.6
d) r% = 5.5%

12. Peak Vent Header Pressure Impulse, from load cell (PVM).

PVM = 0.0882 - 0.0230 (TYPE) - 0.0021 (CW/DC) - 0.0007 (ΔP)
-0.0014 (VH-W) - 0.0323 (DF/VH)

a) R^2 = 0.70228
b) SEE = 0.01017
   1) 90% CI = 0.0167
   2) CV = 50.3%

c) Overall $F_{5,96} = 45.3$
d) r% not calculated

The regression equations can be summarized by examining the effects of the plant parameters on the pool swell as a whole.

The most important determinant of all torus phenomena is ΔP. As ΔP is increased, peak torus downforce and downpressure, peak force impulse and pressure impulse, peak upforce and uppressure are all mitigated by the tendency of increased ΔP to cause vent clearing to occur sooner and at a lower drywell pressure, thus decreasing the driving force of the bubble. In addition, increased ΔP, tends to speed up the occurrence of peak downforce and upforce for the same reason. The coefficients of ΔP are negative in the predictive equations for all eight torus pool swell variables.

The second most important determininant of all torus phenomena is submergence (SUB). As submergence is increased and everything else is held constant, time to vent clearing is increased which causes the driving pressure at vent clearing to be higher. Thus peak torus downforce and pressure, peak torus impulse and pressure impulse, time to peak torus downforce, peak torus upforce and uppressure, and time to peak torus upforce are all increased by increases in SUB.

As the rate of pressurization of the drywell (PDOT) is increased and everything else is held constant, vent clearing time is speeded up and the driving force of the bubble at vent clearing time is increased. Thus all torus forces and pressures are increased and the times of peak torus downforce and upforce are reduced.

Increases in cell width have a positive effect on peak torus forces and peak torus force impulse, because as the area over which the torus pressures are integrated goes up, the total goes up even though the size of the incremental addition decreases as the distance from the downcomers

increases. Similarly, increases in cell width have a negative effect on peak torus pressures and peak torus pressure impulse, since the incremental addition to torus force per unit area tends to decrease as the distance from the downcomers increases.

The ratio of cell width to number of downcomers was included in the set of explaining variables to help account for the differences between the one-downcomer-per-cell Duane Arnold tests and the remaining tests which are strictly two-downcomer. Imagine that the two downcomer configuration, is actually one cell of a normal Duane Arnold torus which has been modified by doubling the number of downcomers. Increasing the number of downcomers per cell will increase the rate at which the vent system can transmit mass into the cell and so increase torus loads.

Vent Capacitance (CAP) is a measure of the ability of the vent system to transiently store and discharge air into the LOCA bubble. As the CAP increases, everything else being equal, the rate at which mass is transmitted to the torus following vent clearing increases, increasing torus loads and decreasing times to peak loads. CAP and all subsequent variables discussed in this section, unlike the previously discussed variables, were not found to be significant in all eight torus equations. CAP appears only in the equations for peak torus downforce, peak torus pressure impulse, peak torus upforce and uppressure and time to peak torus uppressure.

As the total vent system resistance is increased, the ability of the vent system to transmit mass is decreased, so an increase in fL/D would have an opposite effect from an increase in CAP. Total vent system resistance appears in the equations for peak torus pressure impulse, time to peak torus downforce, and peak torus upforce and uppressure.

As the deflector is moved farther from the water surface (within the range examined in this study), peak torus upforce and uppressure is

reduced, possibly because the deflector is more effective in promoting breakthrough of the bubble. (DF-W) appears in the equations for peak torus upforce and uppressure.

The variables which were found to be significant determinants of vent header forces are the distance from the deflector bottom to water surface (DF-W), the distance from the vent header bottom to water surface (VH-W), the ratio of deflector width to vent header diameter (DF/VH), vent header diameter (VHD), the type of deflector used (TYPE), ΔP and the ratio of cell width to the number of downcomers. Increases in all of these variables tended to decrease vent header loads. For the range of values evaluated, increases in the deflector to water distance (DF-W) increase the pool velocity and decrease the slug thickness at deflector impact. Both these effects tend to enhance the effectiveness of the deflector. Increases in the vent header to water distance (VH-W) reduce the slug thickness at impact and extend the impact time into the upload transient. This delay allows the pool to decelerate some before impact. A larger deflector in front of a given vent header will deflect more of the flow. Hence an increase in deflector width/header diameter (DF/HD) decreases vent header forces. Increases in vent header diameter (VHD) will tend to decrease the header pressure impulse and average pressure. This effect occurs because, for Mark I vent header impact, the size (hence the deeply submerged hydrodynamic mass) of the vent header is significant with respect to the slug thickness at impact. The results of the present study agree with the results of the previous one in implying that an angle or "T" deflector is more effective in deflecting water flow and decreasing vent header forces than a pipe deflector of the same width. Increases in ΔP and cell width/number of downcomers (CW/DC) tend to decrease vent header forces because they reduce pool momentum at the time of vent header impact.

C.4.5 Conclusions

The objectives of this study were: 1) to make the regression equations more useful and flexible by eliminating all but one of the second degree

variables (CW/DC) and by including more plant parameters in the set of explaining variables; 2) to show that the 5.5.3-1 and 5.5.4 tests belong to a common distribution with the 5.5.3-2 tests; 3) to improve the explanation of upload; 4) to correlate the Duane Arnold tests with the rest of the data base; and 5) to better explain vent header forces. To evaluate progress in each of these areas, the regression equations developed in this study were compared to the equations from the previous study. The regressions of the previous study used a combination of largely second degree variables (i.e., products and quotients of the plant parameters) and a few simple plant parameters as explanatory variables, and used fewer of these first and second degree variables in each equation, and so are not strictly comparable with the equations presented here. The R^2 and F of the torus and vent header equations from the previous study are presented with these statistics from the present study, in Tables C-13 and C-14. Alternative formulations of the data base and set of explaining variables are included for the discussion of the Duane Arnold tests. Also included is the range of the number of different plant parameters included in the regression equations for each alternative approach.

Two of the most important criteria on which to judge regression equations are the proportion of observed variation in the dependent variable for which the equation accounts (R^2), and the overall significance of the equation (F). R^2 increases monotonically as explaining variables are added to a regression. The overall F-statistic measures the degree of confidence with which it can be said that the vector of correlation coefficients produced by the regression is different from a vector of zeroes. The F-statistic for the equation will increase with the addition of a new variable only if the new variable increases R^2 enough to overcome the built in bias of the F statistic against new variables.

Recall that the F-test for the equation as a whole is:

$$F = \frac{SS_{EXP/k}}{SS_{ERR/n-k-1}}, \text{ and } R^2 = SS_{EXP} + SS_{ERR}$$

where SS_{EXP} is the sum of squared deviations (from the mean of the dependent variable), which is explained by the regression; SS_{ERR} is the complement to SS_{EXP} in the total sum of squared deviations from the mean, (or the sum of squared deviations of the observed from the estimate); n is the number of tests and k is the number of variables in the regression equation.

So for the F-statistic to increase with the addition of a new variable, the ratio of (SS_{EXP}/SS_{ERR} after the new variable is added) to (SS_{EXP}/SS_{ERR} before the new variable is added) must be greater than,

$$\frac{k+1}{k} \cdot \frac{n-k-1}{n-k-2}$$

Thus, even though the addition of less significant variables will increase R^2 slightly, the F-statistic will finally decrease as less significant explaining variables are added to the regression.

The present regression equations for the torus variables have, in general, levels of R^2 and F which are comparable to R^2 and F values for the previous equation set. In the present study, the size of the data base was substantially increased, the ranges of the variables in the data base increased, and the Duane Arnold tests included. Although one to three additional variables were included in equations in the new study, F-values were only slightly lowered. The goal of expanding the set of explaining variables was achieved without substantially reducing the significance levels of the equations, implying that the new variables were only marginally less significant than the old ones. It also appears

that the new tests have been successfully integrated into the data base, since there were no sharp drops in R^2 or F.

In the case of upforce and uppressure, R^2 levels rose and F levels were only slightly lower; in the case of torus force and pressure impulses, both R^2 and F levels rose despite the addition of two to three variables to all four equations. These gains in R^2 can be attributed not simply to the addition of variables, but must be partially attributed to better modeling. If the gains in R^2 were due only to the addition of less significant variables, the F-values would drop sharply. Thus the added variables are about as significant as the original ones.

In the case of uploads, part of the gains in R^2 can be attributed to the addition of deflector data to the set of explaining variables.

In order to demonstrate the relationship of the Duane Arnold tests to the rest of the data base, and to show the importance of the ratio of cell width to number of downcomers to the set of explaining variables, R^2 and F values for two alternative approaches are included. Alternatives A and B are regression sets with the same set of explaining variables and data base as the regressions presented in Secton C.4.4, except in alternative B the explaining variable set lacks (CW/DC), and in alternative A, the data set lacks the Duane Arnold tests. Overall, R^2 and F levels tend to drop sharply when the Duane Arnold tests are incorporated into the data base correlated against a set of explaining variables without (CW/DC). When (CW/DC) is introduced, R^2 and F values return to their former levels. So (CW/DC) is of significant value in correlating the Duane Arnold tests with the rest of the data base.

The vent header regression results for this study are compared to the results in the previous study in Table C-14. The F and R^2 values are substantially worse in the present study. This corresponds to the high number of outliers in the set of estimates produced by the old equations

for the new data. The outliers were produced by using the previous equations to estimate the vent header loads for new plant configurations with larger deflectors higher above the water surface than were present in the previous data base (the Task 5.5.3 tests). This implies that the effects of either deflector size or height of deflector above the water surface or both are significantly non-linear and, as the ranges of these variables are increased, the inaccuracies associated with a linear approximation become more apparent.

Also, the ratio of measurement error to signal size is increased for the vent header variables, especially for large deflectors which substantially reduce the vent header forces. An indirect measure of this effect is provided by the r% statistic presented in Section C.4.4. The r% is that fraction of total observed variation which, because it comes from tests run under identical conditions, cannot be explained by any model, given our set of explaining variables.

The five times higher level of r% for peak vent header loads is due to higher levels of measurement uncertainty. Higher levels of measurement uncertainty and non-linear aspects associated with some vent header variables combine to make the R^2 and F values lower for the vent header variables than for the torus variables.

The torus equations with their high R^2 and F values and low standard errors are useful for fairly accurate predictions of the effect of changes in a set of plant parameters on the set of variables they describe. More importantly, the high R^2 and F values affirm the high degree of internal consistency and even linearity of the data.

C.5 Plant Unique Effects

C.5.1 Duane Arnold Delayed Download Oscillations

C.5.1.1 Introduction

A torus downforce spike with subsequent oscillations appeared during Duane Arnold Plant Unique Test 5 (Task 5.5.3-2) at approximately 600 milliseconds after test initiation. Since this spike occurred well after the time of peak upload and roughly coincided with the time of air supply valve closure, the spike was attributed to noise from the electrical signal which initiated valve closure. During the Supplemental Plant Unique Tests, four additional Duane Arnold tests (Tests 6 - 9) were conducted under the same conditions as the earlier Test 5. When the downforce spike reappeared and was insensitive to changes in the timing of the valve closure signal, additional investigations were conducted. The results of that study are presented in this section.

C.5.1.2 Discussion

Figures C-8 and C-9 show the delayed torus downforce spike and oscillations which appeared in the Test 5 corrected pressure integral and corrected torus load cell, respectively. This oscillatory force at 600 milliseconds after test initiation is typical of Tests 5 through 9.

The configuration of torus pressure transducers for Test 5 is shown in Figure C-10. This arrangement of transducers was also utilized for Tests 6 through 9, except that PT-1007 (195°) was deleted. Figure C-11 presents the torus pressure transducer outputs for Test 5. This transducer output is typical of Tests 5 through 9. The spread of pressures at the beginning of each test was caused by the differences in water head above each transducer. Between 300 and 600 milliseconds after initiation of each test, all torus pressure transducers had approximately the same output. This indicates that the dynamic effects of the expanding bubble compensated for the differences in hydrostatic head and probably

indicates that portions of the torus bot' m were uncovered. Immediately after 600 milliseconds the transducer outputs began to diverge. This change indicates that the water was flowing back to the torus floor.

During each test, transducer PT-1006 recorded a pressure surge at approximately 600 milliseconds, followed by approximately 50 milliseconds of oscillation at a frequency of about 160 Hz. Outputs from transducers PT-1008, -1007, and -1002 were significantly less oscillatory than PT-1006 (see Figure C-12). Figure C-13 shows a detailed diagram of the placement of transducers PT-1006, -1008, -1007, and -1002. Since PT-1006 sensed a higher pressure than the other transducers, the center of impact was evidently localized at the bottom-dead-center of the torus.

A sequence of sketches made from the Test 5 movie is presented in Figures C-14 and C-15. The interfaces which were visible through the front window are shown with solid lines. Extrapolated interfaces which were not visible are indicated with dashed lines. The extrapolated portions of the diagrams were developed from visible interfaces and bubble shapes observed in Tests 1-4, where more of the bubble was visible. The torus pressure spike appears to have occurred at the time that the lower portion of the bubble began to collapse (t = .600 sec). Collision of two downward-moving waves of water from the torus sides would have produced the local pressure pulse that was recorded by the lower torus pressure transducers.

Figure C-16 shows that the uncorrected load cell only registered a downforce of approximately 500 pounds, which excited the 50 Hz. natural frequency of the torus. This indicates that the force was applied over a time that was short compared to the torus period of approximately 20 milliseconds. The relative positions of the torus accelerometer and PT-1006 are shown in Figure C-18. The location of the accelerometer would allow it to see any torus vibrations localized around PT-1006.

The irregular oscillatory output (approximately 200 Hz for the first two cycles and about 160 Hz thereafter) of the torus accelerometer indicates that the force was applied over a time that was slightly longer than the first pulse (i.e., 6-8 milliseconds). Since the pressure transducer and accelerometer achieved an approximate 160 Hz sinusoidal motion (180° out of phase) after about 10 milliseconds, the oscillations from that time on can be assumed to be due to localized structural ringout (refer to Figure C-21).

Since the accelerometer is used to correct the torus load cell output for combined torus and water inertia, its use during periods of localized vibration would result in calculation of erroneous force oscillations. The large downforce spike and 160-170 Hz oscillations seen in the inertia-corrected load cell plot (Figure C-9) were, therefore, erroneously introduced by an inertia correction which used the local vibrations sensed by the torus accelerometer.

Since the pressure spike was localized around PT-1006, integration of this local high pressure over the entire 15° segment of torus bottom would result in calculation of erroneously high force oscillations in the torus pressure integral. This effect would then be compounded by using the oscillating torus accelerometer output to correct the pressure integral for water inertia. The large downforce spike and 160-170 Hz oscillations seen in the inertia-corrected pressure integral plot (Figure C-8) were erroneously introduced by integrating the PT-1006 output over too large an area and using the local vibrations sensed with the torus accelerometer to perform the inertia correction of the torus pressure integral.

There is some evidence that repeated tests can reduce the magnitude of the delayed downforce spike and oscillations, possibly by removal of dissolved air. Figure C-19 presents the plots of PT-1006 output for Tests 8 and 9, which were run 2 hours apart. The pressure trace from

Test 9 showed smaller pressure oscillations and more rapid damping than that from Test 8.

C.5.1.3 Determination of Applied Force (Quarter Scale)

Since impulse imparted to the torus should equal impulse imparted to the load cell, impulse should also equal the integral of the load cell plot over the time interval that the initial torus kinetic energy is being absorbed by the load cell, 596 to 601.5 milliseconds. Integration of this portion of the load cell plot (Figure C-21) yields an impulse of 1.70 lb-sec.

If the force-time plot is assumed to be triangular and have a 7 millisecond duration, the peak force can be approximated by

$$F = \frac{2I}{t} = \frac{2(1.7)}{.007} = 485.7 \text{ lb}$$

The responses of pressure transducers PT-1002, -1007, and -1008 (Figure C-12) indicates that the force was attenuated to zero within a distance of 6 inches from PT-1006. The assumption of a conical pressure distribution with a 6 inch radius yields a peak load pressure of

$$P = \frac{(486 \text{ lb})(3)}{\pi R^2} = 12.9 \text{ psi}$$

This calculated pressure agrees reasonably well with the 11 psi rise recorded by PT-1006.

C.5.1.4 Conclusions

1. The observed torus downforce at 600 milliseconds is a real phenomenon and the localized impulsive loading should be considered in the load evaluations. However, the measured oscillations are primarily the structural response of the QSTF to the nearly impulsive loading.

2. This phenomenon seems to be caused in Duane Arnold by the single downcomer and zero ΔP which allow the bubble to penetrate essentially to the bottom of the torus. As this bubble collapses, waves rolling down the sides of the torus appear to meet in the center causing the observed local loading phenomenon.

3. Values of 1.7 lbf-sec, 7 milliseconds and 490 lbf seem to be reasonable subscale estimates for the impulse, duration and peak force for this phenomenon.

4. The QSTF instrumentation provides valid force measurements throughout the main downforce, upforce and breakthrough phases of the transient. The loading phenomenon at 600 ms causes oscillations in the output of the torus accelerometer and several pressure transducers which produce subsequent erroneous oscillations in the torus force measurements.

5. Measurements of the torus forces after the impulsive loading can be obtained by combining a measurement of the loading such as given in 3 above with a mean curve drawn through the oscillations in the torus force measurements.

C.5.2 Oyster Creek Torus Force Plots

Because the torus accelerometer failed during Oyster Creek Tests 7 and 15, the Q- and P-plots (inertia-corrected torus load cell and inertia-corrected torus pressure integral, respectively) were not corrected with the appropriate acceleration terms. Since Test 6 was conducted under the same conditions as Test 7, the accelerometer output for Test 6 was used to obtain the "correct" Test 7 torus force plots. Similarly, the 2A shakedown test data was used to obtain "correct" Test 15 torus force plots.

The Test 6 torus accelerometer plot is shown in Figure C-22. Also shown are the plots of the acceleration multiplied by water mass and the acceleration multiplied by the combined water and torus mass. The acceleration times water mass values were subtracted from the torus pressure integral values to produce the inertia-corrected plot shown in Figure C-23. The acceleration times water plus torus mass values were subtracted from the thrust-corrected load cell values to produce the corrected plot shown in Figure C-24.

The Test 2A (shakedown) torus accelerometer plot is shown in Figure C-25, along with the plots of the water and water-plus-torus multiples. The inertia-corrected torus force plot obtained from the pressure integral is shown on Figure C-26. The inertia-corrected torus force plot obtained from the load cell is shown on Figure C-27.

The similarity between these manually-corrected torus force plots and routine inertia-corrected torus force plots for the remaining Oyster Creek tests substantiates the assumption that acceleration data are reproducible for tests with identical hydrodynamic and facility design parameters.

FIGURE C-1

NORMALIZED MAXIMUM LOCAL IMPACT PRESSURE VERSUS NORMALIZED DEFLECTOR WIDTH

Tasks 5.5.3-2 and 5.5.4 Tests

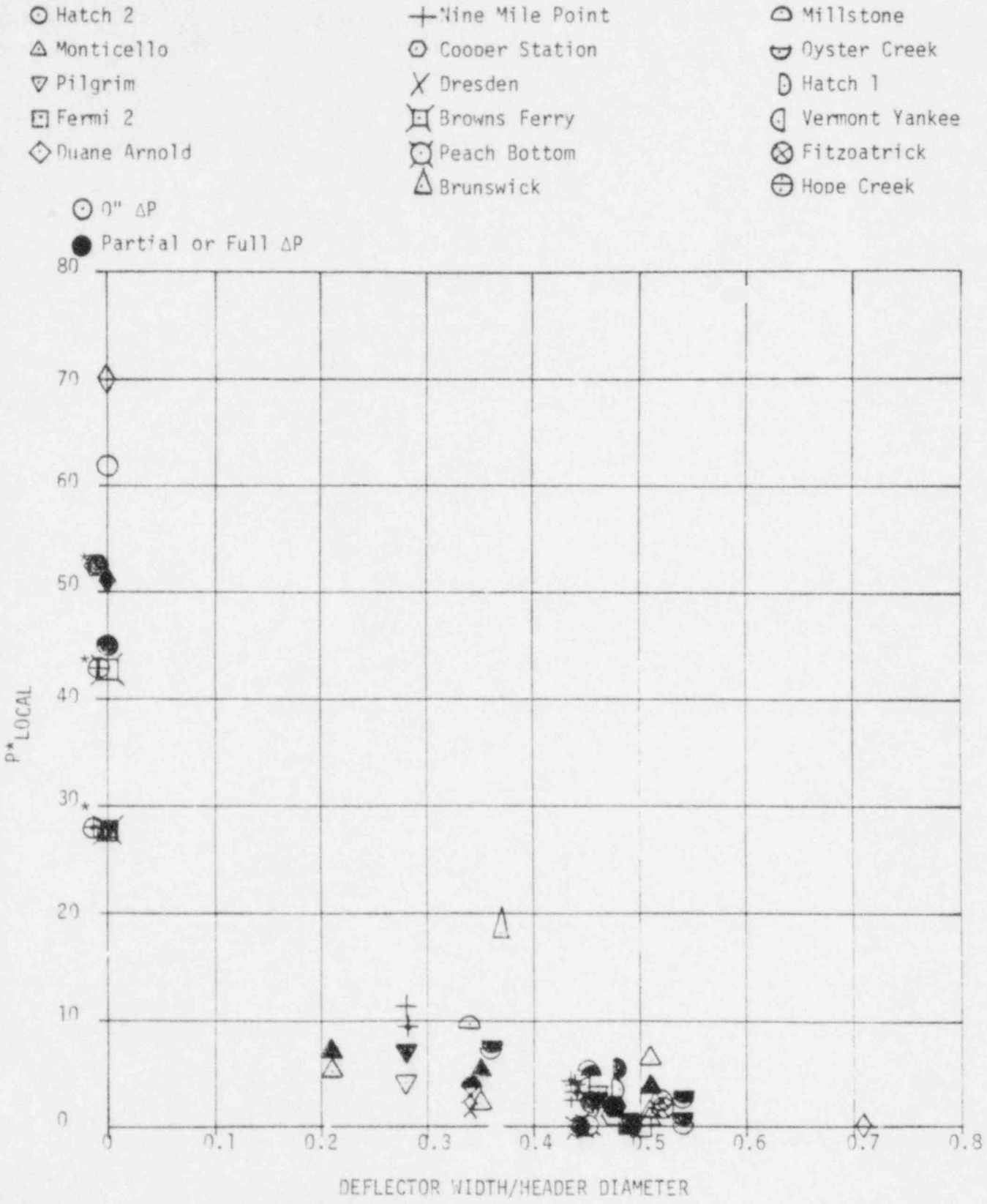

*Displaced for Readability

FIGURE C-2

NORMALIZED MAXIMUM VENT HEADER FORCE VERSUS NORMALIZED DEFLECTOR WIDTH

Tasks 5.5.3-2 and 5.5.4 Tests

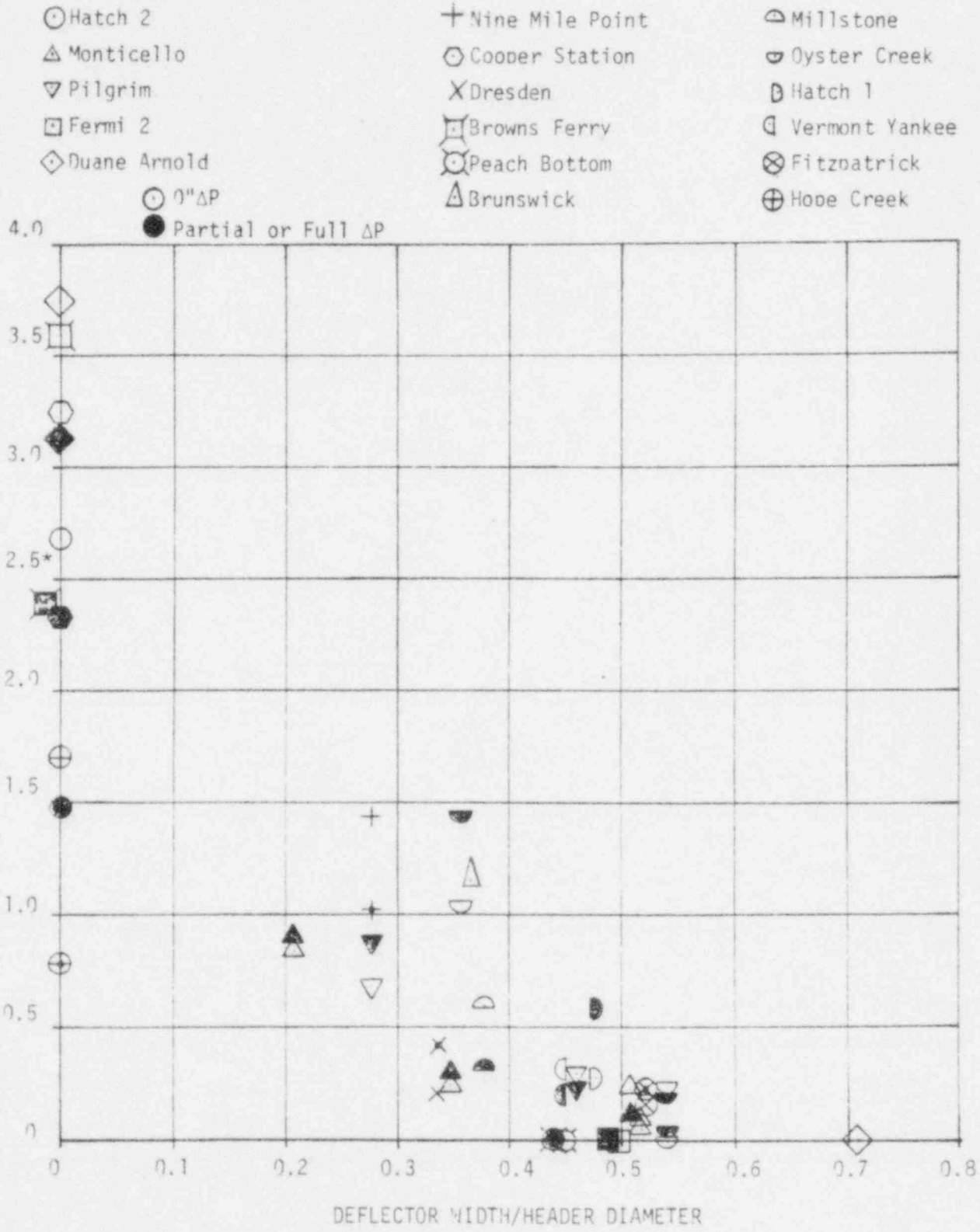

*Disolaced for readability

FIGURE C-3

NORMALIZED IMPACT FORCE IMPULSE VERSUS NORMALIZED DEFLECTOR WIDTH

Tasks 5.5.3-2 and 5.5.4 Tests

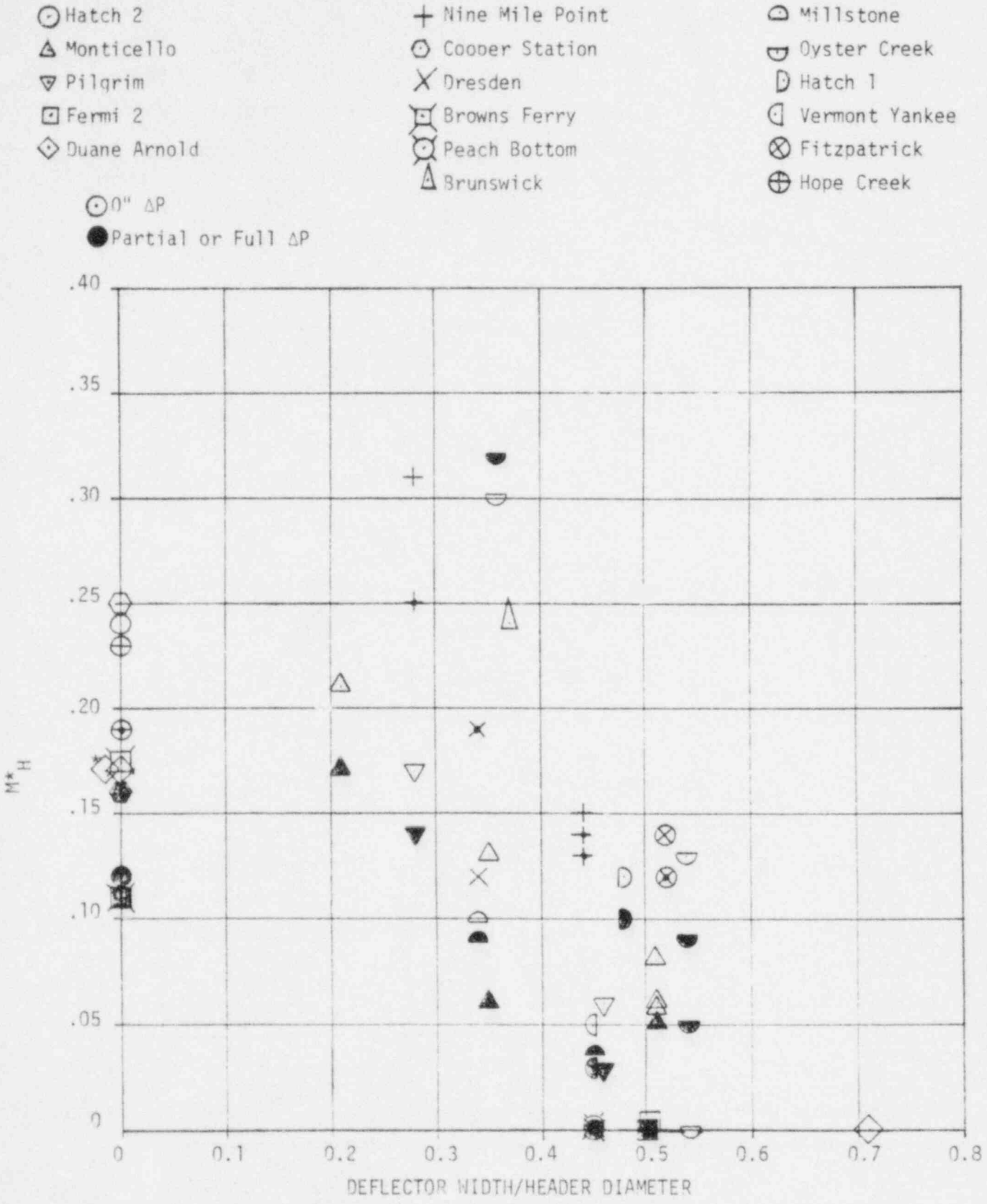

*Displaced for readability

FIGURE C-4

PEAK DOWNFORCE

Task 5.5.3-2 and 5.5.4 Tests

⊙ Hatch 2	+ Nine Mile Point	Millstone
△ Montice'lo	⊙ Cooper Station	Oyster Creek
▽ Pilgrim	X Dresden	Hatch 1
⊡ Fermi 2	⊡ Browns Ferry	Vermont Yankee
◇ Duane Arnold	⊡ Peach Bottom	⊗ Fitzpatrick
		⊕ Hope Creek

Note: (1) Brunswick only tested at zero ΔP.

(2) Solid symbol is used for mean of 4 tests with standard deviation.

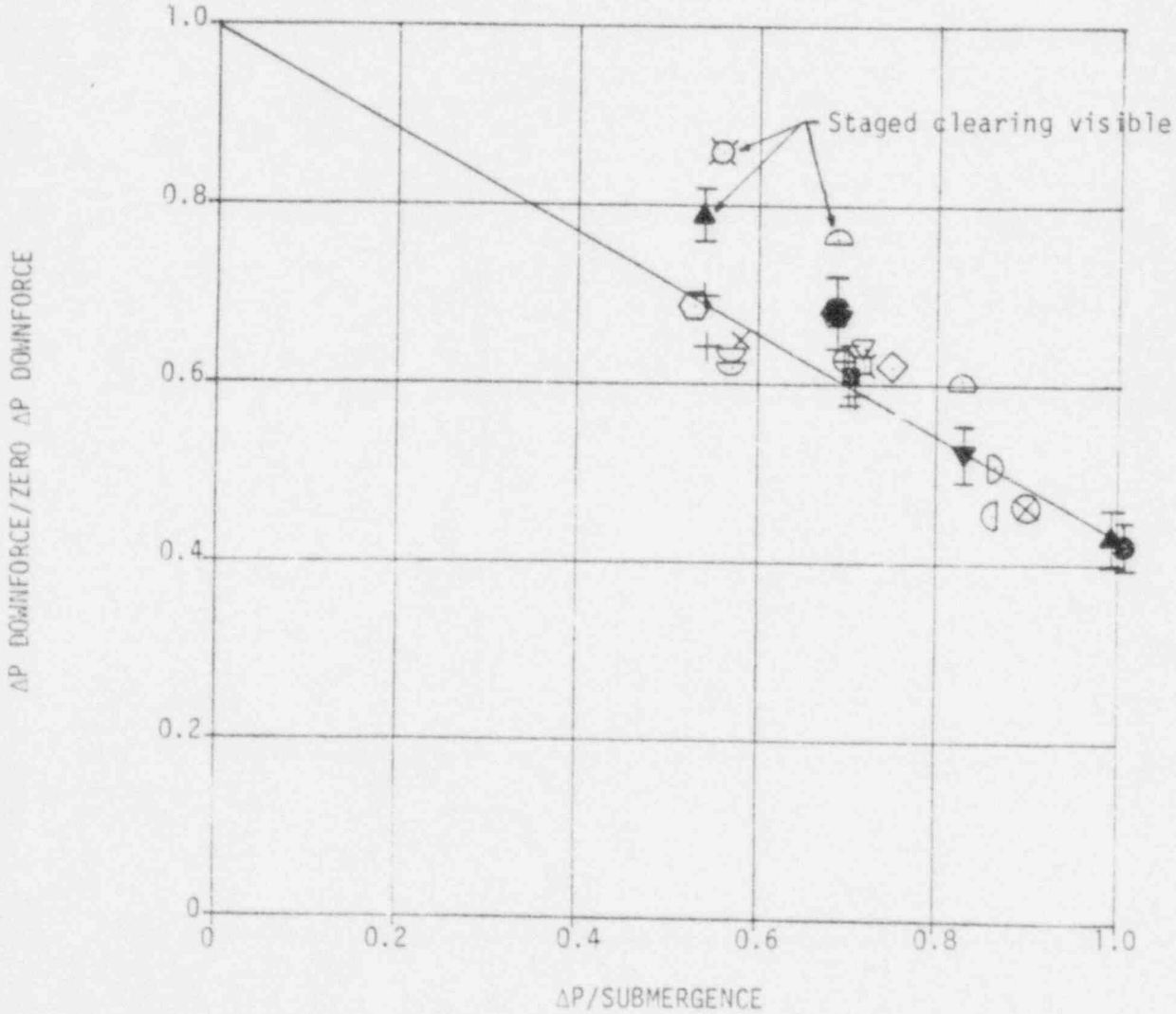

FIGURE C-5

DOWNFORCE IMPULSE
Task 5.5.3-2 and 5.5.4 Tests

- Hatch 2
- Monticello
- Pilgrim
- Fermi 2
- Duane Arnold
- Nine Mile Point
- Cooper Station
- Dresden
- Browns Ferry
- Peach Bottom
- Millstone
- Oyster Creek
- Hatch 1
- Vermont Yankee
- Fitzpatrick
- Hope Creek

Note: (1) Brunswick only tested at zero ΔP.
(2) Solid symbol is used for mean of 4 tests with standard deviation

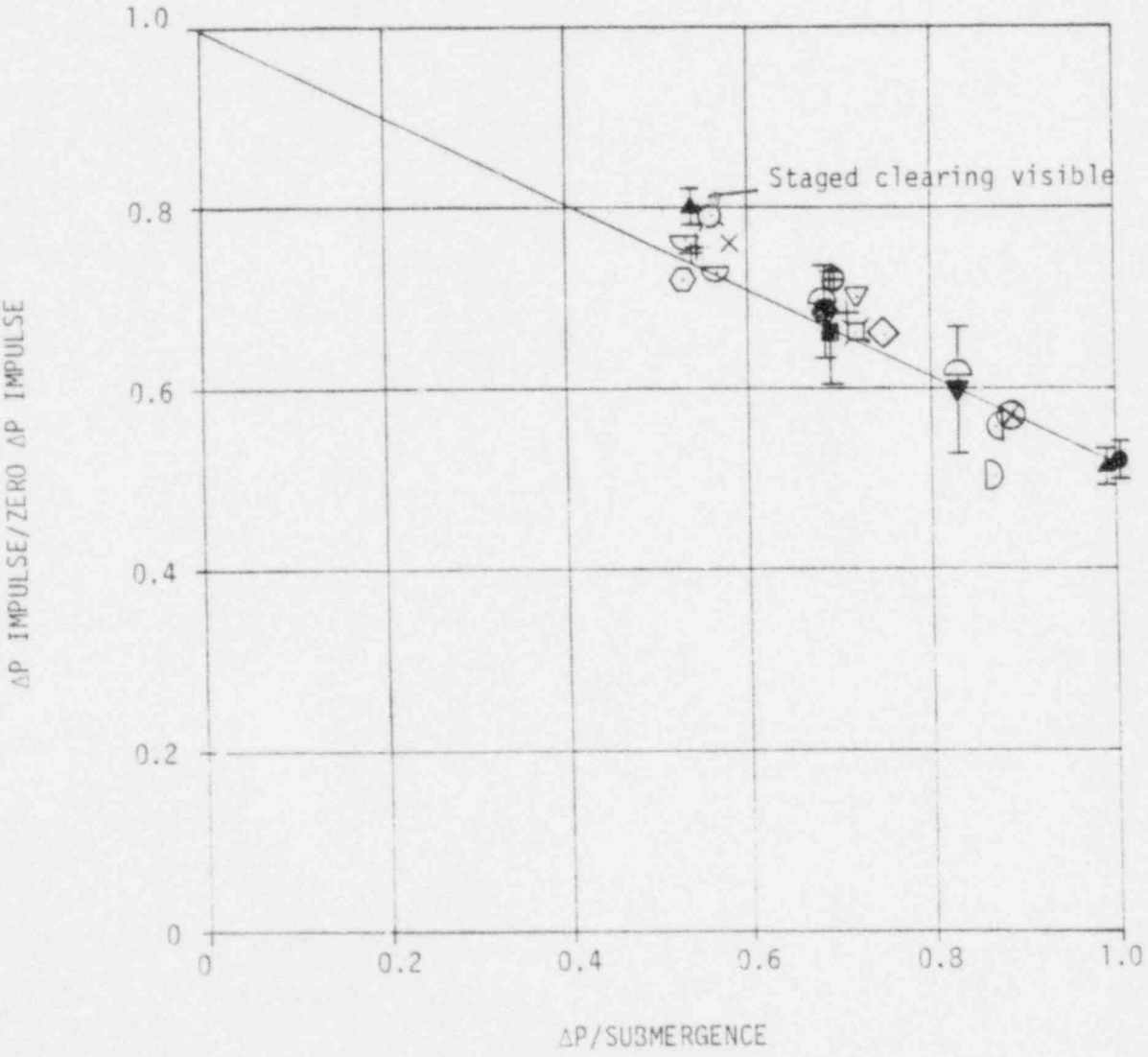

FIGURE C-6

PEAK UPFORCE

Task 5.5.3-2 and 5.5.4 Tests

- Hatch 2
- Monticello
- Pilgrim
- Fermi 2
- Duane Arnold
- Nine Mile Point
- Cooper Station
- Dresden
- Browns Ferry
- Peach Bottom
- Millstone
- Oyster Creek
- Hatch 1
- Vermont Yankee
- Fitzpatrick
- Hope Creek

Note: (1) Brunswick only tested at zero ΔP.

(2) Solid symbol is used for mean of 4 tests with standard deviation.

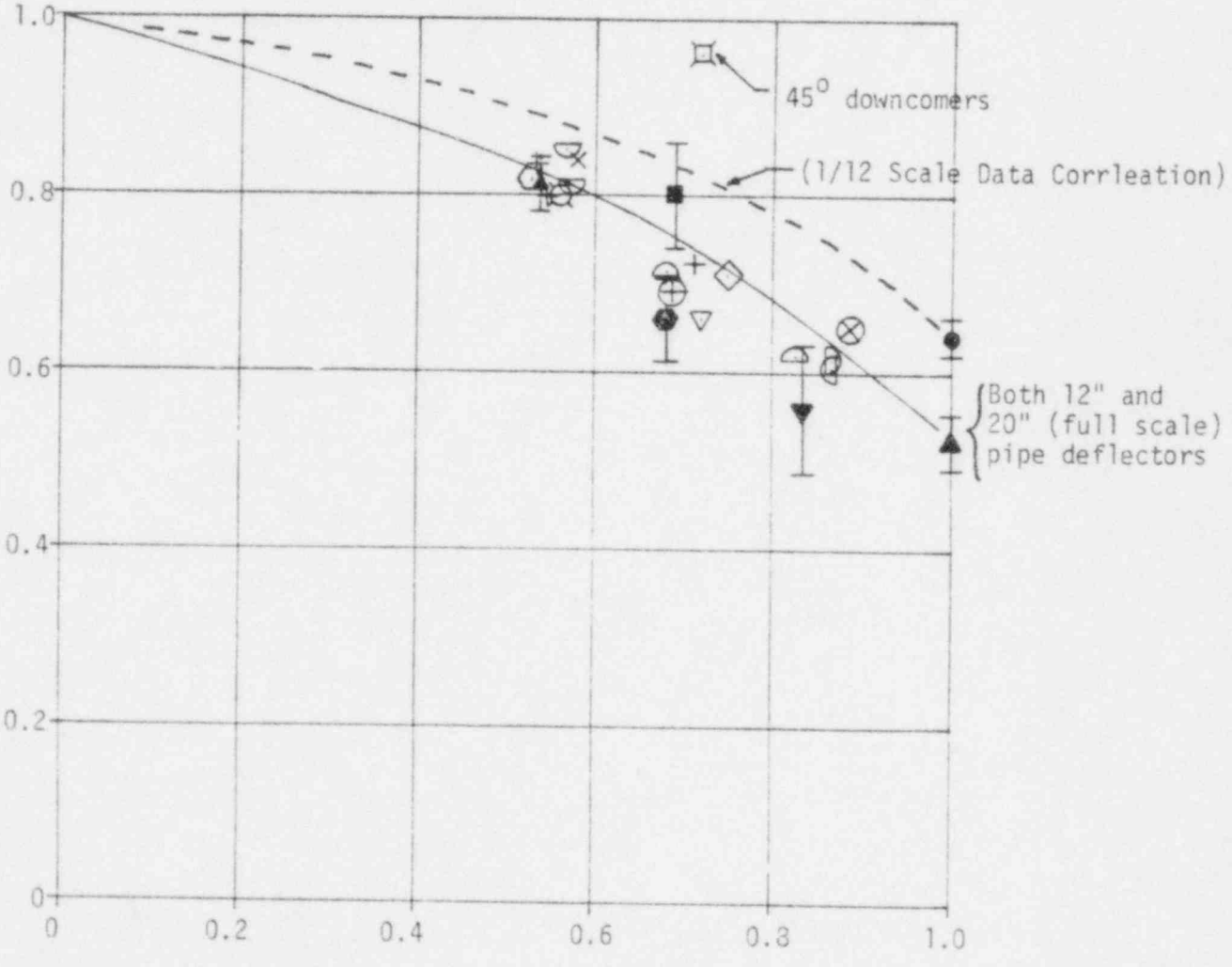

FIGURE C-7

PEAK LOCAL VENT HEADER IMPACT PRESSURE RISE

Tasks 5.5.3-2 and 5.5.4 Tests

- Hatch 2
- Monticello - "T" deflector
- Monticello - 20" pipe deflector
- Monticello - 12" pipe deflector
- Pilgrim - 16" pipe deflector
- Pilgrim - 25.6" winged deflector
- Duane Arnold
- Nine Mile Point - 16" pipe deflector
- Nine Mile Point - 25.6" winged deflector
- Cooper Station - 25.3" winged deflector
- Dresden - 20" pipe deflector
- Browns Ferry
- Peach Bottom
- Millstone
- Millstone - 30" "T" Deflector
- Oyster Creek
- Oyster Creek - 30" "T" deflector
- Hatch 1
- Vermont Yankee
- Fitzpatrick
- Hope Creek

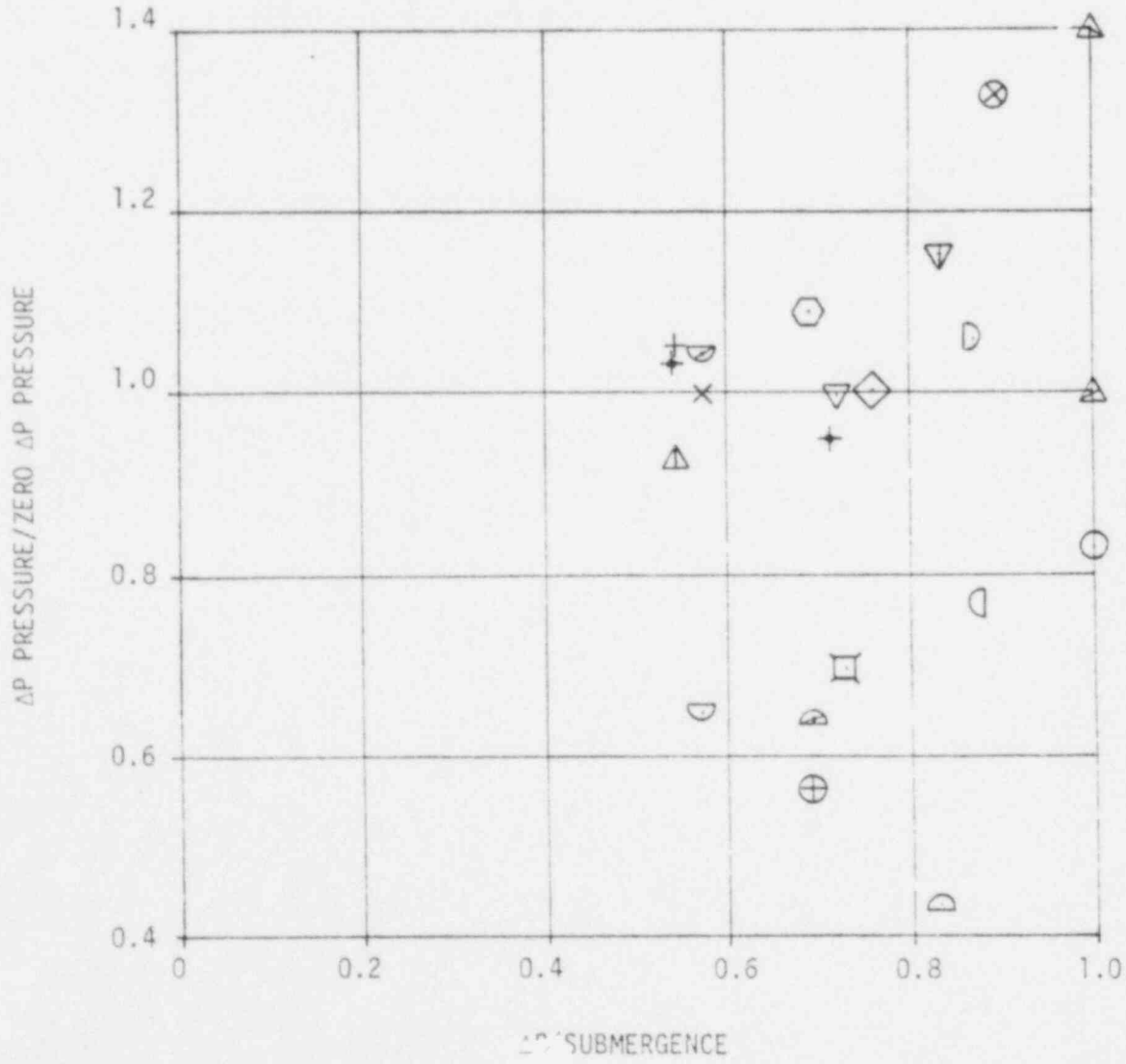

FIGURE C-8

TORUS FORCE FROM PRESSURE INTEGRAL,
WATER INERTIA CORRECTED

DUANE ARNOLD TEST 5

*General Electric Company proprietary information has been deleted.

FIGURE C-9

TORUS FORCE FROM LOAD CELL,
TORUS INERTIA CORRECTED

DUANE ARNOLD TEST 5

*

*General Electric Company proprietary information has been deleted.

FIGURE C-10

TEST INSTRUMENTATION

*

*General Electric Company proprietary information has been deleted.

FIGURE C-11

TORUS WATER PRESSURES

DUANE ARNOLD TEST 5

*General Electric Company proprietary information has been deleted.

FIGURE C-12

EXPANDED OUTPUTS FROM TORUS PRESSURE TRANSDUCERS

DUANE ARNOLD TEST 5

*

*General Electric Company proprietary information has been deleted.

FIGURE

PLACEMENT OF TRANSDUCERS

ON TORUS FLOOR

*

*General Electric Company proprietary information has been deleted.

FIGURE C-14

SEQUENCE OF EVENTS - TEST 5

DUANE ARNOLD

*

*General Electric Company proprietary information has been deleted.

FIGURE C-15

SEQUENCE OF EVENTS - TEST 5, CONT.

DUANE ARNOLD

*

*General Electric Company proprietary information has been deleted.

FIGURE C-16

NET TORUS FORCE FROM LOAD CELL,

NOT CORRECTED FOR INERTIA

Duane Arnold Test 5

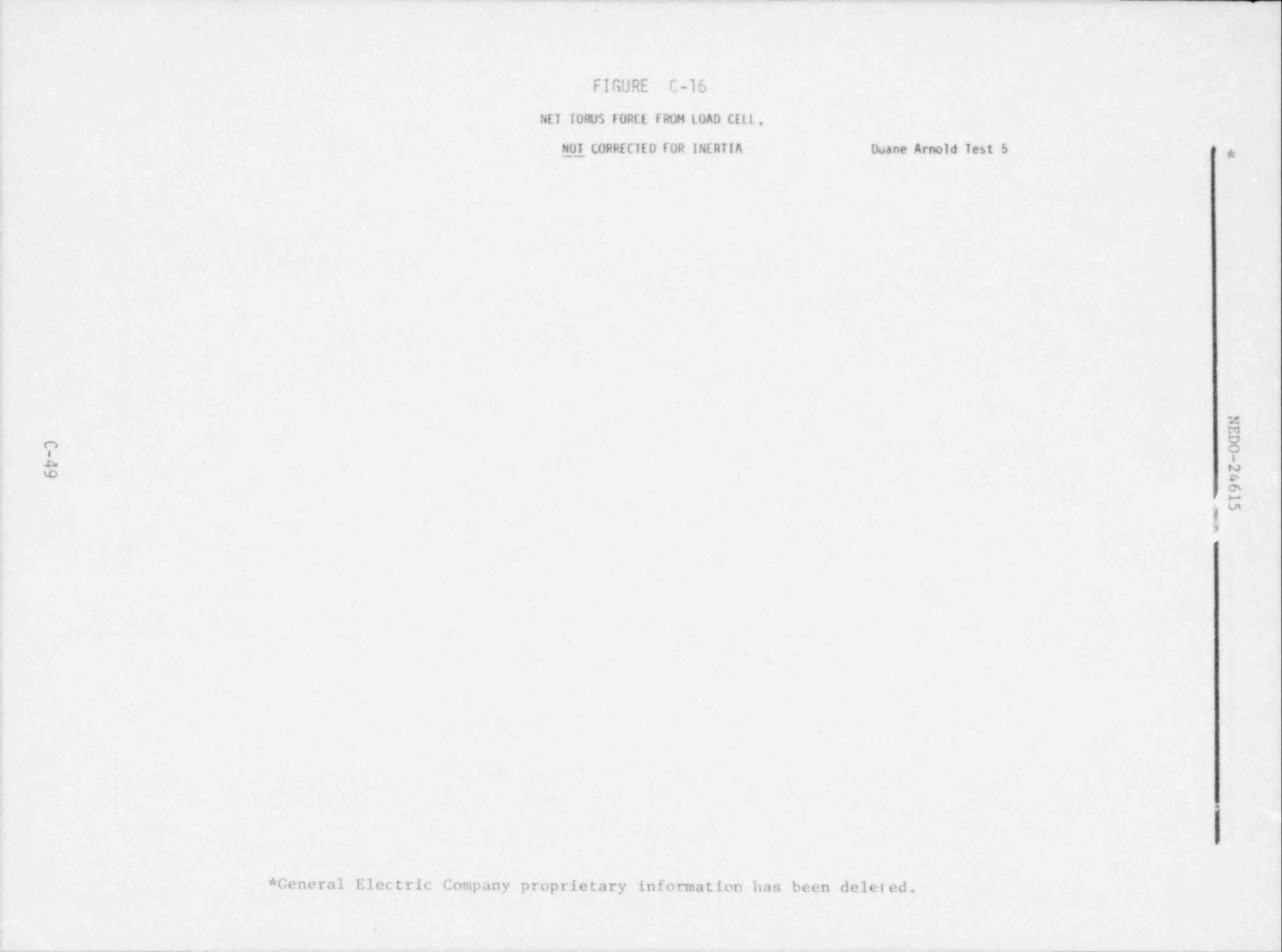

*General Electric Company proprietary information has been deleted.

FIGURE C-17

OSCILLATING TORUS ACCELEROMETER

Duane Arnold - Test 5

*

*General Electric Company proprietary information has been deleted.

FIGURE C-18

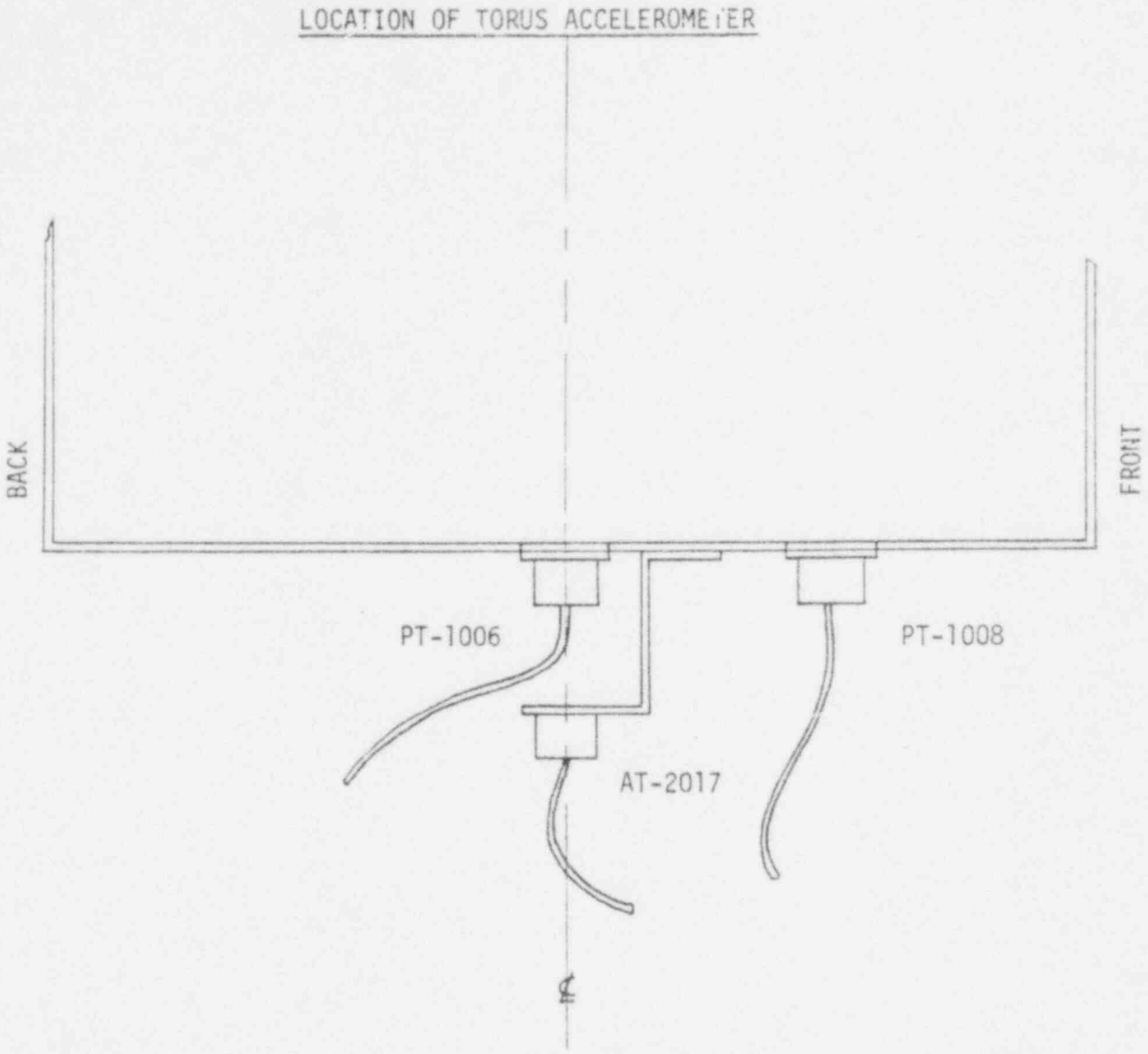

SIDE VIEW - TORUS BOTTOM

FIGURE C-19

EFFECT OF REPEAT TESTS ON PRESSURE OSCILLATIONS

*

*General Electric Company proprietary information has been deleted.

FIGURE C-20

TEST 5 PRESSURE AND ACCELERATION

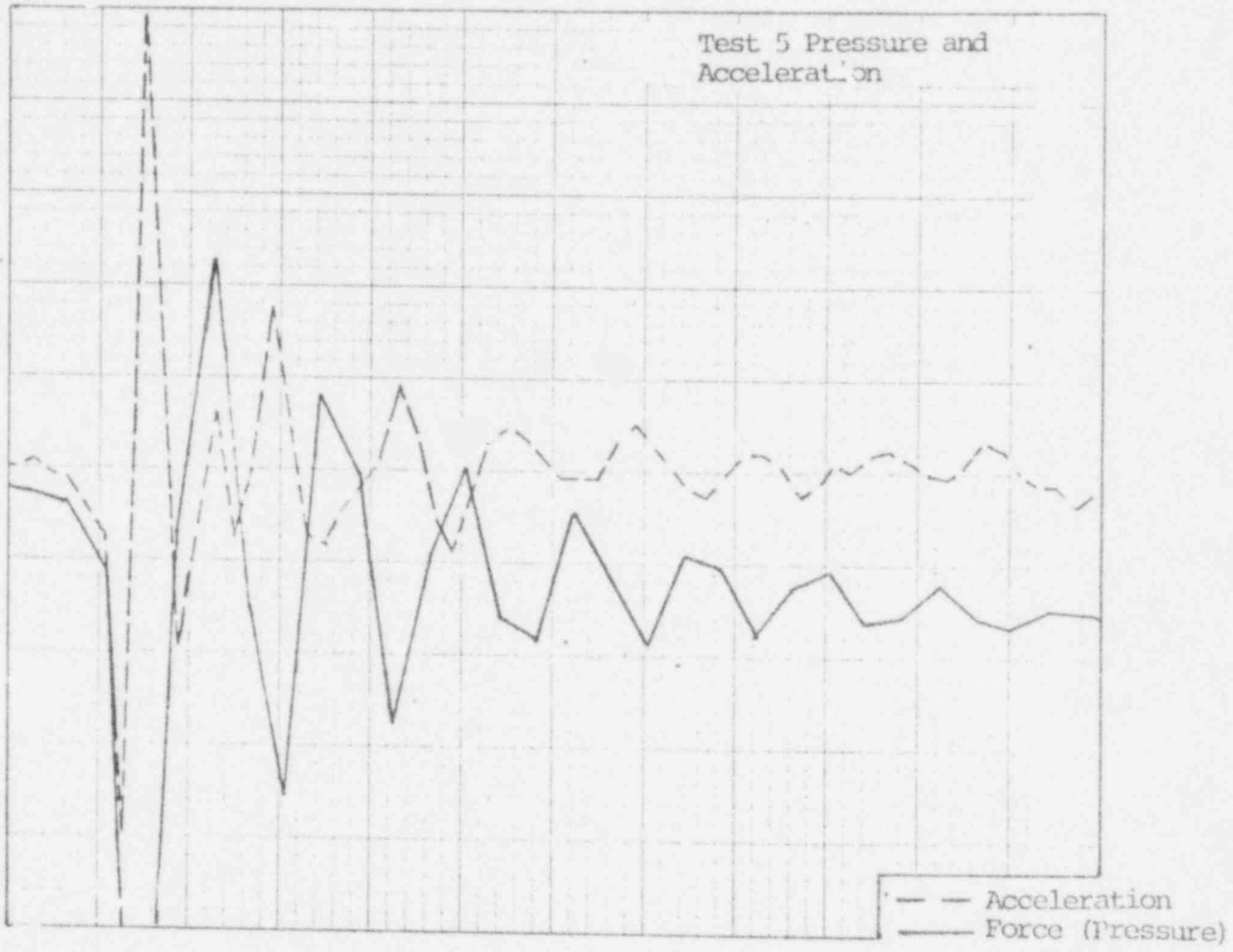

TIME

FIGURE C-21

EXPANDED LOAD CELL PLOT, UNCORRECTED

Duane Arnold Test 5

*

*General Electric Company proprietary information has been deleted.

FIGURE C-22

ACCELERATION PLOTS

*

*General Electric Company proprietary information has been deleted.

FIGURE C-23

NET TORUS FORCE FROM PRESSURE INTEGRAL CORRECTED FOR POOL INERTIA

Task 5.5.4 Oyster Creek Test 7 (Modified)

*

*General Electric Company proprietary information has been deleted.

FIGURE C-24

NET TORUS FORCE FROM LOAD CELL CORRECTED FOR INERTIA

Task 5.5.4 Oyster Creek Test 7 (Modified)

*

*General Electric Company proprietary information has been deleted.

FIGURE C-25

ACCELERATION PLOTS

*

*General Electric Company proprietary information has been deleted.

FIGURE C-26

NET TORUS FORCE FROM LOAD CELL CORRECTED FOR INERTIA

Task 5.5.4 Oyster Creek Test 15 (Modified)

*

*General Electric Company proprietary information has been deleted.

FIGURE C-27

NET TORUS FORCE FROM PRESSURE INTEGRAL CORRECTED FOR POOL INERTIA

Task 5.5.4 Oyster Creek Test 15 (Modified)

*

*General Electric Company proprietary information has been deleted.

TABLE C-1

EQUATIONS FOR CONVERTING MEASURED VALUES TO EQUIVALENT 1/4-SCALE VALUES

(1) Peak Average Downforce Pressure = Mean Peak Downforce/$Area_T$ (8) X 0.2500/SF (9)

(2) Average Downforce Impulse per Unit Area (psi-sec) = Mean Downforce Impulse/$Area_T$ X $(0.2500/SF)^{7/2}$

(3) Peak Average Upforce Pressure = Mean Peak Upforce/$Area_T$ X 0.2500/SF

(4) Vent Impact Velocity = Mean Vent Impact Velocity X 0.2500/SF

(5) Average Vent Impact Impulse per Unit Area (psi-sec) = Mean Vent Impact Impulse*/$Area_H$ X $(0.2500/SF)^{7/2}$

(6) Peak Average Vent Impact Pressure = Mean Peak Vent Impact Force**/$Area_H$ (10) X 0.2500/SF

(7) Peak Local Impact Pressure Rise = Peak Local Impact Pressure Rise X 0.2500/SF

(8) $Area_T$ = QSTF Torus Projected Area = 93" X Torus Width

(9) SF = Scale Factor = 93"/Plant Torus Minor Diameter, in

(10) $Area_H$ = QSTF Header Projected Area = Head OD X Length

*from load cell

**from pressure integral

TABLE C-2

SOME BENCHMARK VALUES FOR

QUARTER-SCALE COMPARISON OF PLANT UNIQUE TEST DATA

Test Conditions (Full Scale)	Reference Plant STP	QSTF TASK 5.5.1 Large Orifice	QSTF TASK 5.5.1 Medium Orifice	TASK 5.5.3-1 Reference Condition
Submergence, ft.	4	4	4	3'4"
ΔP, ft.	0	0	4	3'4"
Drywell $\dot{P}$, psi/sec	56	69.2	47.0	56
Deflector	None	None	None	None
Test Data				
(8) Torus Area, in^2		2027	2027	2027
(9) Scale Factor		0.2500	0.2500	0.2500
(10) Header Area, in^2		318	318	318

*

*General Electric Company proprietary information has been deleted.

TABLE C-3[a]

QUARTER-SCALE COMPARISON OF PLANT UNIQUE TEST DATA

Task 5.5.4 Tests

Test Conditions (Full Scale)	Monticello		Duane Arnold
	Tests 17 - 20	Tests 21 - 24	Tests 6 - 9
Submergence, ft.	3.58	3.0	3.33
ΔP, ft.	0	0	0
Drywell $\dot{P}$, psi/sec	72.5	72.5	46.1
Deflector	14" Pipe with "T" Sections 29" Wide		Wedge Deflector 30" Wide
(8) Torus Area, in^2	2027		2194
(9) Scale Factor	0.2801		0.3019
(10) Header Area, in^2	343		297(253)*
(11) Pool Area/Vent Area	29.8		55.5

*

*General Electric Company proprietary information has been deleted.

TABLE C-3b

QUARTER-SCALE COMPARISON OF PLANT UNIQUE TEST DATA

Task 5.5.4 Tests

Test Conditions (Full Scale)	Pilgrim	
	Test 6 - 9	Tests 10 - 13
Submergence, ft.	4.0	4.0
ΔP, ft.	3.46	0
Drywell $\dot{P}$, psi/sec	67.4	67.4
Deflector	16" Pipe with Angles 25.61" wide	

(8)	Torus Area, in^2	1983
(9)	Scale Factor	0.2627
(10)	Header Area, in^2	310
(11)	Pool Area/Vent Area	31.8

*General Electric Company proprietary information has been deleted.

TABLE C-3c

QUARTER-SCALE COMPARISON OF PLANT UNIQUE TEST DATA

Task 5.5.4 Tests

	Oyster Creek			
Test Conditions (Full Scale)	Tests 6 - 9	Test 10	Tests 11 - 14	Test 15
Submergence, ft.	4.06	4.06	3.00	3.00
ΔP, ft	2.31	0	2.31	0
Drywell $\dot{P}$, psi/sec	54.5	54.5	54.5	54.5
Deflector	------16" Pipe with "T" Sections 30" Wide--------			

*

(8)	Torus Area, in^2	1533
(9)	Scale Factor	0.2583
(10)	Header Area, in^2	226
(11)	Pool Area/Vent Area	27.2

*General Electric Company proprietary information has been deleted.

TABLE C-3d

QUARTER-SCALE COMPARISON OF PLANT UNIQUE TEST DATA

Task 5.5.4 Tests

Test Conditions (Full Scale)	Nine Mile Point			
	Tests 6 - 9	Test 10	Tests 11 - 14	Tests 15 - 18
Submergence, ft	4.25	4.25	3.25	3.25
ΔP, ft	2.31	0	2.31	0
Drywell $\dot{P}$, psi/sec	54.0	54.0	54.0	54.0
Deflector	-------16" Pipe with Angles 25.61" Wide----------			

*

(8)	Torus Area, in^2	2086
(9)	Scale Factor	0.2870
(10)	Header Area, in^2	358
(11)	Pool Area/Vent Area	26.7

*General Electric Company proprietary information has been deleted.

TABLE C-3e

QUARTER-SCALE COMPARISON OF PLANT UNIQUE TEST DATA

Task 5.5.4 Tests

	Millstone		Cooper Station	
Test Conditions (Full Scale)	Tests 6 - 9	Test 10	Tests 6 - 9	Tests 10 - 13
Submergence, ft	3.33	3.33	3.33	3.33
ΔP, ft	2.31	0	2.31	0
Drywell $\dot{P}$, psi/sec	66.9	66.9	74.0	74.0
Deflector	16" Pipe with Angles 25.6" Wide		16" Pipe with Angles 25.3" Wide	

*

(8)	Torus Area, in^2	1983	2436
(9)	Scale Factor	0.2627	0.2696
(10)	Header Area, in^2	310	347
(11)	Pool Area/Vent Area	32.1	40.1

*General Electric Company proprietary information has been deleted.

TABLE C-4a

NON-DIMENSIONALIZED VENT HEADER IMPACT DATA

Task 5.5.4 Tests

Plant	Monticello		Duane Arnold	Pilgrim		Oyster Creek			
Deflector	8.15" Wide "T" Deflector (29" Full Scale)		9.06" Wide Wedge Deflector (30" Full Scale)	6.73" Wide Winged Deflector (25.61" Full Scale)		7.75" Wide "T" Deflector (30" Full Scale)			
Header Diameter (ft)	1.34		1.07	1.26		1.20			
Header Length (ft)	1.77		1.92	1.68		1.31			
Submergence (in)	12.03	10.08	12.08	10.25		12.59		9.30	
	Tests 17-20	Tests 21-24	Tests 6-9	Tests 6-9	Tests 10-13	Tests 6-9	Test 10	Tests 11-14	Test 15
P^*_{LOCAL} (dimensionless unit)	1.2	1.1	0.0	3.5	3.3	2.9	2.3	0.7	0.0
F^* (dimensionless unit)	0.07	0.06	0.0	0.24	0.31	0.21	0.23	0.05	0.0
M^*_H (dimensionless unit)	0.08	0.06	0.0	0.03	0.06	0.09	0.13	0.05	0.0

P^*_{LOCAL} = (Maximum Local Impact Pressure x $2g_c$ x 144)/([Impact Velocity]^2 x Water Density)

F^* = (Maximum Vent Header Force x $2g_c$)/(Projected Area x [Impact Velocity]^2 x Water Density)

M^*_H = (Impact Force Impulse x g_c)/([π x Diameter^2/4] x Length x [Impact Velocity] x Water Density)

*General Electric Company proprietary information has been deleted.

TABLE C- 4b

NON-DIMESIONALIZED VENT HEADER IMPACT DATA

Task 5.5.4 Tests

Plant	Nine Mile Point				Millstone		Cooper Station	
Deflector	7.35" Wide Winged Deflector (25.6" Full Scale)				6.73" Wide Winged Deflector (25.6" Full Scale)		6.82" Wide Winged Deflector (25.3" Full Scale)	
Header Diameter (ft)	1.39				1.26		1.14	
Header Length (ft.)	1.79				1.71		2.12	
Submergence (in)	14.64		11.19		10.50		10.78	
	Tests 6 - 9	Test 10	Tests 11-14	Tests 15-18	Tests 6 - 9	Test 10	Tests 6 - 9	Tests 10-13
P^*_{LOCAL} dimensionless unit	4.3	4.1	3.8	4.3	3.4	5.4	1.1	1.0
F*(dimensionless unit)	0.33	0.29	0.41	0.43	0.31	0.32	0.12	0.07
M^*_H(dimensionless unit)	0.14	†††	0.13	0.15	0.03	†††	---	---

P^*_{LOCAL} = (Maximum Local Impact Pressure x $2g_c$x144)/([Impact Velocity]^{2}x Water Density)

F* = (Maximum Vent Header Force x $2g_c$)/(Projected Area x [Impact Velocity]^{2}x Water Density)

M^*_H = (Impact Force Impulse x g_c)/([π x Diameter^2/4] x Length x Impact Velocity x Water Density)

†††Not applicable because impulse from corrected load cell includes deflector load.

---Impulse from corrected load cell is not available.

*General Electric Company proprietary information has been deleted.

TABLE C-5

COMPARISON OF TASK 5.5.4 TEST DATA WITH

ESTIMATES FROM TASK 5.5.3-2 REGRESSION ANALYSIS

		Peak Downforce		(Actual - Predicted) Variation in
		Actual	Predicted	Standard Deviations**
Monticello	17 - 20	4573 lb_f*	5037 lb_f*	-1.5*
	21 - 24	4323	4768	-1.5
Duane Arnold	6 - 9	1950	4134	-7.0***
Pilgrim	6 - 9	2438	2295	0.5
	10 - 13	4724	4739	-0.1
Oyster Creek	6 - 9	2808	2780	0.1
	10	4534	4373	0.5
	11	1486	1698	-0.7
	12 - 14	1487	1716	-0.6
	15	3227	3921	-2.2
Nine Mile Point	6 - 9	2752	3231	-1.5
	10	4399	4781	-1.2
	11 - 14	2196	2176	0.0
	15 - 18	3723	4215	-1.6
Millstone	6 - 9	2393	2845	-1.5
	10	3904	4876	-0.4
Cooper Station	6 - 9	2559	3336	-2.5
	10 - 13	4948	5376	-1.3

*Values given are averages for tests at the same conditions

**90% of the variations are expected to lie within approximately two standard deviations of the mean if the "Actual" comes from the distribution which underlies the "Predicted".

***As discussed in the text, the correlations were developed for dual downcomer tests. They do not therefore, provide particularly good predictions for the Duane Arnold single downcomer geometry.

TABLE C-6

COMPARISON OF TASK 5.5.4 TEST DATA WITH

ESTIMATES FROM TASK 5.5.3-2 REGRESSION ANALYSIS

		Peak Upforce		(Actual - Predicted)
		Actual	Predicted	Variation in Standard Deviations**
Monticello	17 - 20	2441 lb_f*	2400 lb_f*	0.2*
	21 - 24	1832	1996	-0.7
Duane Arnold	6 - 9	883	1939	-4.1***
Pilgrim	6 - 9	1275	1206	0.3
	10 - 13	2246	2137	0.5
Oyster Creek	6 - 9	1617	1822	-0.8
	10	2008	2429	-1.6
	11	913	815	0.4
	12 - 14	849	820	0.1
	15	1196	1658	-1.8
Nine Mile Point	6 - 9	2086	2090	-0.1
	10	2592	2679	-0.3
	11 - 14	1332	1140	0.8
	15 - 18	1852	1915	-0.3
Millstone	6 - 9	1954	1453	1.9
	10	2790	2225	2.2
Cooper Station	6 - 9	1578	1693	-0.5
	10 - 13	2402	2473	-0.2
Generic Sensitivity	1 - 8	1042	995	0.2
	29 - 32	1540	1471	0.3
	33 - 36	961	1743	-3.0

*Values given are averages for tests at the same conditions

**90% of the variations are expected to lie within approximately two standard deviations of the mean if the "Actual" comes from the distribution which underlies the "Predicted".

***As discussed in the text, the correlations were developed for dual downcomer tests. They do not, therefore, provide particularly good predictions for the Duane Arnold single downcomer geometry.

TABLE C-7

COMPARISON OF TASK 5.5.4 TEST DATA WITH

ESTIMATES FROM TASK 5.5.3-2 REGRESSION ANALYSIS

		Downforce Impulse		(Actual - Predicted)
		Actual	Predicted	Variation in Standard Deviations**
Monticello	17 - 20	314 lb_f*	291 lb_f*	1.5*
	21 - 24	266	252	1.0
Duane Arnold	6 - 9	143	202	-3.8***
Pilgrim	6 - 9	160	138	1.4
	10 - 13	268	270	-0.2
Oyster Creek	6 - 9	217	236	-1.2
	10	285	323	-2.5
	11	116	126	-0.6
	12 - 14	129	127	0.2
	15	209	247	-2.5
Nine Mile Point	6 - 9	229	245	-1.0
	10	305	329	-1.6
	11 - 14	162	144	1.2
	15 - 18	239	256	-1.1
Millstone	6-9	191	187	0.3
	10	272	299	-1.7
Cooper Station	6 - 9	201	191	0.7
	10 - 13	295	302	-0.5

*Values given are averages for tests at the same conditions

**90% of the variations are expected to lie within approximately two standard deviations of the mean if the "Actual" comes from the distribution which underlies the "Predicted".

***As discussed in the text, the correlations were developed for dual downcomer tests. They do not, therefore, provide particularly good predictions for the Duane Arnold single downcomer geometry.

TABLE C-8

COMPARISON OF TASK 5.5.4 TEST DATA WITH

ESTIMATES FROM TASK 5.5.3-2 REGRESSION ANALYSIS

		Time to Peak Downforce		(Actual - Predicted) Variation in Standard Deviations**
		Actual	Predicted	
Monticello	17 - 20	1[illegible] lb_f*	130 lb_f*	-0.5*
	21 - 24	110	129	-2.0
Duane Arnold	6 - 9	141	137	0.4***
Pilgrim	6 - 9	92	74	1.9
	10 - 13	121	124	-0.3
Oyster Creek	6 - 9	94	100	-0.6
	10	147	136	1.1
	11	65	81	-1.7
	12 - 14	64	81	-1.8
	15	126	129	-0.3
Nine Mile Point	6 - 9	99	114	-1.6
	10	149	148	0.1
	11 - 14	102	97	0.5
	15 - 18	131	142	-1.2
Millstone	6 - 9	66	89	-2.5
	10	118	131	-1.4
Cooper Station	6 - 9	67	82	-1.6
	10 - 13	118	124	-0.6

*Values given are averages for tests at the same conditions.
**90% of the variations are expected to lie within approximately two standard deviations of the mean if the "Actual" comes from the distribution which underlies the "Predicted".
***As discussed in the text, the correlations were developed for dual downcomer tests. They do not therefore, provide particularly good predictions for the Duane Arnold single downcomer geometry.

TABLE C-9

COMPARISON OF TASK 5.5.4 TEST DATA WITH
ESTIMATES FROM TASK 5.5.3-2 REGRESSION ANALYSIS

		Peak Downforce		(Actual - Predicted)
		Actual	Predicted	Variation in Standard Deviations**
Monticello	17 - 20	264 lb_f*	263 lb_f*	0.3
	21 - 24	239	233	0.8
Duane Arnold	6 - 9	287	269	2.5***
Pilgrim	6 - 9	184	186	-0.4
	10 - 13	265	254	1.4
Oyster Creek	6 - 9	248	242	0.9
	10	304	300	0.5
	11	192	190	0.3
	12 - 14	192	190	0.2
	15	256	247	1.2
Nine Mile Point	6 - 9	259	254	0.7
	10	306	311	-0.7
	11 - 14	213	203	1.3
	15 - 18	271	260	1.4
Millstone	6 - 9	197	197	0.1
	10	258	253	0.7
Cooper Station	6 - 9	182	193	-1.4
	10 - 13	245	249	-0.5
Generic Sensitivity	1 - 8	159	181	-3.0
	29 - 32	209	212	-0.4
	33 - 36	171	205	-4.2

*Values given are averages for tests at the same conditions
**90% of the variations are expected to lie within approximately two standard deviations of the mean if the "Actual" comes from the distribution which underlies the "Predicted".
***As discussed in the text, the correlations were developed for dual downcomer tests. They do not, therefore, provide particularly good predictions for the Duane Arnold single downcomer geometry.

TABLE C-10

COMPARISON OF TASK 5.5.4 TEST DATA WITH

ESTIMATES FROM TASK 5.5.3-2 REGRESSION ANALYSIS

(Actual - Predicted)

		Peak Vent Header Force		
		Actual	Predicted	Variation in Standard Deviations**
Monticello	17 - 18	64 lb_f*	-17 lb_f*	1.1*
	21 - 22	71	-199	3.5
Duane Arnold	6 - 7	0	-570	7.3***
Pilgrim	6 - 7	130	-347	6.2
	10 - 11	157	-347	6.5
Oyster Creek	6 - 7	71	41.5	0.4
	10	95	41.5	0.7
	11	18	41.5	-0.3
	12	14	41.5	-0.4
	15	0	41.5	-0.5
Nine Mile Point	6 - 7	88	129.1	-0.5
	10	99	129.1	-0.4
	11 - 12	119	129.1	-0.2
	15 - 16	139	129.1	0.2
Millstone	6 - 7	94	178	-1.1
Cooper Station	6 - 7	84	32	0.7
	10 - 11	16	32	-0.2

*Values given are averages for tests at the same conditions

**90% of the variations are expected to lie within approximately two standard deviations of the mean if the "Actual" comes from the distribution which underlies the "Predicted".

***As discussed in the text, the correlations were developed for dual downcomer tests. They do not, therefore, provide particularly good predictions for the Duane Arnold single downcomer geometry.

TABLE C-11

COMPARISON OF TASK 5.5.4 TEST DATA WITH

ESTIMATES FROM TASK 5.5.3-2 REGRESSION ANALYSIS

(Actual - Predicted)

		Peak Vent Header Impulse		
		Actual	Predicted	Variation in Standard Deviations**
Monticello	17 - 18	1.9 lb_f*	5.2 lb_f*	-1.4 lb_f
	21 - 22	2.3	5.2	-1.3
Duane Arnold	6 - 7	0	-7.6	3.3***
Pilgrim	6 - 7	2.6	4.2	-0.7
	10 - 11	2.3	4.4	-0.9
Oyster Creek	6 - 7	3.5	-1.2	2.0
	10	5.8	-1.2	3.0
	11	1.3	-1.6	1.2
	12	2.9	-0.9	1.6
	15	4.5	-1.4	2.5
Nine Mile Point	6-7	6.4	1.0	2.3
	10	13.5	1.3	5.2
	11 - 12	6.4	0.6	2.1
	15 - 16	7.2	0.8	2.7
Millstone	6 - 7	1.6	5.3	-1.6
Cooper Station	6 - 7	0.0	5.4	-2.3
	10 - 11	0.0	6.0	-2.5

*Values given are averages for tests at the same conditions.

**90% of the variations are expected to lie within approximately two standard deviations of the mean if the "Actual" comes from the distribution which underlies the "Predicted".

***As discussed in the text, the correlations were developed for dual downcomer tests. They do not, therefore, provide particularly good predictions for the Duane Arnold single downcomer geometry.

TABLE C-12

CORRELATION MATRIX FOR ALL VARIABLES IN REGRESSIONS

*

*General Electric Company proprietary information has been deleted.

TABLE C-13

COMPARISON OF RESULTS OF NEW REGRESSIONS

TO PREVIOUS STUDY FOR TORUS VARIABLES

*

*General Electric Company proprietary information has been deleted.

TABLE C-14

COMPARISON OF RESULTS OF NEW REGRESSIONS

TO PREVIOUS STUDY FOR VENT HEADER VARIABLES

*

*General Electric Company proprietary information has been deleted.

APPENDIX D

MEASUREMENT UNCERTAINTY ANALYSIS

An uncertainty analysis was performed to ensure that the error bands associated with calculated test results fell within acceptable limits. Many of the important test values (such as enthalpy flow) were calculated from several measured test parameters. While each of the individual parameters has its own error band, the combination of several different parameters has an entirely different error band. In addition, the errors associated with a single sensor may not reflect the total error band of the data from the system using that sensor.

To arrive at the compound error bands, each sensor system was analyzed as a number of different sources of error. For example, a pressure transducer would be assumed to have a specified error inherent in its construction, an analog to digital conversion error, a signal conditioning error and a frequency response error. The total uncertainty for this single sensor was assumed to be the square root of the sum of the squares of errors contributed by each component part.

To combine the errors of several different sensors in order to achieve a calculated total value, it was assumed that each of the independent errors was normally distributed over its range and the calculated value was a linear function of its independent variables.

Table D-1 lists the major variables of interest, their nominal values, range of values during the Supplemental Plant Unique Tests, and uncertainty intervals based on a 95% confidence level.

TABLE D-1

SUMMARY OF UNCERTAINTY ANALYSIS

TASK 5.5.4 SUPPLEMENTAL PLANT UNIQUE TESTS

Variable	Nominal Value	Range of Variable	% Uncertainty of Nominal Value (95% Confidence Level)
Measured Values:			
Drywell Orifice Upstream Pressure, psia	60	45→75	±0.12
Wetwell Pressure, psia	7.5	4.2→16.0	±0.4
Drywell Pressure, psia	7.5	3.7→16.0	±0.4
Torus Load Cell, lbf Maximum Downforce	17,000	13,000→ 19,000	±0.15
Maximum Upforce	8,000	9,000→ 6,000	±0.31
Vent Header Load Cell, lbf	300	0→400	±3.3
Downcomer Orifice ΔP, psid	3.5	2.5→5.0	±1.4
Torus Accelerometer, g	0.15	-0.3→+0.3	±6.7
Downcomer Air Temperature °F	115	100→135	±1.4
Vent Header Impact Pressure, psia	10	0→15	±5.0
Vent Header Accelerometer, g	0.8	-1.0→+1.0	±12.5
Initial Submergence, Inches	12.0	9.3 →14.6	±0.6
Drywell/Wetwell ΔP, in. of water	8.5	0→8.5	±0.8
Vent Resistance Calibration:			
Total fL/D	16.0	13.25→18.0	6.0

TABLE D-1 (continued)

SUMMARY OF UNCERTAINTY ANALYSIS

TASK 5.5.4 SUPPLEMENTAL PLANT UNIQUE TESTS

Variable	Nominal Value	Range of Variable	% Uncertainty of Nominal Value (95% Confidence Level)
Calculated Values:			
Critical Nozzle Flow Rate, lbm/sec	7.7	6.9→10.6	±1.8
Enthalpy Flow into Pool, Btu/sec (based on downcomer orifice differential pressure and upstream temperature)	450	300→700	±4.8
Spatial Integral of Torus Pressures (force), lbf			
Maximum Downforce	4,700	2,100→ 6,400	±1.6
Maximum Upforce	2,700	950 → 3,900	±1.7
Inertia Corrected Torus Load Cell, lbf			
Maximum Downforce	5,000	2,100→ 7,500	±1.9
Maximum Upforce	2,800	1,100→ 4,000	±2.3
Impulse of Torus Spatial Pressure Integral, lbf-sec	330	140→ 500	±2.0
Spatial Integral of Vent Header Impact Pressures (force), lbf	150	0→240	±10.4
Inertia Corrected Vent Header Load Cell, lbf	200	0→350	±14.1
Impulse of Vent Header - Load Cell Corrected, lbf-sec	2.5	0→11.6	±14.1

APPENDIX E

PHOTOGRAPHIC RESULTS

Figures E-1 through E-7 present the sequence of major events, which occurred during a typical load definition test from each plant tested during the Supplemental Plant Unique Tests. The photographs are from the high speed movies taken during the tests.

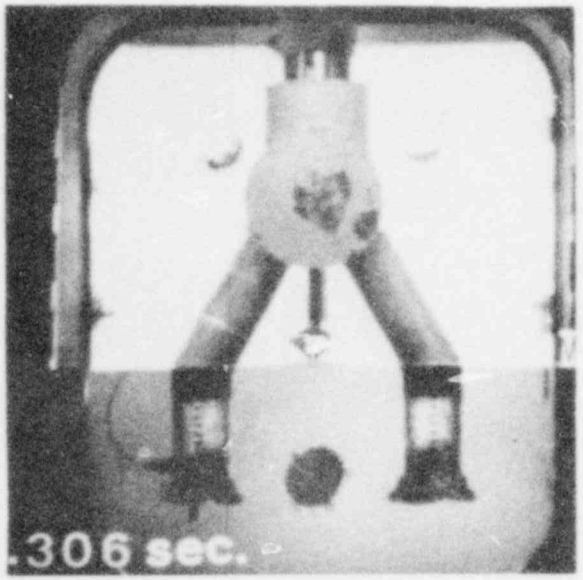

PEAK DOWNFORCE

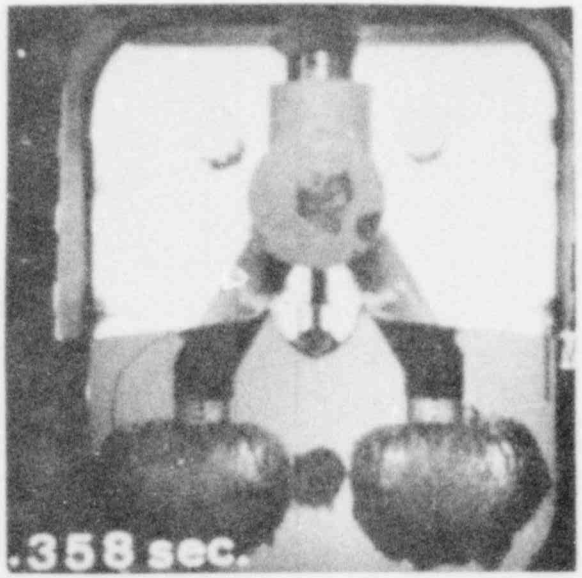

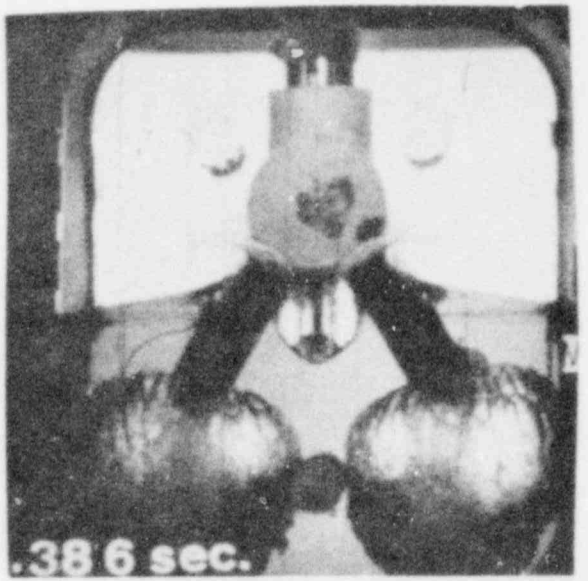

VENT HEADER IMPACT

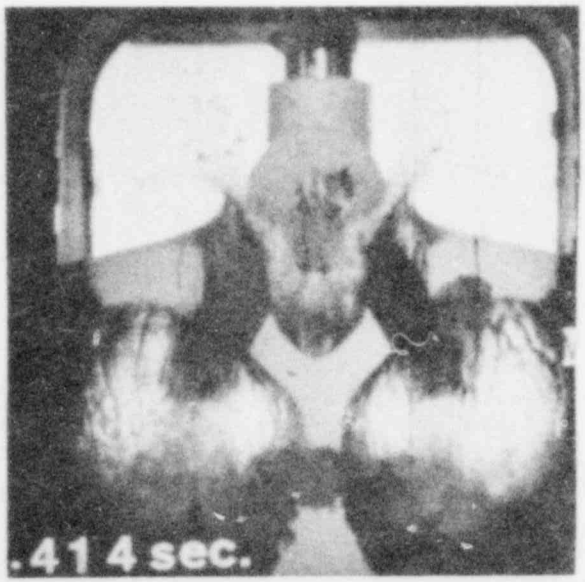

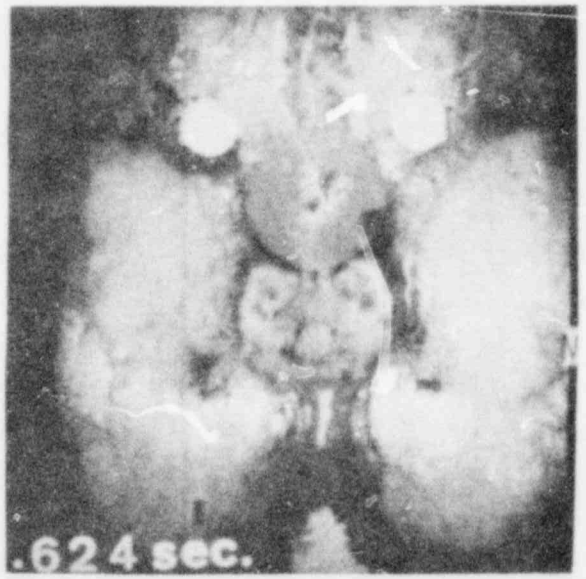

PEAK UPFORCE

TIMES UNCORRECTED FOR T_0, T_0 = .180 sec.

Figure E-1
MONTICELLO, TEST 19

Figure E-2

JUANE ARNOLD, TEST 8

TIMES UNCORRECTED FOR T_0, T_0 = .198 sec.

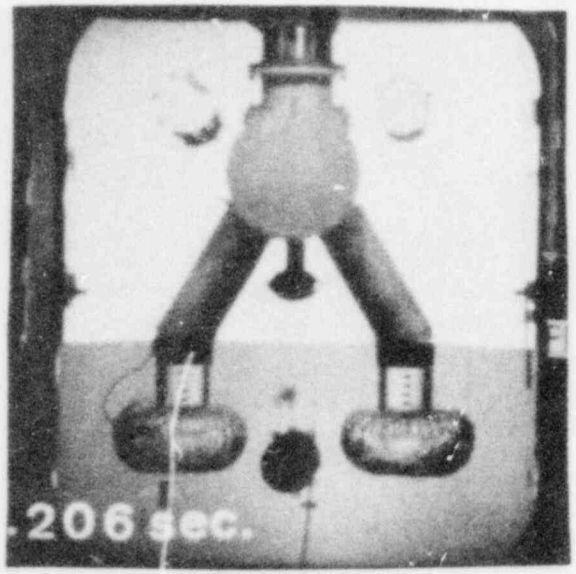

PEAK DOWNFORCE

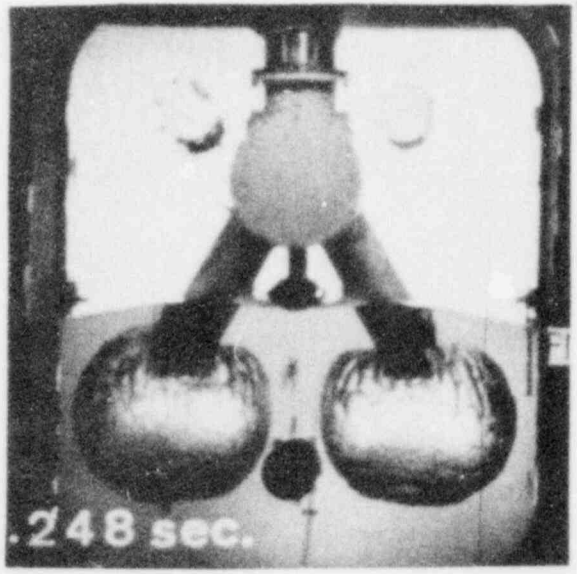

DEFLECTOR IMPACT

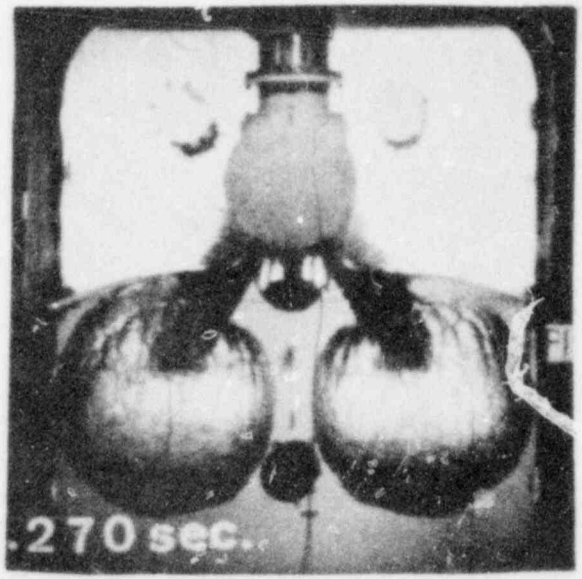

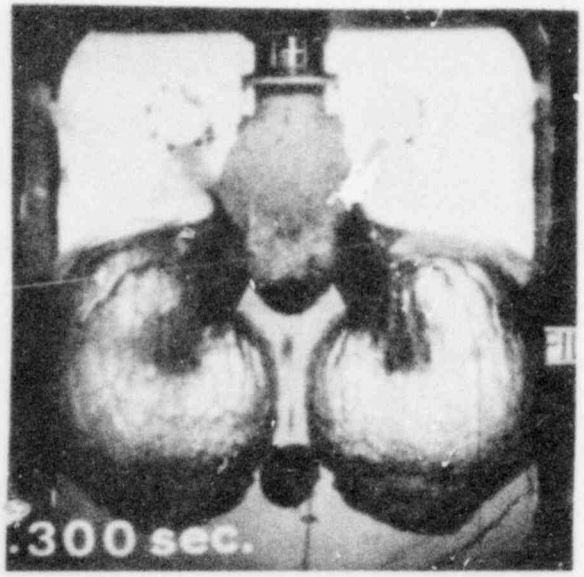

PEAK UPFORCE

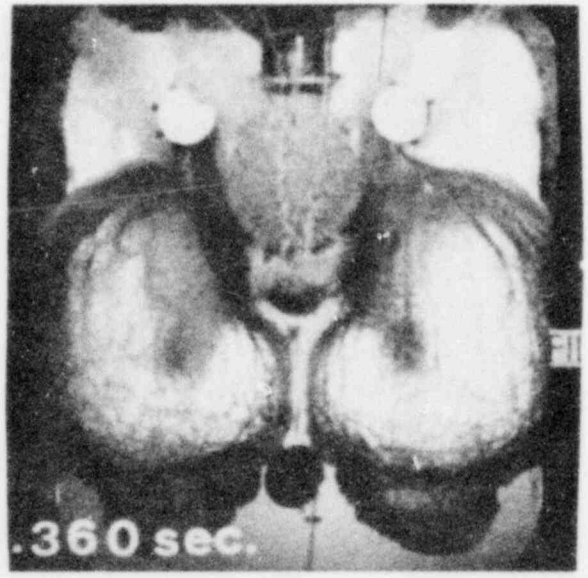

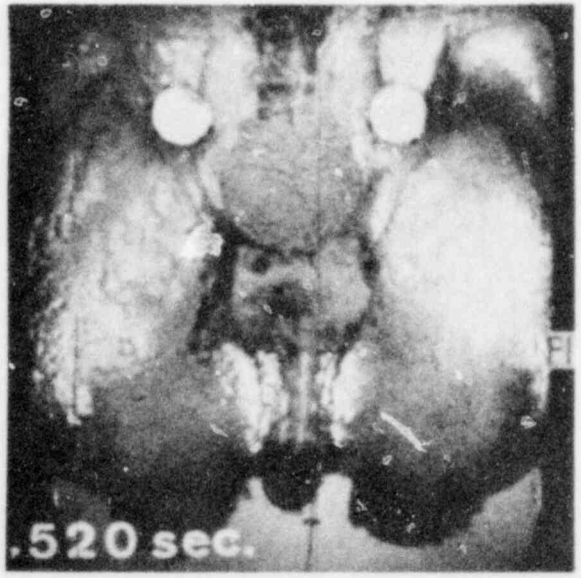

TIMES UNCORRECTED FOR T_0, T_0 = .110 sec.

Figure E-3
PILGRIM, TEST 8

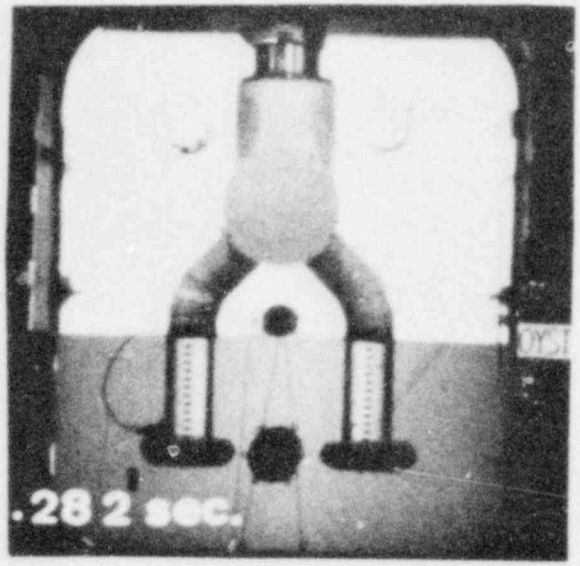

PEAK DOWNFORCE

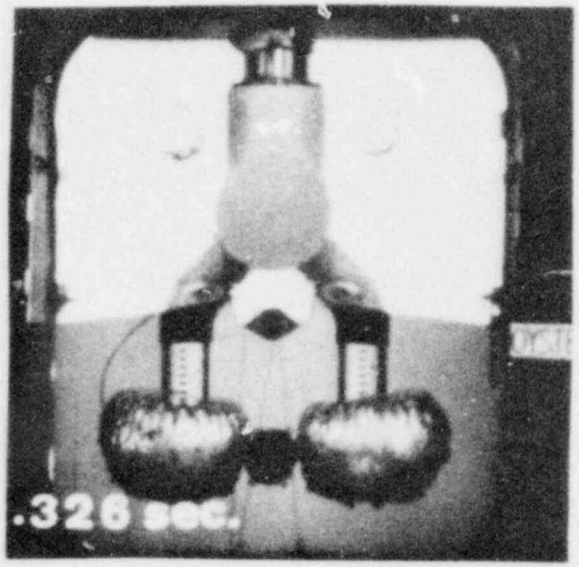

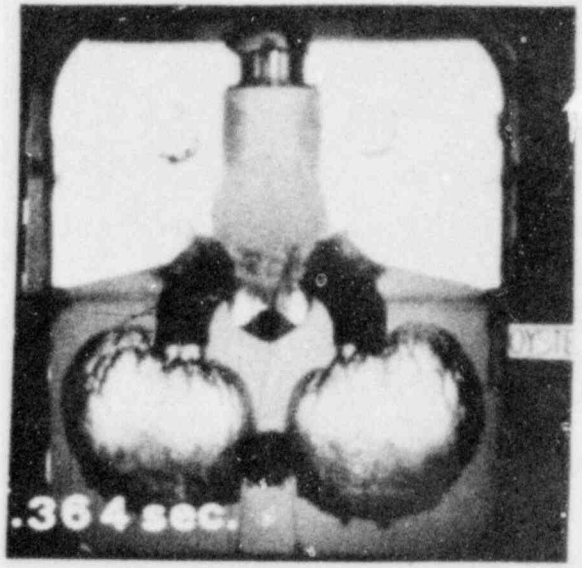

VENT HEADER IMPACT

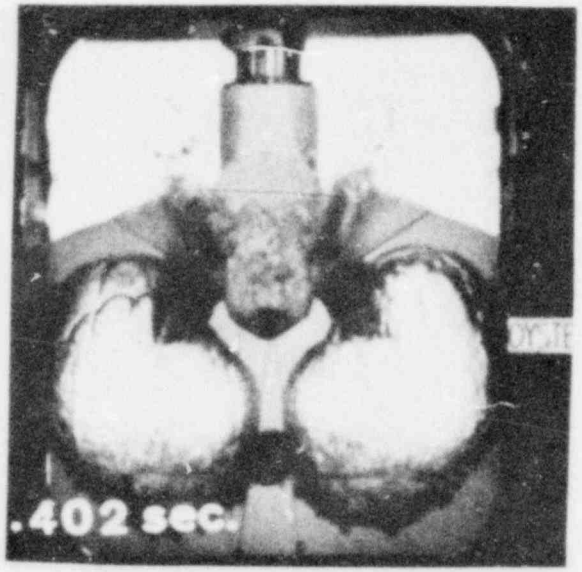

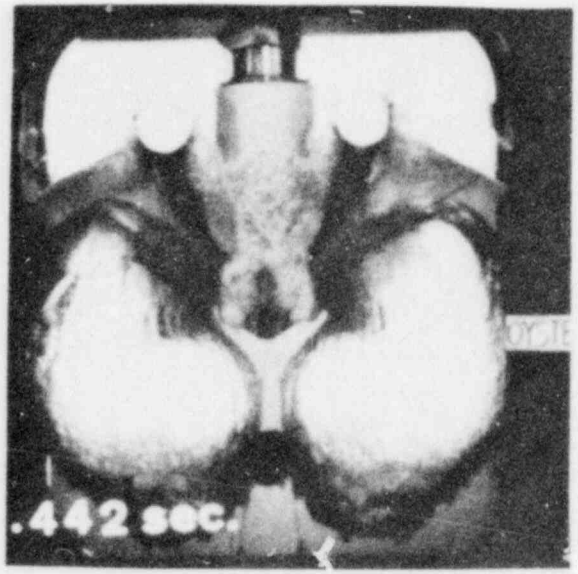

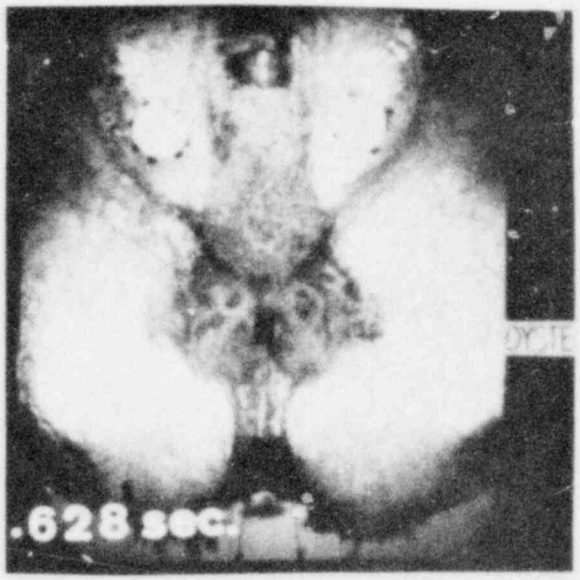

PEAK UPFORCE

TIMES UNCORRECTED FOR T_0, T_0 = .186 sec.

Figure L-4
OYSTER CREEK, TEST 8

NEDO-24615

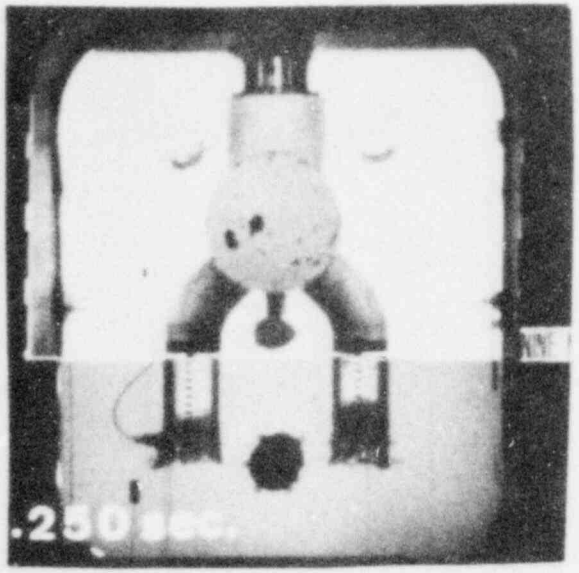

PEAK DOWNFORCE

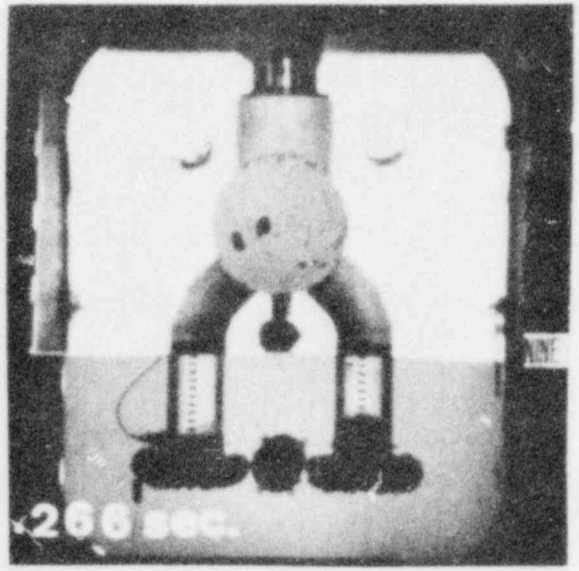

DEFLECTOR IMPACT

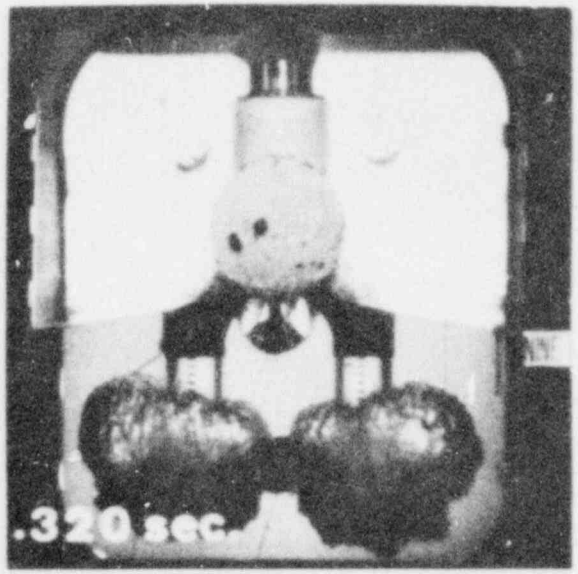

VENT HEADER IMPACT

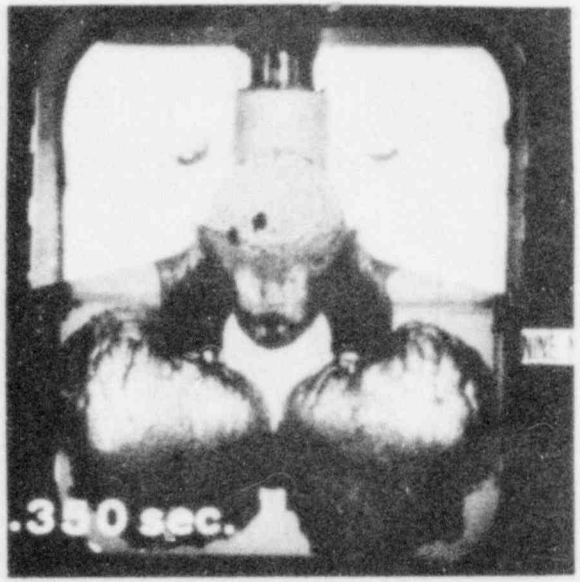

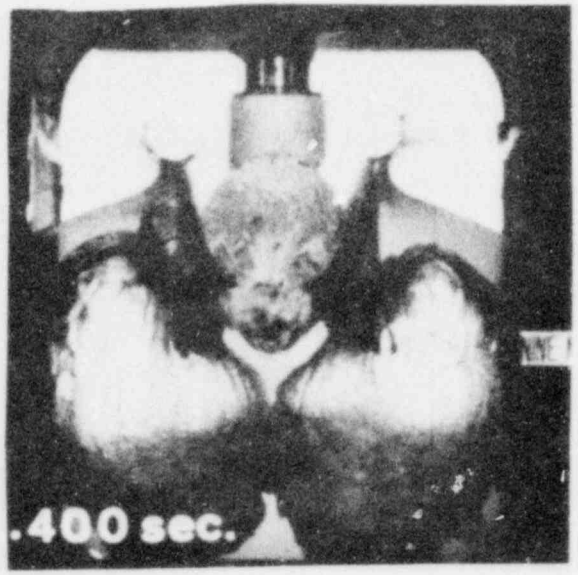

PEAK UPFORCE

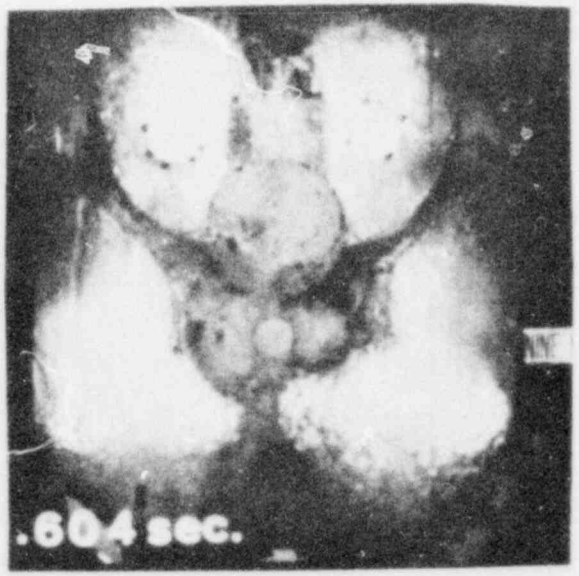

TIMES UNCORRECTED FOR T_0, T_0 - .112 sec.

Figure E-5
NINE MILE POINT, TEST 17

PEAK DOWNFORCE

VENT HEADER IMPACT

PEAK UPFORCE

TIMES UNCORRECTED FOR T_0, T_0 = .100 sec.

Figure E-6
MILLSTONE, TEST 8

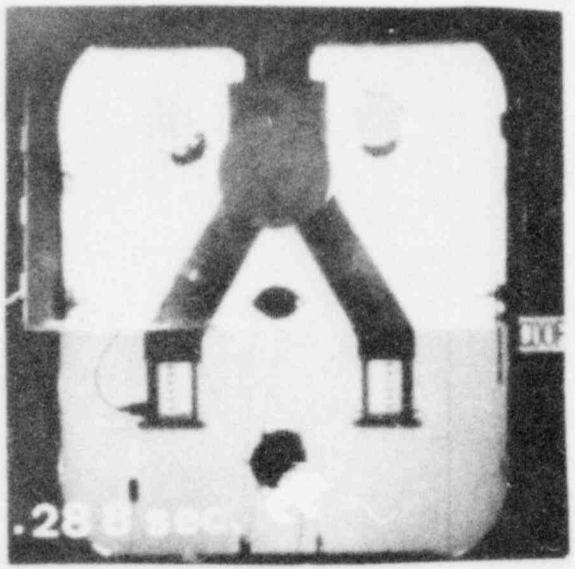

PEAK DOWNFORCE

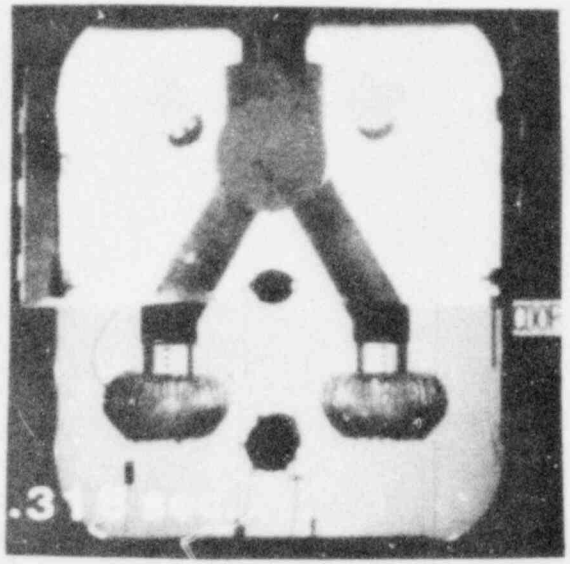

DEFLECTOR IMPACT

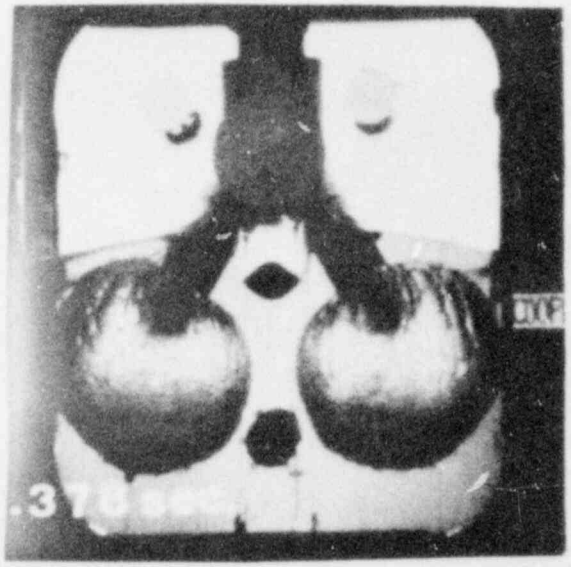

VENT HEADER IMPACT

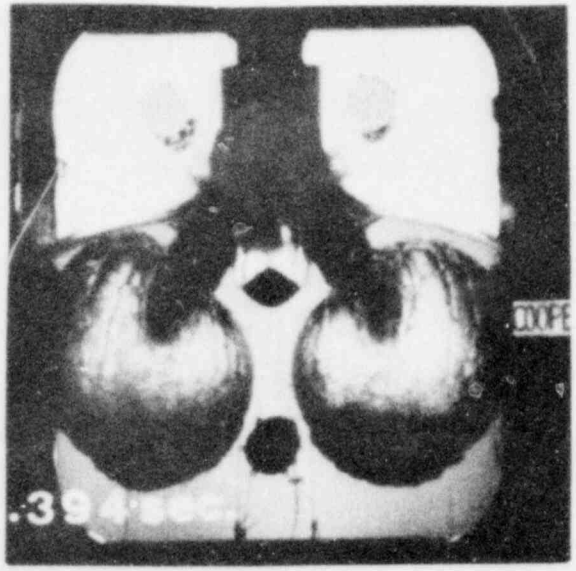

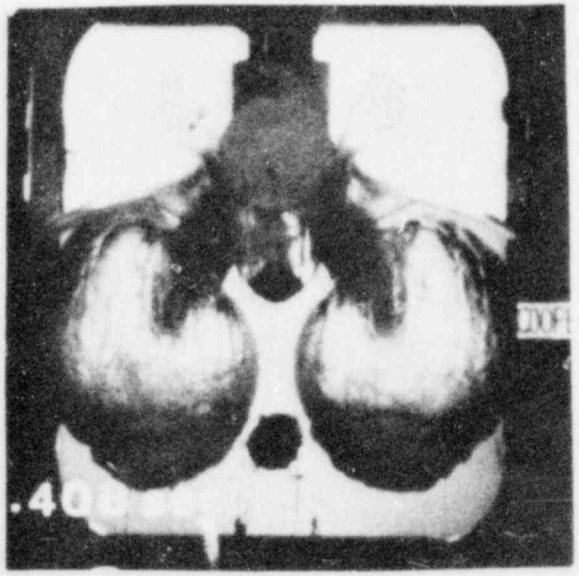

PEAK UPFORCE

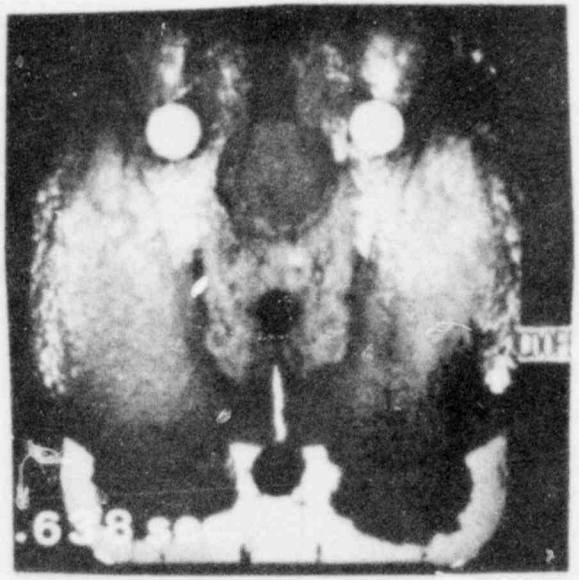

TIMES UNCORRECTED FOR T_0, T_0 = .216 sec.

Figure E-7
COOPER STATION, TEST 7

APPENDIX F

SMOOTHING WINDOW-RELATED DOWNLOAD OSCILLATIONS IN TORUS LOAD DATA

Three plants in the Task 5.5.4 series of testing (Millstone, Oyster Creek, and Cooper Station) exhibited window-related torus download oscillations of sufficient magnitude to warrant filtering (as discussed in Appendix H of Reference 2) to remove these non-prototypical effects. The technique used for digitally filtering the acceleration-corrected torus pressure integral data to eliminate oscillations was discussed in detail in the referenced report and is summarized below:

(1) Perform a Power Spectral Density (PSD) analysis of the window accelerometer and corrected pressure integral data for each test.

(2) Compare the window accelerometer and corrected pressure integral PSDs to determine natural window frequency. Select an appropriate notch filter.

(3) Filter the corrected pressure integral data over the frequency band determined in (2).

Figures F-1 through F-3 present sample PSD plots of window acceleration and corrected torus pressure integral for each plant. Also shown are the notch filter frequency range selected from each plant's data. Figures F-4 through F-8 present filtered pressure integral (corrected) plots for Millstone tests, Figures F-9 through F-18 present filtered pressure integral (corrected) plots for Oyster Creek tests, and Figures F-19 through F-26 present filtered pressure integral (corrected) plots for Cooper Station tests. The filtered and unfiltered curves were compared in Appendix A. In general, the filtering succeeded in removing window-related sinusoidal oscillatons without disturbing the basic character of the force plot. Filtering did not remove the download oscillations thought to be caused by vent clearing phenomena.

FIGURE F-1
Millstone - Test 7

*

*General Electric Company proprietary information has been deleted.

FIGURE F-2
Oyster Creek - Test 9A

*

*General Electric Company proprietary information has been deleted.

FIGURE F-3
Cooper Station - Test 7

*

*General Electric Company proprietary information has been deleted.

FIGURE F-4

MILLSTONE TORUS LOADS (TEST 6B)

Filtered 87.5 - 117.5 Hz

*

*General Electric Company proprietary information has been deleted.

FIGURE F-5
MILLSTONE TORUS LOADS (TEST 7A)

Filtered 87.5 - 117.5 Hz

*

*General Electric Company proprietary information has been deleted.

FIGURE F-6
MILLSTONE TORUS LOADS (TEST 8)

Filtered 87.5 - 117.5 Hz

*

*General Electric Company proprietary information has been deleted.

FIGURE F-7
MILLSTONE TORUS LOADS (TEST 9A)

Filtered 87.5 - 117.5 Hz

*

*General Electric Company proprietary information has been deleted.

FIGURE F-8
MILLSTONE TORUS LOADS (TEST 10)

Filtered 87.5 - 117.5 Hz

*

*General Electric Company proprietary information has been deleted.

FIGURE F-9
OYSTER CREEK TORUS LOADS (TEST 6)

Filtered 105 - 125 Hz

*

*General Electric Company proprietary information has been deleted.

FIGURE F-10
OYSTER CREEK TORUS LOADS (TEST 7)
Filtered 105 - 125 Hz

*

*General Electric Company proprietary information has been deleted.

FIGURE F-11
OYSTER CREEK TORUS LOADS (TEST 8A)

Filtered 105 - 125 Hz

*

*General Electric Company proprietary information has been deleted.

*

FIGURE F-12
OYSTER CREEK TORUS LOADS (TEST 9A)

Filtered 105 - 125 Hz

*General Electric Company proprietary information has been deleted.

*

FIGURE F-13

OYSTER CREEK TORUS LOADS (TEST 10)

Filtered 105 - 125 Hz

*General Electric Company proprietary information has been deleted.

FIGURE F-14

OYSTER CREEK TORUS LOADS (TEST 11)

Filtered 105 - 125 Hz

*

*General Electric Company proprietary information has been deleted.

*

FIGURE F-15
OYSTER CREEK TORUS LOADS (TEST 12)

Filtered 105 - 125 Hz

*General Electric Company proprietary information has been deleted.

FIGURE F-16
OYSTER CREEK TORUS LOADS (TEST 13)

Filtered 105 - 125 Hz

*

*General Electric Company proprietary information has been deleted.

FIGURE F-17
OYSTER CREEK TORUS LOADS (TEST 14)

Filtered 105 - 125 Hz

*

*General Electric Company proprietary information has been deleted.

FIGURE F-18
OYSTER CREEK TORUS LOADS (TEST 15)

Filtered 105 - 125 Hz

*

*General Electric Company proprietary information has been deleted.

FIGURE F-19

COOPER STATION TORUS LOADS (TEST 6)

Filtered 80 - 120 Hz

*

*General Electric Company proprietary information has been deleted.

FIGURE F-20

COOPER STATION TORUS LOADS (TEST 6)

*

*General Electric Company proprietary information has been deleted.

FIGURE F-21
COOPER STATION TORUS LOADS (TEST 8A)

Filtered 80 - 120 Hz

*

*General Electric Company proprietary information has been deleted.

FIGURE F-22
COOPER STATION TORUS LOADS (TEST 9)

Filtered 80 - 120 Hz

*

*General Electric Company proprietary information has been deleted.

FIGURE F-23
COOPER STATION TORUS LOADS (TEST 10)

Filtered 80 - 120 Hz

*

*General Electric Company proprietary information has been deleted.

FIGURE F-24
COOPER STATION TORUS LOADS (TEST 11)

Filtered 80 - 120 Hz

*

*General Electric Company proprietary information has been deleted.

FIGURE F-25
COOPER STATION TORUS LOADS (TEST 12A)

Filtered 80 - 120 Hz

*

*General Electric Company proprietary information has been deleted.

FIGURE F-26
COOPER STATION TORUS LOADS (TEST 13)

Filtered 80 - 120 Hz

*

*General Electric Company proprietary information has been deleted.

APPENDIX G

VENT RESISTANCE EVALUATION

Prior to each set of Supplemental Plant Unique Tests it was necessary to experimentally determine the vent resistance in the Quarter-Scale Test Facility and, if necessary, adjust flow orifices to bring the vent system fL/D and the fL/D split within the required range. This Appendix describes the test requirements and the experimental method and discusses the analytical technique used for data reduction.

G.1 Test Requirements

Based on the scaling laws (Section 2.1.1), the enthalpy flow ($\dot{H} \propto \rho AVC_pT$) is scaled by $SF^{7/2}$ where SF is the scaling factor. Since ρ is equal to P/RT from the ideal gas law, the enthalpy flow can be expressed as follows:

$$\dot{H} \propto PAV$$

where P = pressure
A = flow area
V = velocity

Since the pressures are proportional to scale factor and areas are proportional to the scale factor squared,

$$\dot{H} \propto (SF)(SF^2)V$$

Consequently, for subscale tests the vent system velocities must be proportional to the square root of the scale factor. This scaling requirement has been met in all QSTF tests by placing flow orifices in the vent system.

For the quarter-scale tests performed to evaluate scaling (Reference 3, Figure 3-5), the quarter-scale exit velocity-pressure ratio characteristic was calibrated to match scaled-up, 1/12-scale values. However, for

plant unique testing, vent resistance requirements were based on calculated full-scale plant unique vent system fL/D values, adjusted to subscale by the relationship

$$(fL/D)_{SS} = (fL/D)_{FS} \times (1/SF) \times (T/T_D)$$

where

$(fL/D)_{SS}$ = vent system total fL/D for subscale test

$(fL/D)_{FS}$ = vent system total fL/D for full scale plant

SF = scaling factor

T = initial test temperature

T_D = initial nominal bulk drywell temperature

The initial test temperature was 70°F (530°R) and the initial nominal bulk drywell temperature was a utility input.

For compressible flow the use of the Fanno equations (see Section G.3) with the above scaling relationship is slightly conservative, because it results in a slightly higher subscale flow velocity than required. For a full scale fL/D of 5 at a pressure ratio of 0.8, the Fanno equations would predict an exit velocity of 321 ft/sec which, scaled to quarter scale, requires a velocity of 160.5 ft/sec (neglecting temperature differences). This is equivalent to a quarter scale fL/D of 20.5 which is slightly higher than the 20.0 obtained by using the fL/D scaling relationship. For additional conservatism, the plant unique vent resistance tested was always equal to or less than the scaled, full-scale vent fL/D. An fL/D tolerance of +0, -2 was allowed from the scaled, full-scale vent fL/D (except for Nine Mile Point, for which the tolerance was revised to +0, -2.5).

Tests conducted during Task 5.5.3-1 (Reference 1) with flow orifices located only in the main vent showed that increasing the vent system volume downstream of the vent system flow orifice increased the torus and vent header loads. Prior to vent clearing and during the early stages of bubble growth, the volume downstream of the orifice acts as an

accumulator which helps to maintain bubble pressure when the bubble begins to overexpand. This effect is referred to as vent system capacitance.

The Mark I vent system capacitance can be closely modeled for subscale tests with two properly placed orifices (Reference 2). For an orifice at the entrance to the vent system and an orifice in each downcomer a 50%, 50% split in vent system resistance provides a good simulation of the full-scale Mark I vent system capacitance characteristics.

G.2 Experimental Method

The basic experimental method consisted of discharging the facility air reservoir (about 500 cubic feet initially charged with air) through the vent system. During this test, the front door was removed from the wetwell so that the downcomer exit was at ambient pressure. A typical reservoir blowdown would last approximately 15 seconds and during this time sufficient data was taken to allow determination of the instantaneous mass flux into the drywell as well as the pressure drop across the vent system. A quasi-steady flow was established within one to two seconds. Neglecting mass storage terms in the drywell and vent system during the quasi-steady portion of the test, allows the system fL/D to be calculated as described in the following section.

The following measurements were digitally sampled at 500 samples per second during the test (see Figure G-1 for measurement locations):

P_c = Pressure at the charging orifice
T_c = Temperature at the charging orifice
P_o = Drywell pressure
T_o = Vent total temperature (assume equal to downcomer temperature)
P_2 = Vent header static pressure

In addition to these measurements, the ambient pressure (P_3) was recorded from a barometer located at the facility. Due to the temperature sensitivity of the pressure transducers (Sensometrics SP-65), it was necessary to thermally isolate them from direct contact with test flow. This was accomplished by attaching the transducers to a length of copper tubing which communicated with the location at which the pressure measurement was to be made.

The digitally sampled data was stored on magnetic tape and later plotted as a function of time. Data was read off the graphs and entered into a computer code which made the vent resistance calculations.

G.3 Analytical Methods

Plant unique vent flow losses are simulated by the use of two flow orifices (Figure G-1). One of the flow orifices is placed at the main vent entrance and a pair of identical orifices are installed, one in each downcomer. The total flow loss is then obtained by summing the losses through the two flow orifices.

The vent system fL/D was calculated from measured data by using the Fanno equations which describe compressible flow with friction. This method requires that the mass flow through the system ($\dot{m}$) be known. The mass flow was calculated from measured fluid properties upstream of the drywell flow control (inlet) orifice using the orifice flow equations in the following form:

$$\dot{m} = \frac{0.4739\, A_c\, P_c}{\sqrt{1-\beta^4}} \sqrt{\frac{2g}{R\, T_c}} \quad ; \quad \frac{P_o}{P_c} \leq 0.528$$

$$\dot{m} = \frac{0.98\, A_c\, Y\, 2g}{\sqrt{1-\beta^4}} \sqrt{\frac{(P_c - P_o)\, P_c}{R\, T_c}} \quad ; \quad \frac{P_o}{P_c} > 0.528$$

where A_c = Flow orifice area (in^2)

R = Gas constant (53.3 ft. lbf/lbm °R)

g = 32.17 lbm ft./lbf sec^2

$\beta = D_c/D_o$ (where D_o is the diameter of the pipe containing the flow orifice and D_c is the flow orifice diameter)

$$\text{and } Y \equiv \left\{ 3.5\, P_R^{1.429} \left[\frac{1-(P_R)^{0.286}}{1-P_R} \right] \left[\frac{1-\beta^4}{1-\beta^4 (P_R)^{1.429}} \right] \right\}^{1/2}$$

$$P_R = P_o/P_c$$

P_c, T_c, and P_o are defined earlier (see Figure G-1). Having determined the mass flow into drywell ($\dot{m}$), the vent fL/D was calculated with the Fanno equations as follows:

$$W_1 = \frac{\dot{m}}{P_0 Ag}\sqrt{\frac{R\,T_o}{\gamma}}; \quad W_1 = M_1 \left(1 + \frac{\gamma-1}{2} M_1^2\right)^{\frac{-(\gamma+1)}{2(\gamma-1)}}$$

$$W_2 = \frac{\dot{m}}{P_2 Ag}\sqrt{\frac{R\,T_o}{\gamma}}; \quad W_2 = M_2 \left(1 + \frac{\gamma-1}{2} M_2^2\right)^{\frac{-(\gamma+1)}{2(\gamma-1)}}$$

$$W_3 = \frac{\dot{m}}{P_3 Ag}\sqrt{\frac{R\,T_o}{\gamma}}; \quad W_3 = M_3\sqrt{1 + \frac{\gamma-1}{2} M_3^2}$$

$$(fL/D)_1 = \frac{1}{\gamma}\frac{M_2^2 - M_1^2}{M_2^2\, M_1^2} + \frac{\gamma+1}{2\gamma} \ln\left(\frac{\left(1+\frac{\gamma-1}{2} M_2^2\right) M_1^2}{\left(1+\frac{\gamma-1}{2} M_1^2\right) M_2^2}\right)$$

$$(fL/D)_2 = \frac{1}{\gamma}\frac{M_3^2 - M_2^2}{M_3^2\, M_2^2} + \frac{\gamma+1}{2\gamma} \ln\left(\frac{\left(1+\frac{\gamma-1}{2} M_3^2\right) M_2^2}{\left(1+\frac{\gamma-1}{2} M_2^2\right) M_3^2}\right) + 1$$

$$(fL/D) = (fL/D)_1 + (fL/D)_2$$

Here P_0 = Drywell pressure, P_2 = Vent header pressure, P_3 = Ambient pressure, T_0 = Drywell temperature, A = Reference downcomer area from hydrodynamic conditions, and γ = 1.4.

For each selected data point during the test, W_1, W_2, and W_3 are calculated from measured or derived quantities. The corresponding values of M_1, M_2, and M_3 are calculated by an iterative procedure, and the flow losses through the vent orifice $(fL/D)_1$ and downcomer orifice $(fL/D)_2$ are calculated from the above algebraic expressions. Finally, the total vent resistance (fL/D) is obtained from the sum of $(fL/D)_1$ and $(fL/D)_2$.

G.4 Typical Test Data

The calculated total vent resistance (fL/D) and its distribution as a function of the ratio between the ambient and the drywell pressure for the seven Mark I plants tested are presented in Figures G-2 through G-15 and summarized in Table G-1.

Although the calculated values of vent system fL/D presented in Figures G-2 through G-15 exhibit some scatter, this scatter is felt to be primarily caused by uncertainties in the calculated fL/D and not by real variations in fL/D with vent system pressure ratio. Therefore, the fL/D values presented in Table G-1 are the average of the calculated fL/D values over the pressure ratio range from 0.8 to 0.9. The pressure ratio range of 0.8 to 0.9 was selected for fL/D calibration in order to provide a nearly incompressible fL/D at a low enough pressure ratio to minimize measurement error. Since the Fanno equations are based on pressure differences, the calculated fL/D values become more sensitive to uncertainty in the measured pressures at high vent system pressure ratios. The pressure signals (especially in the drywell) contain high frequency acoustic noise with an amplitude of a few tenths of a psi. The pressure uncertainty caused by this noise is felt to be largely responsible for the scatter in calculated fL/D. The measurement uncertainty analysis presented in Appendix D indicated an fL/D uncertainty of 6% at 95% confidence.

FIGURE G-1

FACILITY GEOMETRY

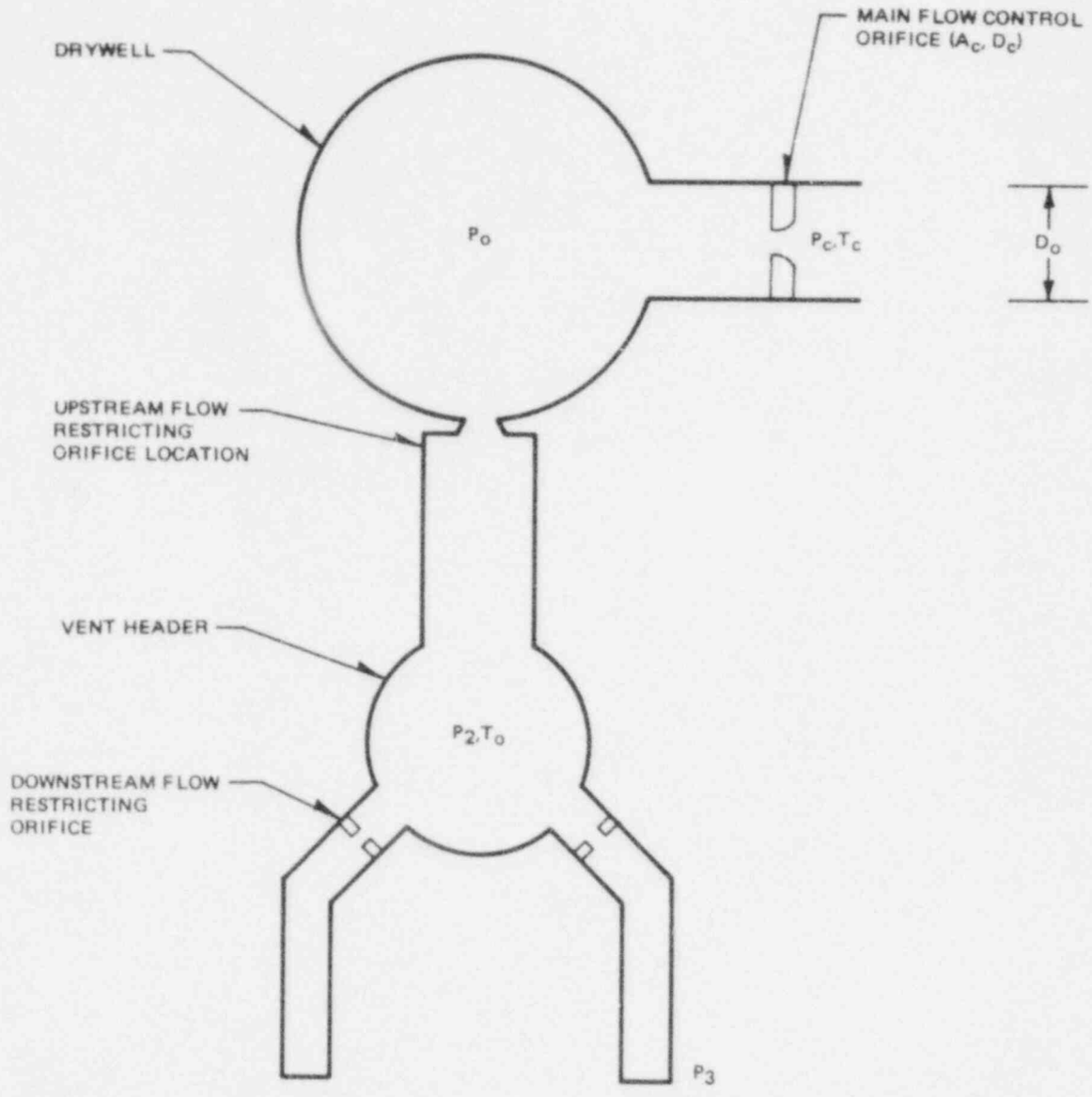

FIGURE G-2

CALCULATED VENT HEADER RESISTANCE fL/D

Task 5.5.4 Monticello Tests

*

*General Electric Company proprietary information has been deleted.

FIGURE G-3

VENT RESISTANCE (fL/D) DISTRIBUTION

Task 5.5.4 Monticello Tests

*General Electric Company proprietary information has been deleted.

FIGURE G-4

CALCULATED VENT HEADER RESISTANCE fL/D

Task 5.5.4 Duane Arnold Tests

*

*General Electric Company proprietary information has been deleted.

FIGURE G-5

VENT RESISTANCE (fL/D) DISTRIBUTION

Task 5.5.4 Duane Arnold Tests

*

*General Electric Company proprietary information has been deleted.

FIGURE G-6

CALCULATED VENT HEADER RESISTANCE $f_{L/D}$

Task 5.5.4 Pilgrim Tests

*

*General Electric Company proprietary information has been deleted.

FIGURE G-7

VENT RESISTANCE (fL/D) DISTRIBUTION

Task 5.5.4 Pilgrim Tests

*

*General Electric Company proprietary information has been deleted.

FIGURE G-8

CALCULATED VENT HEADER RESISTANCE fL/D

Task 5.5.4 Oyster Creek Tests

*

*General Electric Company proprietary information has been deleted.

FIGURE G-9

VENT RESISTANCE (fL/D) DISTRIBUTION

Task 5.5.4 Oyster Creek Tests

*

*General Electric Company proprietary information has been deleted.

FIGURE G-10

CALCULATED VENT HEADER RESISTANCE fL/D

Task 5.5.4 Nine Mile Point Tests

*

*General Electric Company proprietary information has been deleted.

FIGURE G-11

VENT RESISTANCE (fL/D) DISTRIBUTION

Task 5.5.4 Nine Mile Point Tests

*

*General Electric Company proprietary information has been deleted.

FIGURE G-12

CALCULATED VENT HEADER RESISTANCE fL/D

Task 5.5.4 Millstone Tests

*

*General Electric Company proprietary information has been deleted.

FIGURE G-13

VENT RESISTANCE (fL/D) DISTRIBUTION

Task 5.5.4 Millstone Tests

*

*General Electric Company proprietary information has been deleted.

FIGURE G-14

CALCULATED VENT HEADER RESISTANCE fL/D

Task 5.5.4 Cooper Station Tests

*

*General Electric Company proprietary information has been deleted.

FIGURE G-15

VENT RESISTANCE (fL/D) DISTRIBUTION

Task 5.5.4 Cooper Station Tests

*

*General Electric Company proprietary information has been deleted.

TABLE G-1 *

SUMMARY OF VENT RESISTANCE

Task 5.5.4 Supplemental Plant Unique Tests

*General Electric Company proprietary information has been deleted.

APPENDIX H

FORCE CORRECTION FOR THE VENT HEADER LOAD CELL DATA

Forces measured by the QSTF vent header load cell are a combination of external pressures (water and air) and internal pressure (air). The external forces are properly scaled in the QSTF and when multiplied by the proper scale factor are the expected full scale vent header or deflector loads. The internal (thrust) forces were not intended to be scaled since the QSTF vent system does not model the three-dimensional full-scale flow geometry and since Moody's scaling laws (Reference H-1)* call for an internal pressure loss coefficient of about four times higher than is prototypical.

The vertical flow geometry of the QSTF vent system minimizes the magnitude of the thrust term. The thrust transient typically causes the corrected vent header load cell to fall several hundred pounds after vent clearing indicating a downward force on the vent header due to flow and vent system pressure drop.

The vent header impact as measured by the load cell is superimposed on the thrust transient. In practical terms, this requires a zero offset (the value of vent header impact thrust) in the load cell in order to facilitate a comparison of the load cell force with the vent header pressure integral. This technique was used for vent header load cell data up through the Plant Unique Tests.

The use of large vent header deflectors reduces the measured vent header pressure integral in the QSTF to values of 100 lb_f or less while extending the loading duration. In this range, the uncertainty in the load cell corrections for vent header thrust complicate the comparison of load cell values with the vent header pressure integral.

---

*Reference H-1: Moody, F. J. , "Drag Forces on Submerged Structures in Unsteady Flow," NEDE-2141, September 1976.

This appendix describes the relationships which have been developed to correct the vent header load cell for internal thrust forces. Although the vent header pressure integral remains the primary measurement of the vent header impact, the thrust-corrected load cell is felt to be a more directly comparable value for small impact forces. Thrust-corrected load cell values have been used for all the Supplemental Plant Unique Tests to compare with the impact pressure integral.

This appendix describes the method used to calculate the internal drag forces. Subtracting the internal drag forces from the load cell data leaves the external, properly scaled forces.

Figure H-1 shows a schematic of the vent header force measurement system severed from the facility at the column which connects the header load cell to the drywell (structural ground).

Entrance conditions to the header are through an area A_1, at speed u_1, static pressure p_1 and static density ρ_1. Air exhausts from the header through A_2 (inside area of both downcomers) at static pressure p_2 and static density ρ_2.

Applying the vertical momentum equation to the control volume of the inside of the header with entrance at A_1 and exit at A_2:

$$\frac{d}{dt}\int_1^2 (\rho u A)\, dx + \rho_2 u_2^2 A_2 - \rho_1 u_1^2 A_1 = P_1 A_1 - P_2 A_2 - F_{XI} \qquad (1)$$

The first term is the rate of X momentum storage between station 1 and 2 and can be shown to be negligible. The second and third terms on the left hand side are the momentum flux into and out of the control volume. The magnitude of each term can be shown to be small and the difference negligible. The last term F_{XI} is the X component of the pressure integral over the entire inner surface which would be very difficult to

evaluate by a detailed internal integration but which equation 1 (assuming the momentum storage and flux terms negligible) shows simply to be:

$$F_{XI} = P_1A_1 - P_2A_2 \quad (2)$$

If there were no water in the torus during a QSTF test, the net external hydrodynamic load would be zero, but the load cell would record a change in measured force as flow occurred and P_1 and P_{fs} changed values. Note in particular the region where the vent header vertical vent seals and slides against the torus guide tube. P_1 occurs on one side of the flange and P_{fs} on the other. Since this causes a change in the tare force as P_i and P_{fs} change but has nothing to do with hydrodynamics, the effect must be eliminated.

As a reference force condition it is assumed that P_{fs} applies to the exterior surface of the vent header, except for P_2 on the downcomer lip $-P_2(A_3-A_2)$. This assumption is shown in Figure H-2. It can be shown that the x-component of the pressure integral over the dotted path on Figure H-2 is:

$$F_{external} = P_{fs} (A_3 - A_1)$$

The net tare or datum force on the header is then

$$F_d = P_1A_1 - P_2A_2 + P_{fs} (A_3 - A_1) - P_2 (A_3 - A_2) \quad (3)$$

Combining Terms

$$F_d = A_1 (P_1 - P_{fs}) - A_3 (P_2 - P_{fs}) \quad (4)$$

The last term in (3) is the remaining area to complete the X-component of the pressure integral, the downcomer lip $(A_3 - A_2)$ at pressure P_2.

In the QSTF P_v, P_2 and P_{fs} are measured but P_1 is not. P_1 must be calculated by using test data to calibrate the pressure loss coefficient between station 1 and the interior of the header, station v.

It is assumed that the stagnation pressure loss from station 1 to v is proportional to the square of the mass flow rate between stations.

$$Po_1 - P_v = C\dot{m}^2 \tag{5}$$

Assuming incompressible flow

$$Po_1 = P_1 + \frac{1}{2}\rho_1 u_1^2$$

$$u_1 = \frac{\dot{m}}{\rho_1 A_1}$$

$$P_1 = \rho_1 R T_1$$

$$Po_1 = P_1 + \frac{1}{2}\frac{\dot{m}^2 R T_1}{P_1 A_1^2} \tag{6}$$

$$\text{Thus,}\quad P_1 - Pv = c\dot{m}^2 - \frac{1}{2}\frac{\dot{m}^2 R T_1}{P_1 A_1^2} \tag{7}$$

The coefficient C was evaluated by using equations (4) and (7) and measured values of Pv, P_2, P_{fs}, $\dot{m}$, and F_{LC} (obtained sufficiently late in time so that significant flow exists, but vent header forces due to hydrodynamics have decayed). The following dimensional equation resulted from this evaluation:

$$P_1 = 0.0794\ \dot{m}^2 + Pv - 0.0002\ \frac{\dot{m}^2 T_1}{P_1} \qquad (8)$$

where units are: $P[lb/in^2]$
$m[lb/sec]$
$T[^oR]$

It should be noted that the derivation of the datum force, equation (4), applies after vent clearing. Before vent clearing, water is being ejected at station 2 and its momentum flux is not negligible. However, vent neader impact occurs well after vent clearing when Equation (4) is valid. A computer program was written to evaluate Equation (4) and subtract Fd from the vent header load cell data. The vent header forces from the load cell data, listed in the tables in Section 3 and Appendix A, are corrected for inertia and internal drag forces using the method presented in this appendix.

FIGURE H-1

SCHEMATIC OF VENT HEADER FORCE MEASUREMENT SYSTEM

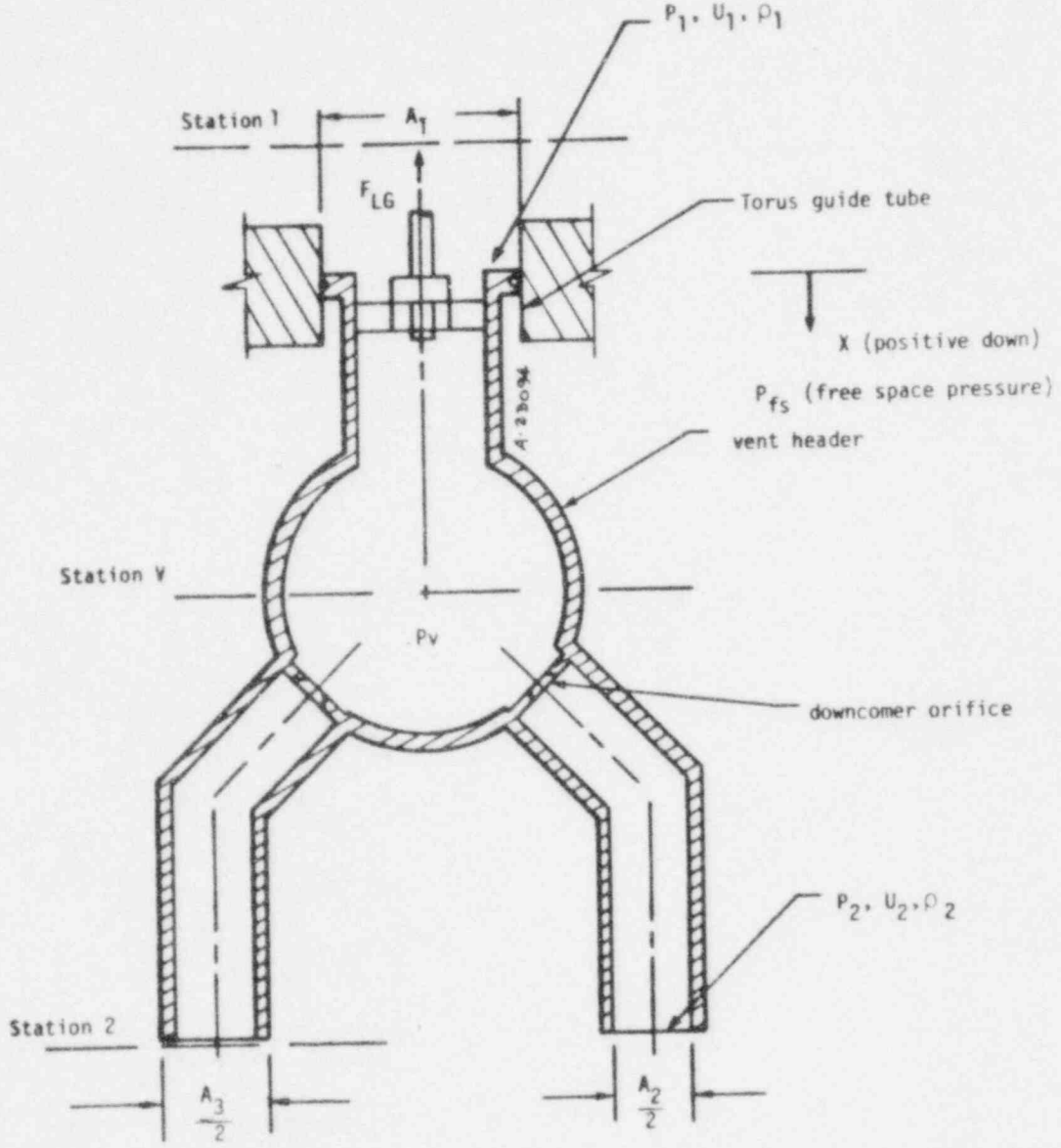

FIGURE H-2

VENT HEADER PRESSURE DISTRIBUTION

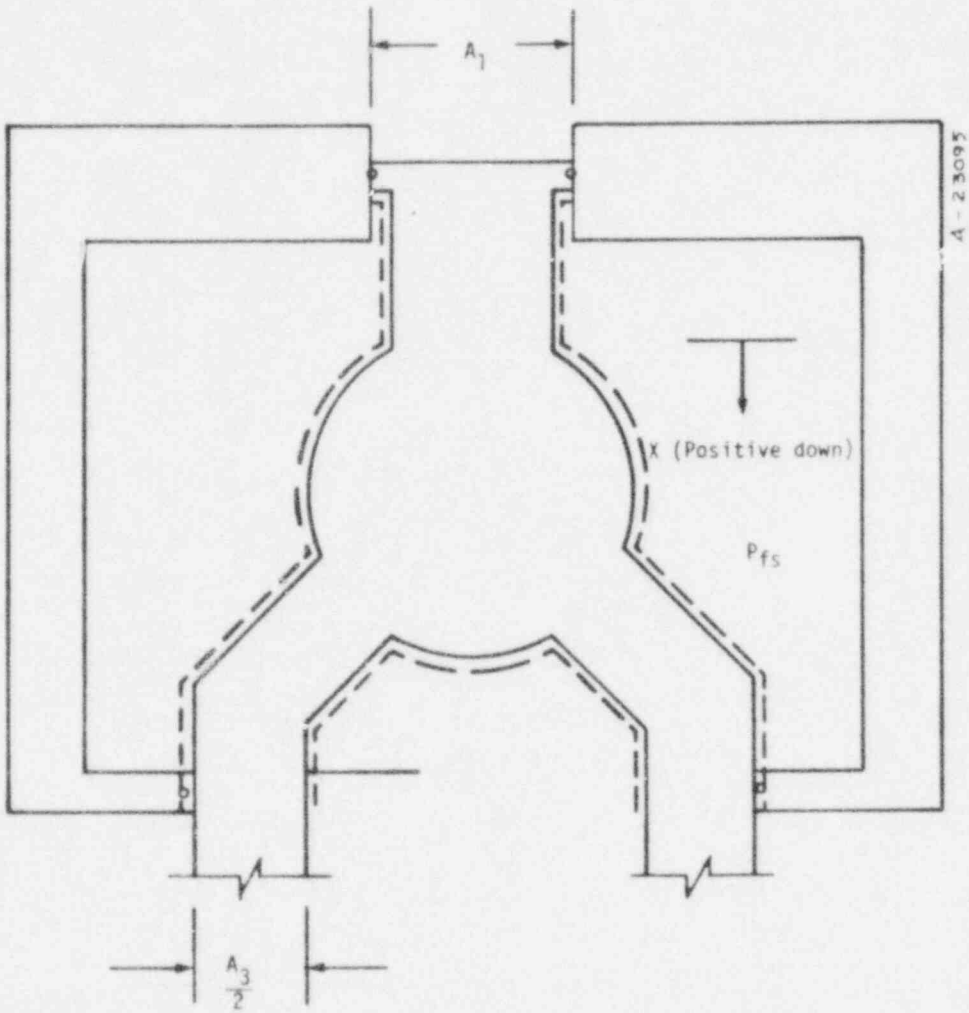

APPENDIX I

DEFLECTOR LOAD ANALYSIS

I.1 Deflector Forces

I.1.1 Introduction

During the Mark I Long Term Program Task 5.5.3, Series 2 testing (Reference 2), most plants elected to test with deflectors installed below the vent header. These deflectors were suspended from the torus by 1/8-inch diameter stainless steel cables. In order to determine forces on the deflector and the amount of force transmitted to the torus through the support cables, the Task 5.5.4 tests were conducted with the deflector suspended first from the torus, then from the vent header. The differences observed in measured torus and vent header forces for each test configuration provided the basis for calculating deflector forces. This section analyzes the deflector loads and impulses for the Monticello, Duane Arnold, Pilgrim, Oyster Creek, Nine Mile Point, Millstone, and Cooper Station test configurations. The test matrix and vent header attachment methods are summarized in Tables I-1, I-2, and I-3.

I.1.2 Deflector Forces Determined From Vent Header Load Cell

Figure I-1 presents the uncorrected vent header load cell outputs for Pilgrim Tests 6 through 9 (8.51" H_2O drywell/wetwell ΔP). The large force oscillations experienced by the vent header during Tests 8 and 9 (deflector bolted to the vent header) make a direct comparison with Tests 6 and 7 (wire-supported) difficult. The vent header load cell output was corrected for vent header inertia by subtracting the product of the averaged upper and lower vent header accelerometer outputs and the vent header mass. The outputs of the upper and lower accelerometers were averaged to reduce the noise and moderate the effect of any surface deflections which might have been measured by either accelerometer. Figure I-2 shows that although correcting the vent header load cell

outputs for inertia (mass times acceleration) results in elimination of the large oscillations, the noise level of the resulting plot is undesirable. Application of a fifteen-point smoothing technique to the data resulted in elimination of most of the noise without significant loss of data (see Figure I-3). Smoothing did, however, both reduce the vent header force rate of rise and eliminate the force spike of 540 pounds at 135 milliseconds which was introduced during acceleration correction. Integration of the smoothed vent header load cell plot (Figure I-4A) shows a maximum difference in impulse between the torus- and header-supported deflector arrangements of approximately 6 lb-sec for the 8.51" H_2O ΔP drywell/wetwell differential pressure. Graphical integration of the uncorrected vent header load cell plot (Figure I-4B) yields the same results. This indicates that the smoothing technique preserves the vent deflector impulse and provides a good indication of the force-time history.

The overlay of net vent header forces obtained with the deflector attached to the torus and net vent header force obtained with the deflector attached to the vent header shows a peak force on the deflector of about 350 pounds at 140 milliseconds (Figure I-3). The small oscillation following the peak is probably the result of not correcting for the mass of the water surrounding the deflector. This "hydrodynamic mass" increases the apparent mass of the deflector and is not included in the acceleration correction. The amount of correction is small and is approximated by the dashed line in Figure I-3.

Figure I-5 presents the uncorrected vent header forces obtained with a zero drywell/wetwell ΔP for Pilgrim Tests 10 through 13.

Figure I-6 illustrates smoothed net vent header forces and Figure I-7 shows integrated vent header forces for 0" ΔP. The overlay of vent header forces shows a peak force on the deflector of about 400 pounds at 190 milliseconds; the overlay of integrated forces gives an impulse of approximately 8 lb-sec.

Figures I-8 through I-35 illustrate the smoothed, inertia-corrected vent header load cell forces, calculated deflector loads, integration of both smoothed and uncorrected vent header load cells, and calculated impulses for the Monticello, Duane Arnold, Oyster Creek, Nine Mile Point, Millstone, and Cooper Station tests.

A summary of test results is presented in Table I-4. Figure I-36 shows the relationship between height of the deflector above the original pool surface and average impact pressure for dual-downcomer plants. The impact pressure was greatest for a height of between 3 and 5 inches; pressure leveled off for heights above 5 inches.

I.1.3 Deflector Forces Determined From Torus Data

In order to determine if deflector forces could be deduced from torus data, the corrected torus load cell plots from the Monticello tests were examined. Although some difference in torus force is evident during the period of deflector upforce, the quantitative difference is indistinct (see Figures I-37 and I-38).

A smoothing of the load cell trace was achieved by correcting for inertia with a "pseudo-weight" of 12,800 lb_f. Although actual weight of the torus was 8,800 lb_f, the pseudo-weight was used to compensate for non-uniform accelerations of torus components. The load cell trace represents the total of forces applied to the torus. This total includes the hydrodynamic forces of water and air bubbles, as well as any external torus forces such as the tensile force on deflector cables.

A comparison of the smoothed load cell plot with the integrated torus pressure plot, which represents the hydrodynamic force against the torus bottom due to water and air bubbles, reveals external torus forces. Figures I-39 and I-40 show the torus load cell and torus pressure integral forces for the Monticello tests. Figures I-41 and I-42 compare the differences between the torus load cell and pressure integral forces for

those tests. The differences represent the external torus forces present in the load cell output which are not present in the torus pressure integral. The dashed lines indicate the average external forces for each test condition. The difference between the average external forces for the deflector "bolted" and "cable-strung" conditions is shown on Figure I-43 and represents the upward force exerted on the torus by the deflector cables. This analysis of torus data indicates that the maximum deflector upforce was 400 pounds for a 12-inch submergence (compared to 420 pounds upforce obtained from vent header data) and 500 pounds for a 10-inch submergence (compared to 440 pounds obtained from vent header data).

Deflector impulse (Figure I-44) was calculated by integrating the deflector upforces shown on Figure I-43. The impulse for a 12-inch submergence was computed from torus data to be 12.5 lb-sec (compared to 20.9 lb-sec obtained from vent header data). The impulse for a 10-inch submergence was computed from torus data to be 10.5 lb-sec (compared to 15.6 lb-sec obtained from vent header data).

I.1.4 Conclusions

- Maximum deflector upforces between 200 and 425 pounds with durations of between 40 to 90 milliseconds have been determined for the Monticello, Duane Arnold, Pilgrim, Oyster Creek, Nine Mile Point, Millstone, and Cooper Station tests. These forces were determined by measuring the differences in smoothed, averaged, acceleration-corrected vent header load cell forces with the deflector alternately attached to the vent header and suspended by cables from the torus.

- As a redundant technique deflector upforces and impulses can be roughly estimated from torus load cell and pressure integral data. Estimates of upforces can probably be assumed to be within 20 percent of actual values; estimates of impulses will probably be within 50 percent of actual values.

- Although vent header deflector upforce was transferred to the torus through the support cables during the Plant Unique Tests (Task 5.5.3-2), the force transfer did not appear to affect the reported peak downforces and upforces. The force transfer definitely did not affect the net torus force plot which was computed from the corrected pressure integral (P-Plot), since the effect of increased torus pressure due to increased upward movement was eliminated with application of the correction for water inertia. Although the vent deflector upforce did reduce the corrected torus load cell force plot (Q-Plot) as discussed in Section I.1.3, it did not appear to affect peak torus downforce or upforce since the deflector loads occurred during the period from peak downforce to peak upforce.

I.2 Dye Injection

In conjunction with the experimental work to measure deflector forces during the Supplemental Plant Unique Tests, an analytical model was developed (Reference 5) to correlate the test data and estimate deflector forces for plants tested during Task 5.5.3-2. One of the primary model inputs was the fluid velocity and acceleration history at the deflector. Early analysis showed that the deflector acted to decelerate the finite fluid mass under the deflector. This finding made the use of free surface velocity inappropriate and overly conservative for deflector force definition. The displacement history of the bubble top (a clearly defined interface) was used to adjust the free surface velocity after deflector impact to obtain a more realistic estimate of the flow conditions acting on the deflector.

A dye injection rake was used (Figure I-45) to provide a measurement of the flow field underneath the deflector in order to corroborate the trend observed in the bubble top. Dye was injected into clear pool water during the Pilgrim shakedown test. Three velocities were obtained from the high-speed movies of that test: pool surface velocity, top of bubble velocity, and subsurface pool velocity under the vent deflector

(see Figure I-46). The results of the dye injection analysis are shown on Figure I-47. At deflector impact (115 milliseconds), the dye was located 8 to 10 inches below the deflector and its velocity had reached 7.5 ft/sec. At that time, surface velocity was approximately 12.5 ft/sec. Dye velocity began to decrease after deflector impact.

The data shown in Figure I-47 seem to indicate that since the bubble top is rising through the fluid, the bubble top displacement and velocity follow the trend of the free surface longer than the dye. The dye probably provides a more realistic picture of the decelerating effect of the deflector on the flow field. These data seem to indicate that use of the trends in bubble top velocity to adjust free surface velocity is a conservative approach for estimating the flow velocity acting on the deflector.

Dye movement was also measured during the Millstone, Cooper Station, and Oyster Creek shakedown tests. The results of those tests followed the same general trends as the results in the Pilgrim test. The results are presented in Figures I-48 through I-50.

In summary the dye displacement data supports the use of the bubble top velocity for vent deflector load definition.

FIGURE I-1

UNCORRECTED VENT HEADER LOAD CELLS - PILGRIM TESTS

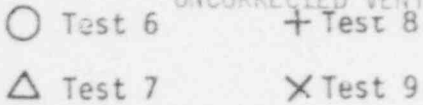

*

*General Electric Company proprietary information has been deleted.

FIGURE I -2

VENT HEADER LOAD CELLS, CORRECTED FOR INERTIA-PILGRIM TESTS

*

*General Electric Company proprietary information has been deleted.

FIGURE I-3

SMOOTHED VENT HEADER LOAD CELLS - PILGRIM TESTS

*General Electric Company proprietary information has been deleted.

FIGURE I-4

INTEGRATED VENT HEADER LOAD CELLS - PILGRIM TESTS

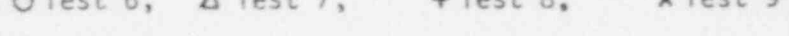

*

*General Electric Company proprietary information has been deleted.

FIGURE I-5

UNCORRECTED VENT HEADER LOAD CELLS-PILGRIM TESTS

○ Test 10 + Test 12

△ Test 11 × Test 13

*

*General Electric Company proprietary information has been deleted.

FIGURE I-6

SMOOTHED VENT HEADER LOAD CELLS - PILGRIM TESTS

A. Overview, B. Detail: Average Forces, C. & Vent Header Forces

○ Test 10 + Test 12

△ Test 11 × Test 13

*General Electric Company proprietary information has been deleted.

FIGURE I -7

INTEGRATED VENT HEADER LOAD CELLS - PILGRIM TESTS

Test 10 Test 11 Test 12 Test 13

*

*General Electric Company proprietary information has been deleted.

FIGURE I-8
SMOOTHED VENT HEADER LOAD CELLS - MONTICELLO TESTS

o Test 17
Δ Test 18
+ Test 19
× Test 20

*General Electric Company proprietary information has been deleted.

FIGURE I-9

INTEGRATED VENT HEADER LOAD CELLS-MONTICELLO TESTS

*General Electric Company proprietary information has been deleted.

FIGURE I-10

SMOOTHED VENT HEADER LOAD CELLS - MONTICELLO TESTS

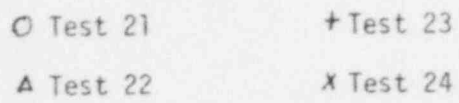

*General Electric Company proprietary information has been deleted.

FIGURE I-11

INTEGRATED VENT HEADER LOAD CELLS-MONTICELLO TESTS

O Test 21, Δ Test 22, + Test 23, x Test 24

*

*General Electric Company proprietary information has been deleted.

FIGURE I-12

SMOOTHED VENT HEADER LOAD CELLS - DUANE ARNOLD TESTS

*

*General Electric Company proprietary information has been deleted.

FIGURE I -13

INTEGRATED VENT HEADER LOAD CELLS - DUANE ARNOLD TESTS

○Test 6, △Test 7, +Test 8 x Test 9

*

*General Electric Company proprietary information has been deleted.

Figure I -14

Smoothed Vent Header Load Cells - Oyster Creek Tests

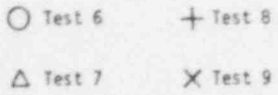

*

*General Electric Company proprietary information has been deleted.

Figure I -15

Oyster Creek Tests

Integrated Vent Header Load Cells

○ Test 6, △ Test 7, + Test 8, × Test 9

*General Electric Company proprietary information has been deleted.

FIGURE I-16

VENT HEADER LOAD CELLS - OYSTER CREEK

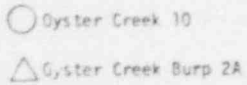

*General Electric Company proprietary information has been deleted.

FIGURE I-17

Oyster Creek Tests

Integrated Vent Header Load Cells

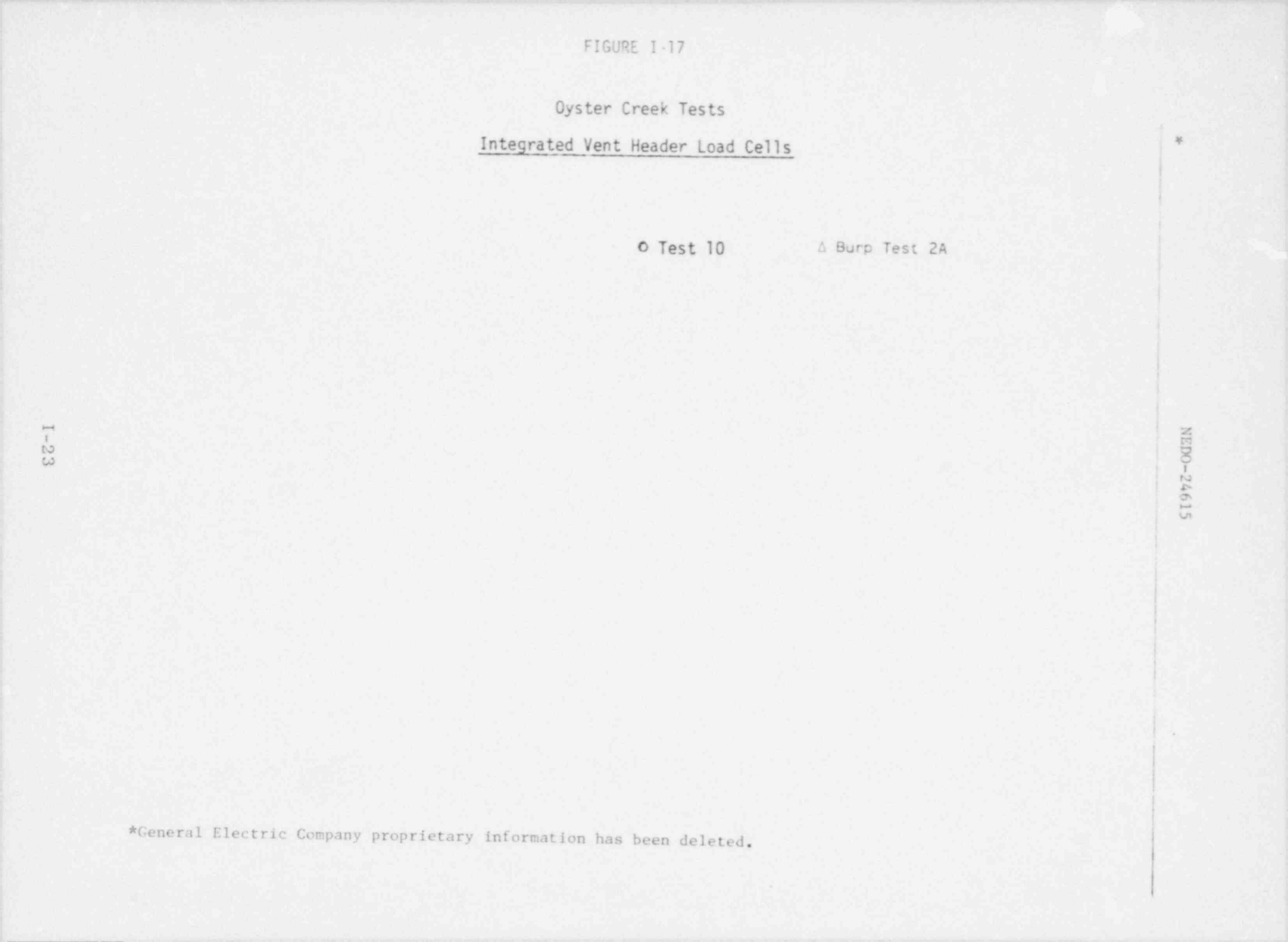

*General Electric Company proprietary information has been deleted.

FIGURE I-18

Smoothed Vent Header Load Cells - Oyster Creek Tests

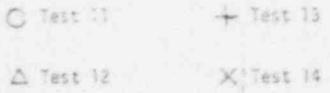

*General Electric Company proprietary information has been deleted.

FIGUREI -19

Oyster Creek Tests

○ Test 11, △ Test 12, + Test 13, × Test 14

*

*General Electric Company proprietary information has been deleted.

Figure I-20

SMOOTHED VENT HEADER LOAD CELLS - NINE MILE POINT

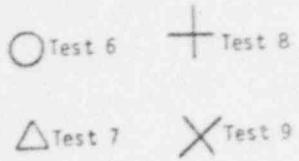

*General Electric Company proprietary information has been deleted.

Figure I - 21

NINE MILE POINT TESTS

INTEGRATED VENT HEADER FORCE

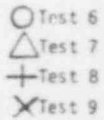

*General Electric Company proprietary information has been deleted.

FIGURE I-22

SMOOTHED VENT HEADER LOAD CELLS - NINE MILE POINT TESTS

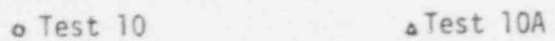

*

*General Electric Company proprietary information has been deleted.

FIGURE I-23

NINE MILE POINT TESTS

INTEGRATED VENT HEADER FORCE

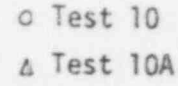

*General Electric Company proprietary information has been deleted.

Figure I-24

SMOOTHED VENT HEADER LOAD CELLS - NINE MILE POINT TESTS

*General Electric Company proprietary information has been deleted.

*

Figure I-25

NINE MILE POINT TESTS

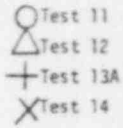

*General Electric Company proprietary information has been deleted.

Figure I-26

SMOOTHED VENT HEADER LOAD CELLS - NINE MILE POINT TESTS

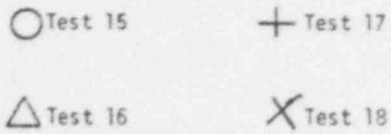

*General Electric Company proprietary information has been deleted.

Figure I-27
Nine Mile Point Tests

Integrated Vent Header Force

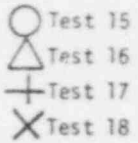

*

*General Electric Company proprietary information has been deleted.

Figure I - 28

SMOOTHED VENT HEADER LOAD CELLS - MILLSTONE

*General Electric Company proprietary information has been deleted.

Figure I - 29
MILLSTONE TESTS

INTEGRATED VENT HEADER FORCE

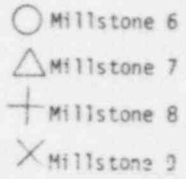

*

*General Electric Company proprietary information has been deleted.

FIGURE I.30

SMOOTHED VENT HEADER LOAD CELLS - MILLSTONE

o Test 10

*

*General Electric Company proprietary information has been deleted.

FIGURE I-31

MILLSTONE TESTS

o Test 10

*

*General Electric Company proprietary information has been deleted.

FIGURE I - 32

SMOOTHED VENT HEADER LOAD CELLS - COOPER STATION

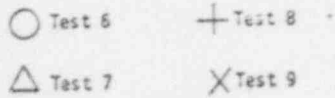

*General Electric Company proprietary information has been deleted.

FIGURE I-33

COOPER STATION TESTS

Integrated Vent Header Force

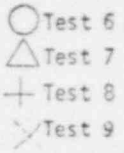

*General Electric Company proprietary information has been deleted.

FIGURE I -34

SMOOTHED VENT HEADER LOAD CELLS - COOPER STATION

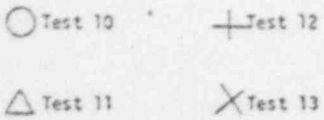

*General Electric Company proprietary information has been deleted.

FIGURE I-35

COOPER STATION TESTS

Integrated Vent Header Force

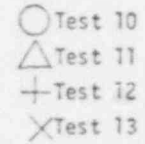

*General Electric Company proprietary information has been deleted.

FIGURE I-36

EFFECT OF DEFLECTOR HEIGHT ON AVERAGE IMPACT PRESSURE

*

*General Electric Company proprietary information has been deleted.

FIGURE I .37

TORUS FORCE FROM LOAD CELL

Monticello Tests
(12-inch Submergence)

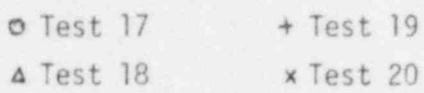

*

*General Electric Company proprietary information has been deleted.

FIGURE I-38

TOTAL FORCE FROM LOAD CELL

Monticello Tests
(10-inch Submergence)

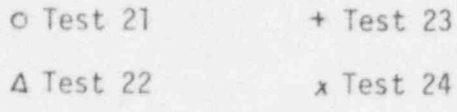

*

*General Electric Company proprietary information has been deleted.

FIGURE 1-39

Monticello Tests

COMPARISON OF NET TORUS FORCE

DETERMINED FROM SMOOTHED LOAD CELL AND PRESSURE INTEGRAL

*

*General Electric Company proprietary information has been deleted.

FIGURE I-40
Monticello Tests
COMPARISON OF NET TORUS FORCE
DETERMINED FROM SMOOTHED LOAD CELL AND PRESSURE INTEGRAL

*

*General Electric Company proprietary information has been deleted.

FIGURE I -41

Monticello Tests

COMPARISON OF TORUS Δ(PRESSURE INTEGRAL-LOAD CELL)

FOR CABLE-SUPPORTED AND BOLTED DEFLECTORS

*General Electric Company proprietary information has been deleted.

FIGURE I-42
Monticello Tests
COMPARISON OF TORUS Δ(PRESSURE INTEGRAL-LOAD CELL)
FOR CABLE-SUPPORTED AND BOLTED DEFLECTORS

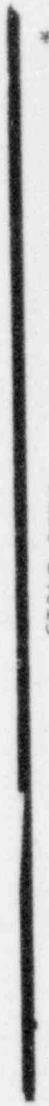

*General Electric Company proprietary information has been deleted.

FIGURE I-43
Monticello Tests
DEFLECTOR UPFORCE FROM TORUS CABLES

*

*General Electric Company proprietary information has been deleted.

FIGURE I-.44

DEFLECTOR IMPULSE

*

*General Electric Company proprietary information has been deleted.

FIGURE I-45

CONFIGURATION OF DYE INJECTION APPARATUS

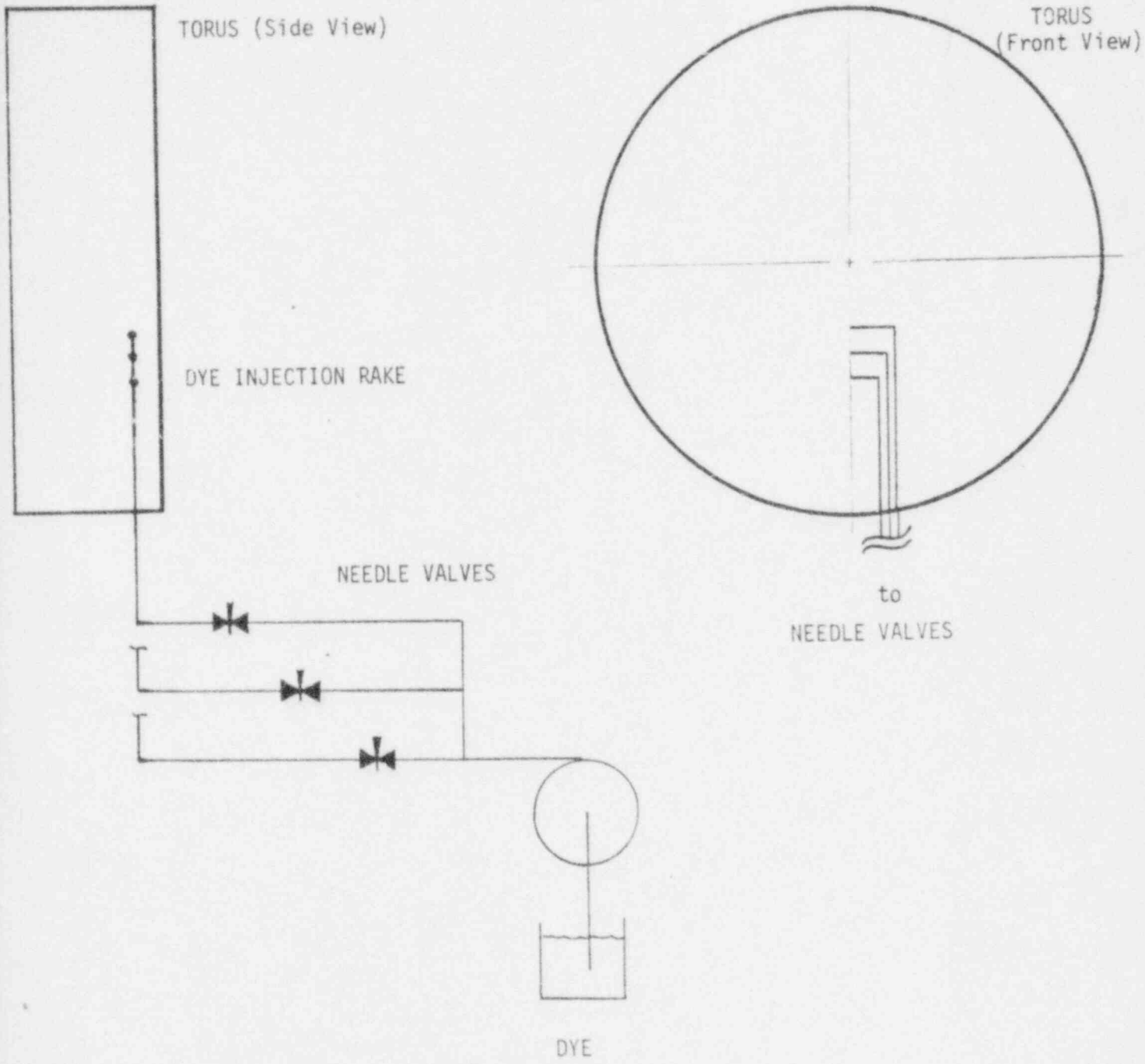

FIGURE I-48

DYE INJECTION RESULTS

MILLSTONE BURP 82

*

*General Electric Company proprietary information has been deleted.

*

*General Electric Company proprietary information has been deleted.

FIGURE I-48

DYE INJECTION RESULTS

MILLSTONE BURP 82

*

*General Electric Company proprietary information has been deleted.

FIGURE I-49

DYE INJECTION RESULTS

COOPER STATION BURP B2

*

*General Electric Company proprietary information has been deleted.

FIGURE I-50
OYSTER CREEK BURP 2A

*

*General Electric Company proprietary information has been deleted.

TABLE I-1

TEST CONDITIONS

MONTICELLO

Test No's.	Test Objective	Test Conditions (quarter scale)		
		Submergence	ΔP	Deflector
17-18	Transmit deflector load to torus	12 inches	0	8.15" *
19-20	Transmit deflector load to vent header	12 inches	0	8.15"
21-22	Transmit deflector load to torus	10 inches	0	8.15"
23-24	Transmit deflector load to vent header	10 inches	0	8.15"

*Tip-to-tip dimension

DUANE ARNOLD

Test No's.	Test Objective	Test Conditions (quarter scale)		
		Submergence	ΔP	Deflector
6, 7	Transmit deflector load to torus	12.08 inches	0	9.06"*
8, 9	Transmit deflector load to vent header	12.08 inches	0	9.06"

*Tip-to-tip dimension

PILGRIM

Test No's.	Test Objective	Test Conditions (quartar scale)		
		Submergence	ΔP	Deflector
6 - 7	Transmit deflector load to torus	10.25 in	8.51	6.73"*
8 - 9	Transmit deflector load to vent header	10.25 in	8.51	6.73"
10 - 11	Transmit deflector load to torus	10.25 in	0	6.73"
12 - 13	Transmit deflector load to vent header	10.25 in	0	6.73"

*Tip-to-tip dimension

TABLE I-2

TEST CONDITIONS

OYSTER CREEK

Test No's.	Test Objective	Test Conditions (Quarter Scale)		
		Submergence	ΔP	Deflector
6, 7	Deflector load transmitted to torus	12.59 inches	7.15"	7.75"*
8, 9	Deflector load transmitted to vent header	12.59 inches	7.15"	7.75"
Surp 2A	Deflector load transmitted to vent header.	12.59 inches	0	7.75"
10	Deflector load transmitted to torus	12.59 inches	0	7.75"
11, 12	Deflector load transmitted to torus.	9.30 inches	7.15"	7.75"
13, 14	Deflector load transmitted to vent header	9.30 inches	7.15"	7.75"
15	Torus load test - QSP.	9.30 inches	0	7.75"

*Tip-to-tip dimension

NINE MILE POINT

Test No's.	Test Objective	Test Conditions (quarter scale)		
		Submergence	ΔP	Deflector
A. Header Centerline to Downcomer Discharge: 31.00 inches				
6, 7	Deflector load transmitted to torus.	14.64 inches	7.94"	7.35"*
8, 9	Deflector load transmitted to vent header.	14.64 inches	7.94"	7.35"
10	Deflector load transmitted to torus.	14.64 inches	0	7.35"
10A	Deflector load transmitted to vent header	14.64 inches	0	7.35"
B. Header Centerline to Downcomer Discharge: 27.55 inches				
11, 12	Deflector load transmitted to torus	11.19 inches	7.94"	7.35"
13, 14	Deflector load transmitted to vent header	11.19 inches	7.94"	7.35"
15, 16	Deflector load transmitted to torus	11.19 inches	0	7.35"
17, 18	Deflector load transmitted to vent header.	11.19 inches	0	7.35"

*Tip-to-tip dimension

TABLE I-3
TEST CONDITIONS

MILLSTONE

Test No's	Test Objective	Test Conditions (Quarter Scale)		
		Submergence	ΔP	Deflector
6, 7	Deflector load transmitted to torus.	10.50 inches	7.27"	6.727"*
8, 9	Deflector load transmitted to vent header	10.50 inches	7.27"	6.727"
10	Torus load test - 0ΔP	10.50 inches	0	6.727"

*Tip-to-tip dimension 

COOPER STATION

Test No's.	Test Objective	Test Conditions (Quarter Scale)		
		Submergence	ΔP	Deflector
6, 7	Deflector load transmitted to torus	10.78 inches	7.46"	6.82"*
8, 9	Deflector load transmitted to vent header.	10.78 inches	7.46"	6.82"
10, 11	Deflector load transmitted to torus	10.78 inches	0	6.82"
12, 13	Deflector load transmitted to vent header.	10.78 inches	0	6.82"

*tip-to-tip dimension 

TABLE I-4

SUMMARY OF DEFLECTOR FORCES

*General Electric Company proprietary information has been deleted.

NUCLEAR ENERGY DIVISIONS • GENERAL ELECTRIC COMPANY
SAN JOSE, CALIFORNIA 95125

GENERAL ELECTRIC

TECHNICAL INFORMATION EXCHANGE

TITLE PAGE

AUTHOR	SUBJECT	TIE NUMBER
	730	80NED023
		DATE: June 1980
TITLE: Mark I Containment Program 1/4 Scale Pressure Suppression Pool Swell Test Program: Supplemental Plant Unique Tests		GE CLASS: I
		GOVERNMENT CLASS: ---
REPRODUCIBLE COPY FILED AT TECHNICAL SUPPORT SERVICES, R&UO, SAN JOSE, CALIFORNIA 95125 (Mail Code 211)		NUMBER OF PAGES: 671

SUMMARY This report presents the results of the Supplemental Plant Unique Tests (Mark I Long-Term Program, Task 10.1/5.5.4) that were conducted in the Mark I Quarter Scale Test Facility (QSTF) for seven Mark I plants. The plants in the order tested were: Monticello, Duane Arnold, Pilgrim, Oyster Creek 1, Nine Mile Point 1, Millstone, and Cooper Station. The objectives of the Supplemental Plant Unique Tests were to obtain subscale two-dimensional net vertical torus forces, vent header impact pressures, and pool surface displacement and velocity transients · test conditions requested by individual utilitie , quantify vent header deflector forces. Individua plant characteristics were modeled in the QSTF so that pool swell could be evaluated on a plant unique basis. Vent reflector forces were determined by the difference in the measured vent header force transients for two test configurations: 1) with the vent deflector suspended from the torus by cables and 2) with the deflector bolted or welded onto the vent header. A total of 56 tests were conducted from November 1978 to March 1979 in the QSTF. The data from these tests will be used as input for plant unique pool swell loads for those conditions selected by the utilities as their design basis.

By cutting out this rectangle and folding in half, the above information can be fitted into a standard card file.

DOCUMENT NUMBER NEDO-24615

INFORMATION PREPARED FOR Nuclear Fuel and Services Division

SECTION Training and Technical Services

BUILDING AND ROOM NUMBER 1887-2007 MAIL CODE 886